

Reactive Flow and Permeability Dynamics I & II

Derek Elsworth, Penn State

Basic Observations of Permeability Evolution - Lab-to-field

Impacts on Permeability

Mechanical effects (pore pressure and thermal effects)

Controls on effective stress

Stress-porosity linkages for fractures

Compaction

Dilation

Rate-state models

Porosity-permeability linkages to fracture dilation

Other mechanical effects (wear)

Reactive chemical effects

Laboratory observations

Linkages among porosity/permeability/dissolution/precipitation

Mechanistic models for chemical-mechanical effects

In situ observations/characterizations of chemical-mechanical effects

Forward/reverse feedbacks on stress-permeability

Reservoir-Scale Evolution of Permeability

Spatial distribution

Timing

Seismicity as an indicator

Summary

Basic Observations of Permeability Evolution

Challenges

- Prospecting (characterization)
- Accessing (drilling)
- Creating reservoir
- Sustaining reservoir
- Environmental issues

Observation

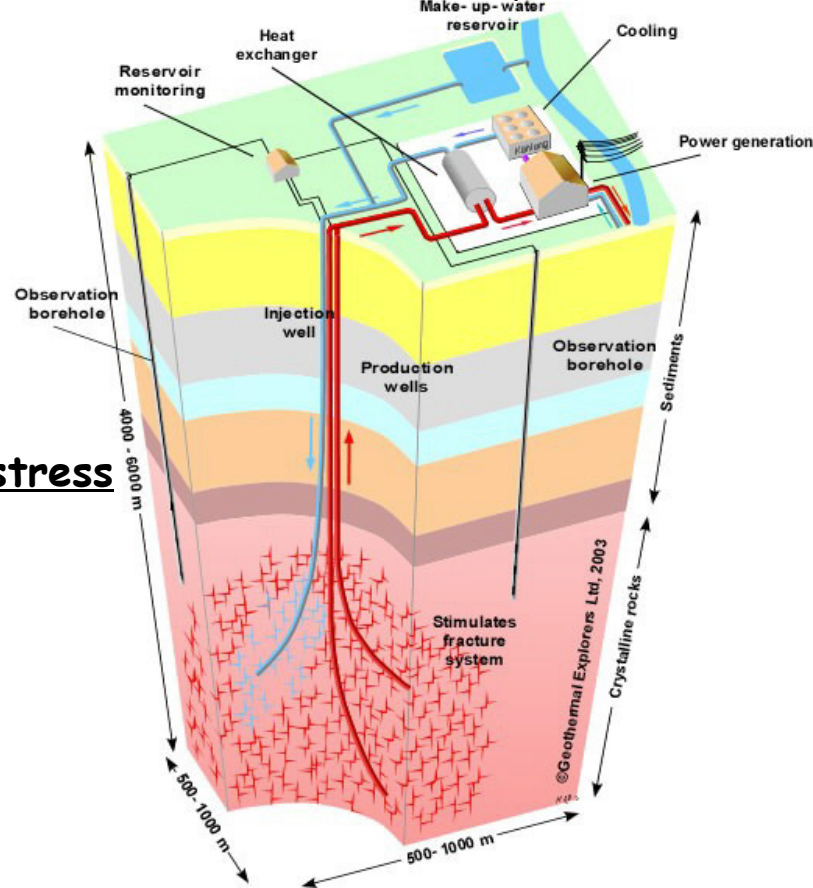
- Stress-sensitive reservoirs
- T H M C all influence via effective stress
- Effective stresses influence
 - Permeability
 - Reactive surface area
 - Induced seismicity

Understanding T H M C is key:

- Size of relative effects of THMC
- Timing of effects
- Migration within reservoir
- Using them to engineer the reservoir

Resource

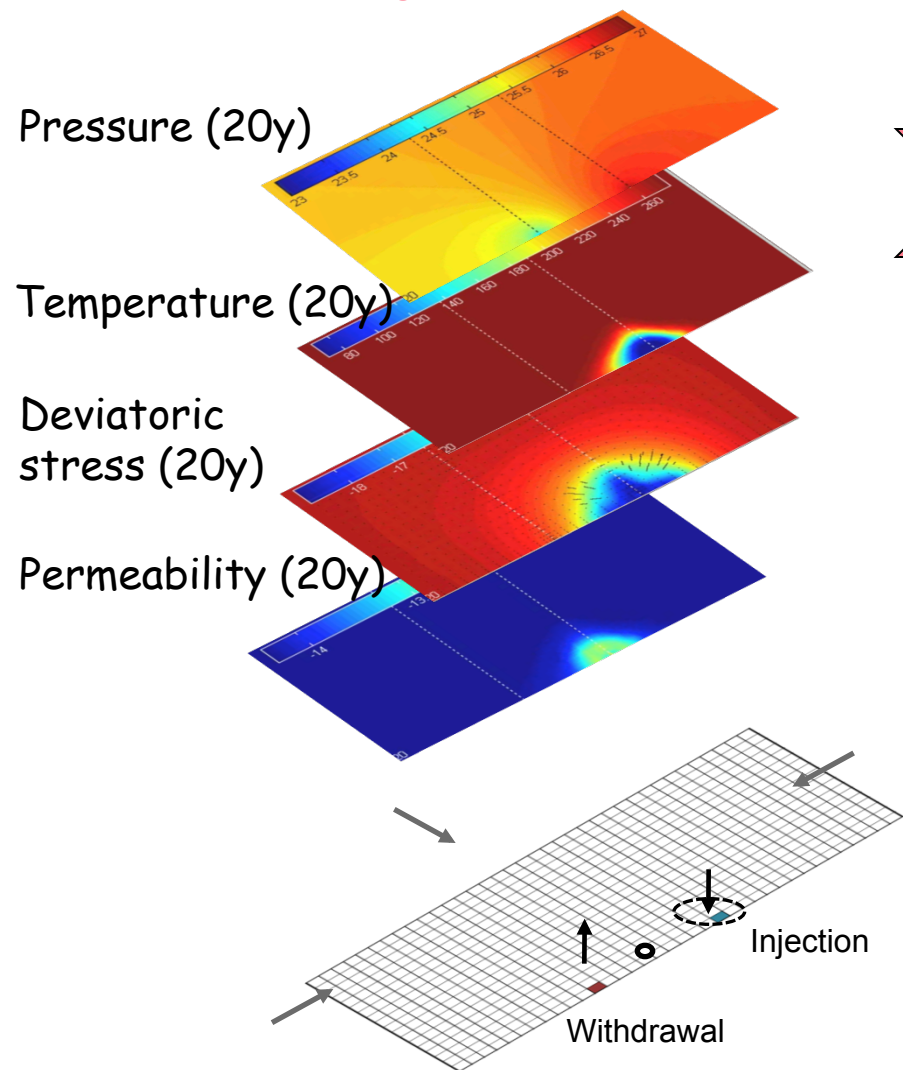
- Hydrothermal (US: 10^4 EJ)
- EGS (US: 10^7 EJ; 100 GW in 50y)



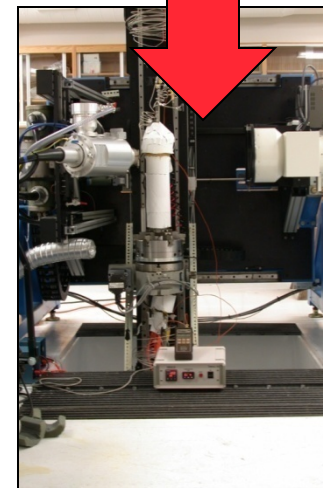
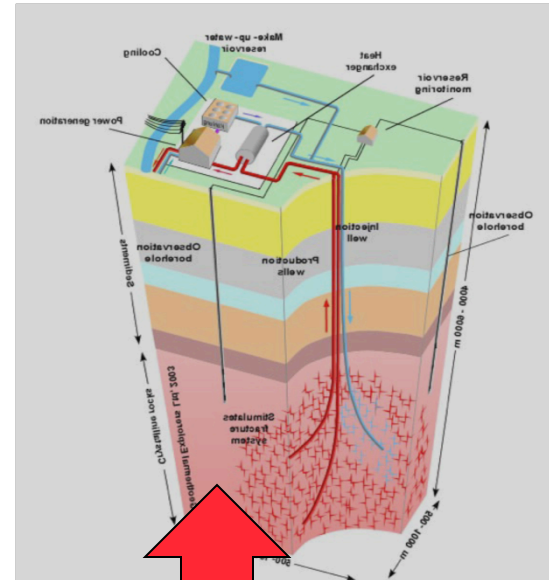
- Permeability
- Reactive surface area
- Induced seismicity

Scaling Between Laboratory and Observation

Model (linkage)



Prototype (reality)



Experiment
(constitutive
behavior):
 $K=f(THMC)$

Controls on Reservoir Evolution

Many processes of vital importance to EGS are defined by coupled THMC processes.

Thermal sweep/fluid residence time

Short circuiting

Induced seismicity

Prolonged sustainability of fluid transmission

Fractures dominate the fluid transfer system

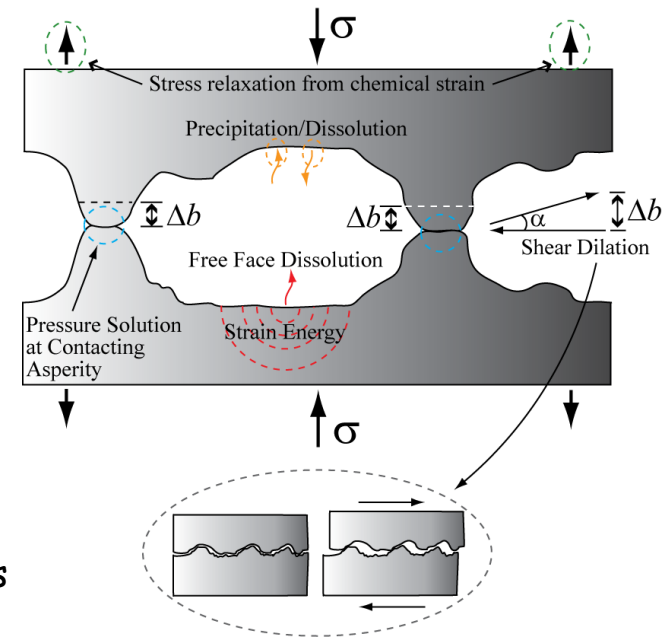
Transmission characterized by:

History of mineral deposition

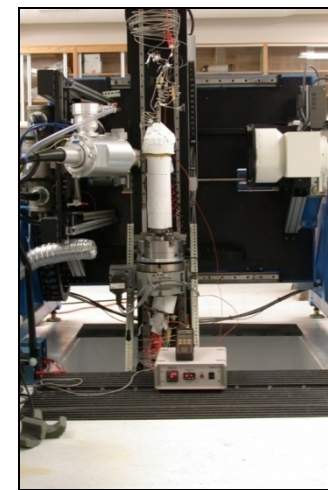
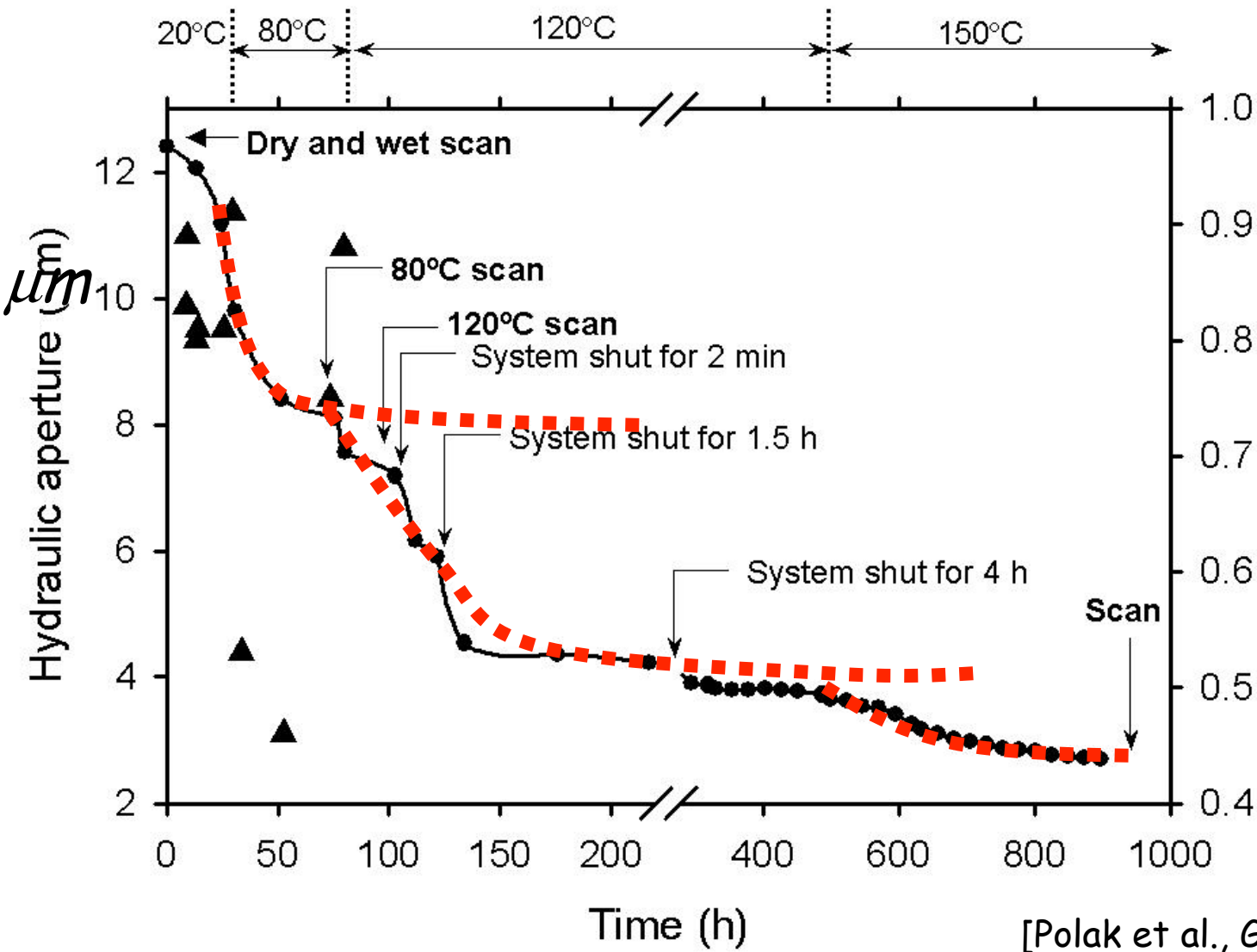
Chemo-mechanical creep at contacting asperities

Mechanical compaction

Shear dilation and the reactivation of relic fractures



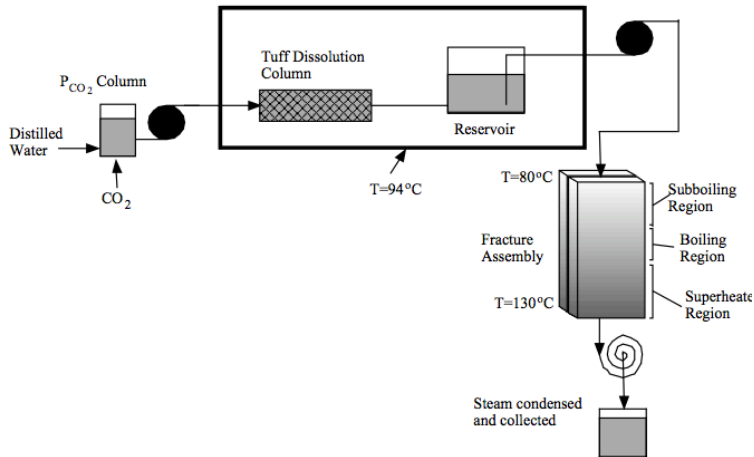
Typical Response of Fractures (Dissolution) ↓



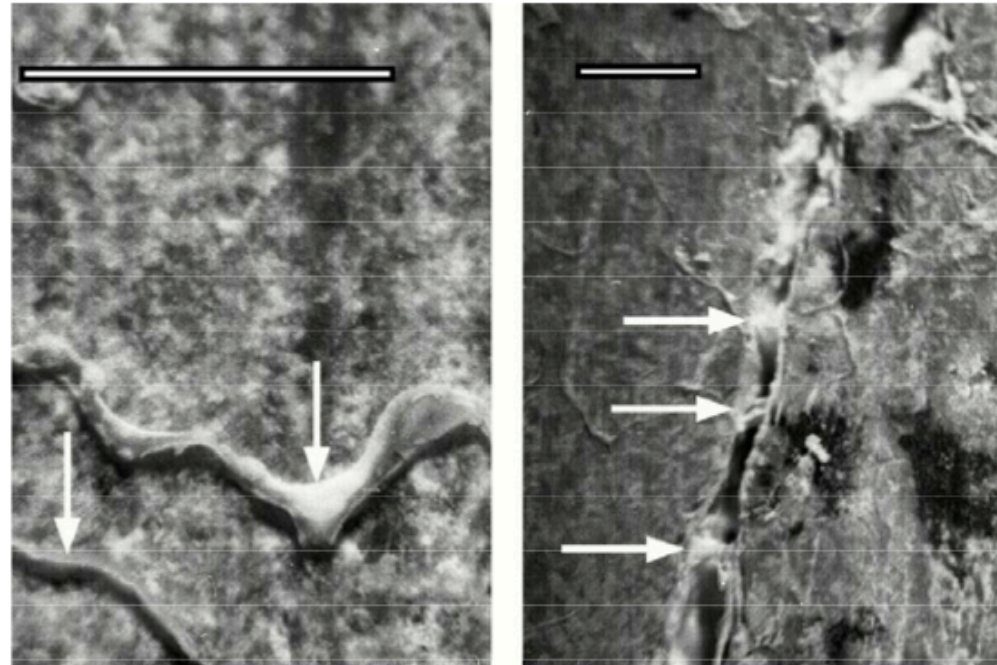
[Polak et al., GRL, 2003]

Typical Response of Fractures (Precipitation)

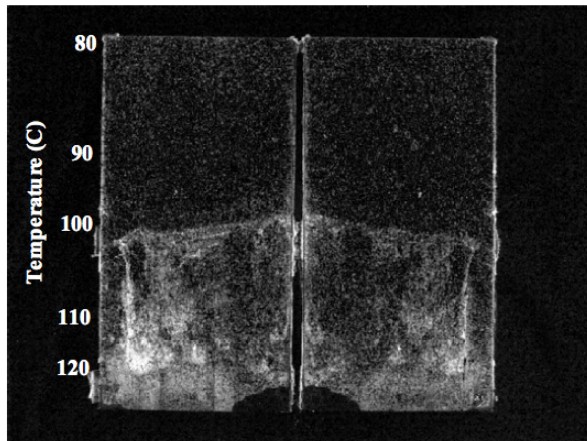
Experimental arrangement



Precipitation



Thermal gradient along fracture



[Dobson et al., 2001]

Reactive Transport [1]

Advection-Dispersion Equation

$$\frac{\partial c_i}{\partial t} + \nabla \cdot (c_i \mathbf{u}) - \nabla \cdot (D_i \nabla c_i) = R_i + k_{i+} (c_i - c_i^{eq}) \quad (1)$$

For the reaction:



$$\text{Forward rate} = k_1[A][B]$$

$$\text{Reverse rate} = k_2[C] \quad (3)$$

At equilibrium:

$$\text{Forward rate} = \text{Reverse rate}$$

$$k_1[A][B] = k_2[C] \quad (4)$$

$$\therefore [A][B] = \frac{k_2}{k_1}[C] \quad (5)$$

For closed system and one mole each of [A] and of [B], with $k_1 = 1$ and $k_2 = 10$, then:

$$\frac{[A][B]}{[C]} = \frac{(1 - X)^2}{X} = \frac{10}{1} \quad (6)$$

And $(1 - X) = [A] = [B] = 0.916$ and $X = [C] = 0.0839$.

Reactive Transport [2]

Implementation:

$$\begin{aligned}R_A &= -k_1[A][B] + k_2[C] \\R_B &= -k_1[A][B] + k_2[C] \\R_C &= +k_1[A][B] - k_2[C]\end{aligned}\tag{7}$$

Generalized:

$$R_i = -k_i^f \prod_{j=1}^N [c_j^f]^{\alpha_j^f} + k_i^r \prod_{j=1}^N [c_j^r]^{\alpha_j^r}\tag{8}$$

Heats of reaction:

$$H_i = R_i \Delta H_i\tag{9}$$

And heat balance requires:

$$\rho c \frac{\partial T}{\partial t} + \nabla \cdot (T \mathbf{u}) - \nabla \cdot (\lambda \nabla T) = H_i\tag{10}$$

Reactive Flow and Permeability Dynamics

Derek Elsworth, Penn State

Basic Observations of Permeability Evolution - Lab-to-field

Impacts on Permeability

Mechanical effects (pore pressure and thermal effects)

- Controls on effective stress

- Stress-porosity linkages for fractures

 - Compaction

 - Dilation

 - Rate-state models

- Porosity-permeability linkages to fracture dilation

- Other mechanical effects (wear)

Reactive chemical effects

- Laboratory observations

- Linkages among porosity/permeability/dissolution/precipitation

- Mechanistic models for chemical-mechanical effects

- In situ observations/characterizations of chemical-mechanical effects

- Forward/reverse feedbacks on stress-permeability

Reservoir-Scale Evolution of Permeability

- Spatial distribution

- Timing

- Seismicity as an indicator

Summary

Basic Observations of Permeability Evolution

Observation

- Stress-sensitive reservoirs
- T H M C all influence via effective stress
- Effective stresses influence
 - Permeability
 - Reactive surface area
 - Induced seismicity

Stress Changes

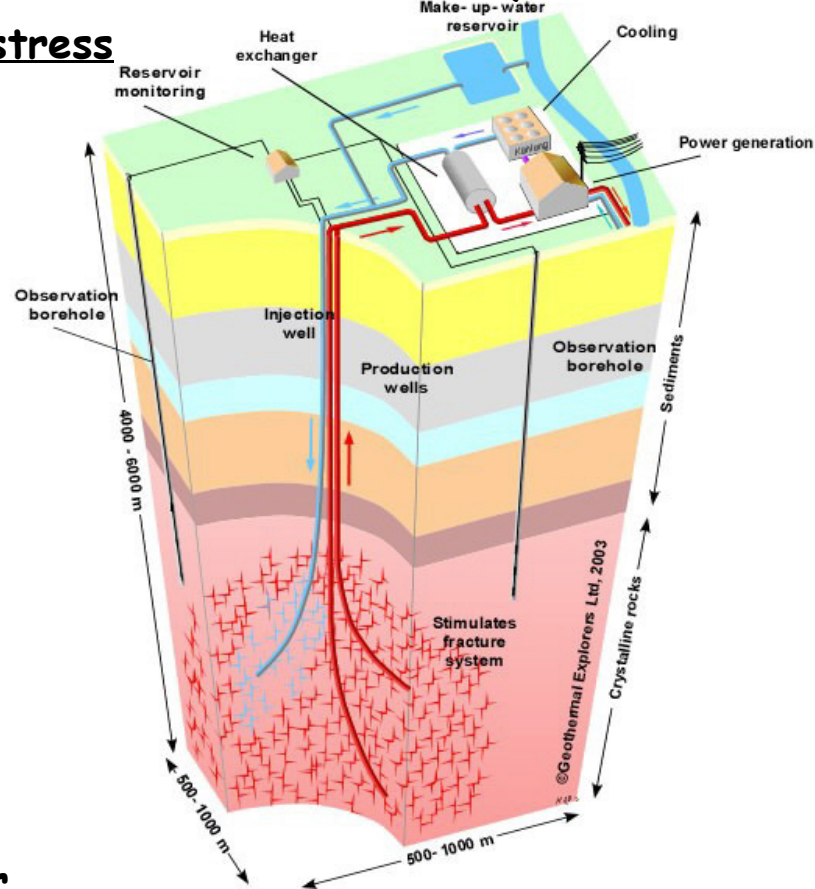
Inert changes (THM)
Reactive changes (MC)

Understanding T H M C is key:

- Size of relative effects of THMC
- Timing of effects
- Migration within reservoir
- Using them to engineer the reservoir

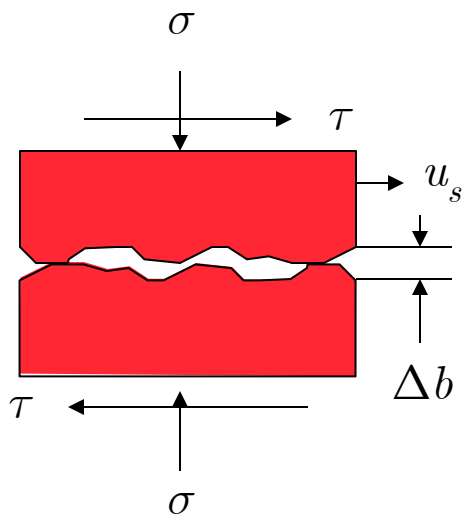
Resource

- Hydrothermal (US: 10^4 EJ)
- EGS (US: 10^7 EJ; 100 GW in 50y)

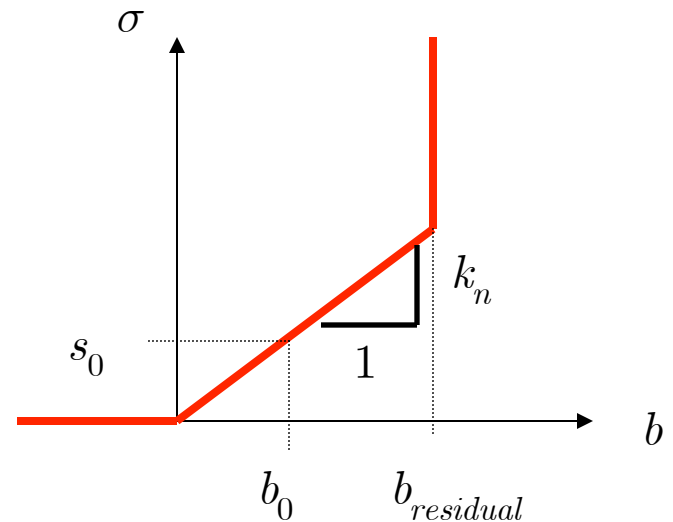


- Permeability
- Reactive surface area
- Induced seismicity

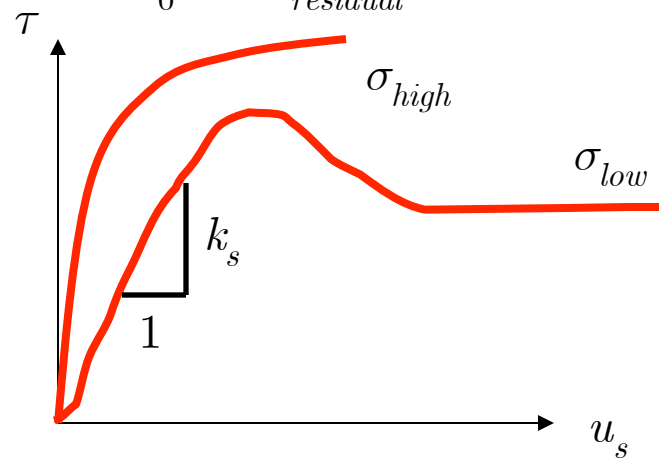
Permeability Changes in Fractures - Deformation



Normal Mode:

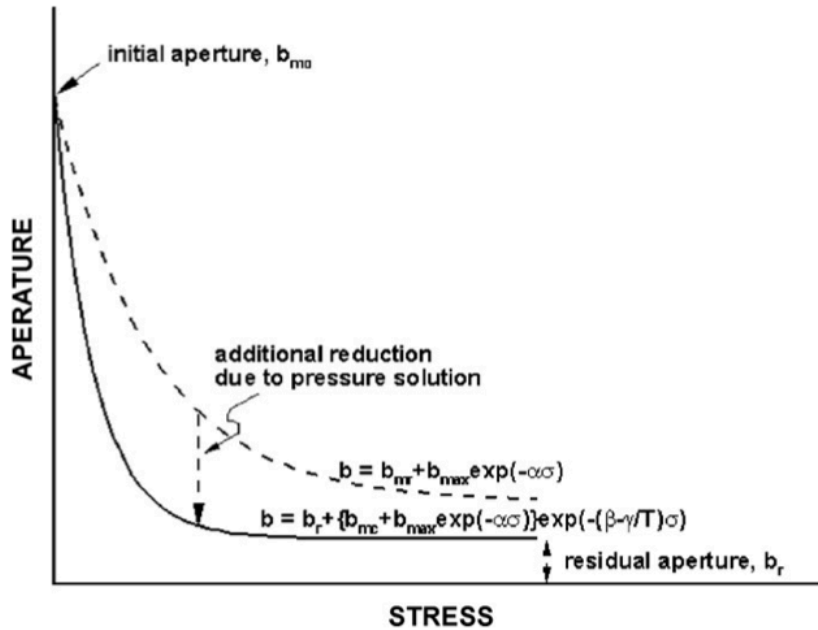


Shear Mode:



Normal Compression of Fractures

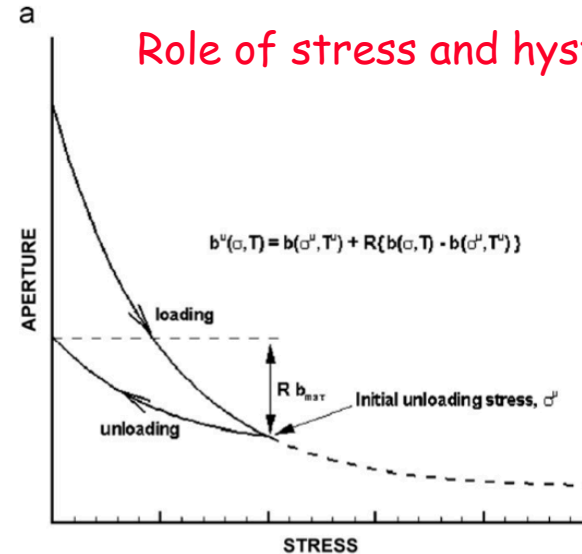
Mechanical closure with stress



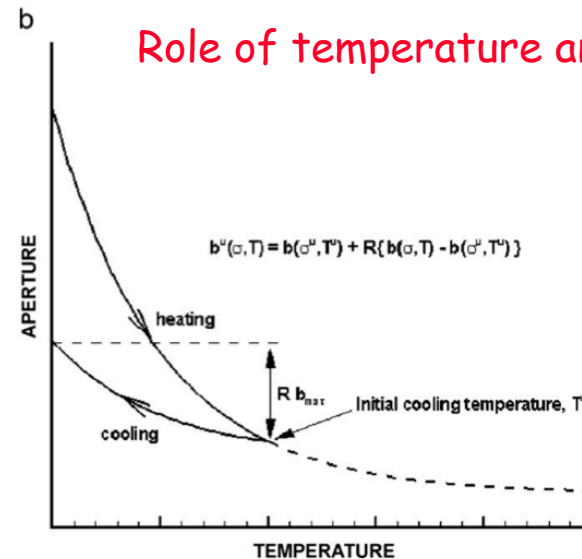
$$b_{normal} = b_r + b_{max} \exp(-\alpha\sigma')$$

$$\Delta b_{normal} = b_{max} \exp(-\alpha\Delta\sigma')$$

Role of stress and hysteresis

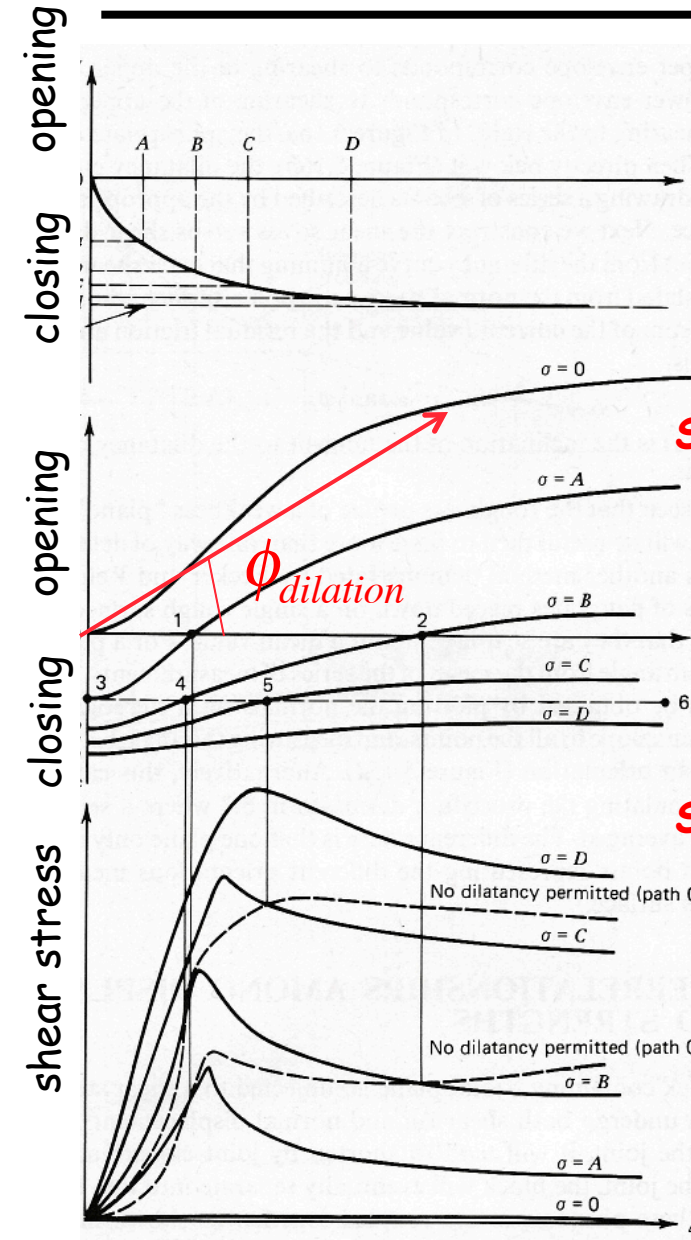


Role of temperature and hysteresis



[Min et al., IJRM, 2009]

Shear Dilation of Fractures



Normal closure behavior

Shear dilatancy behavior

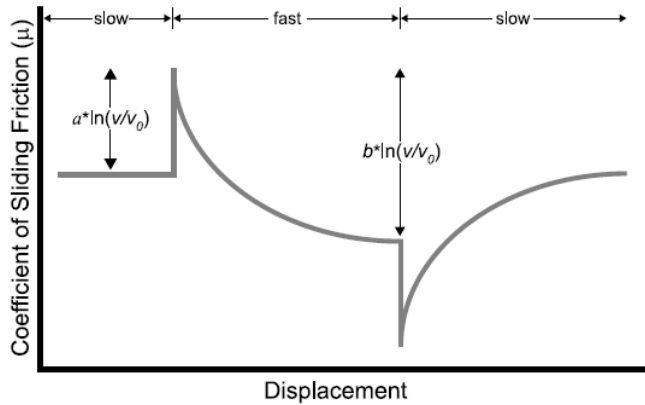
$$\Delta b_{shear} = \tau \left(\frac{s}{G} + \frac{1}{K_{shear}} \right) \tan(\phi_{dilation})$$

Stress-displacement behavior

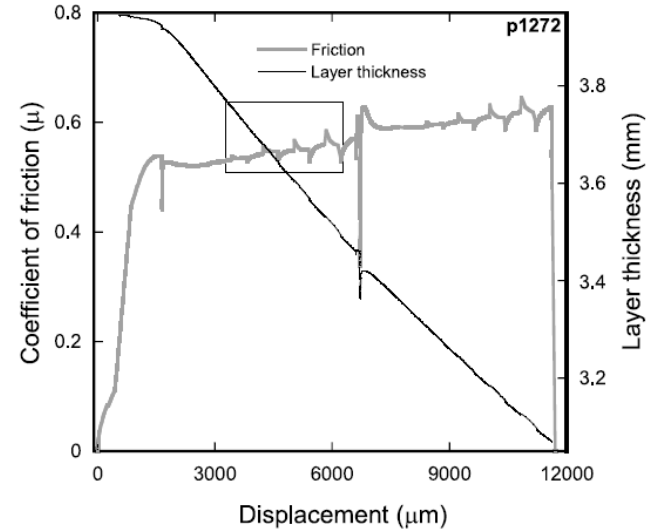
shear displacement

Rate-State Friction [1]

Velocity Steps



Multiple Velocity Steps



R-S Friction

$$\left. \begin{aligned} \mu &= \mu_0 + a \ln\left(\frac{v}{v_0}\right) + b \ln\left(\frac{v_0 \theta}{D_C}\right) \\ \frac{d\theta}{dt} &= 1 - \frac{v\theta}{D_C} \quad (\text{Dieterich Evolution}) \\ \frac{d\theta}{dt} &= \frac{-v\theta}{D_C} \ln\left(\frac{v\theta}{D_C}\right) \quad (\text{Ruina Evolution}) \end{aligned} \right\}$$

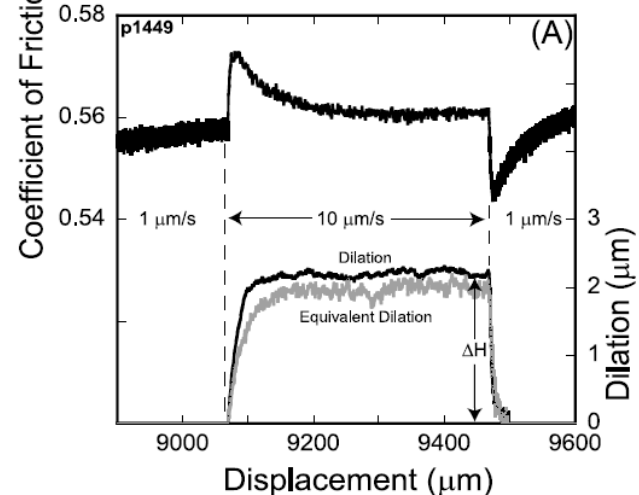
Dilation

$$\frac{\Delta H}{H} \cong \Delta \phi = -\epsilon \ln\left(\frac{v}{v_0}\right) = -\epsilon \ln\left(\frac{v_0 \theta}{D_c}\right)$$

Permeability Evolution

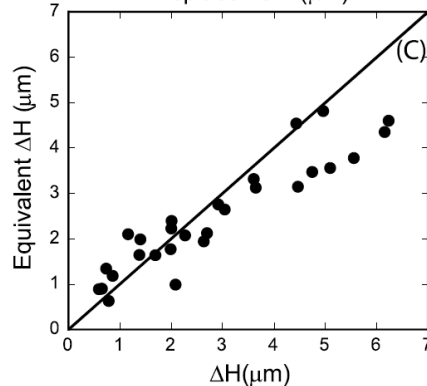
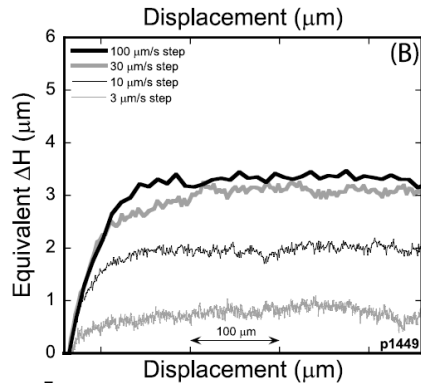
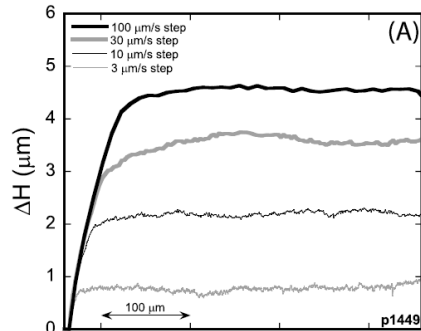
$$\frac{k}{k_0} = \left(1 + \frac{\Delta b}{b_0}\right)^3 = \left(1 + \frac{\Delta H}{H}\right)^3$$

Single Velocity Step

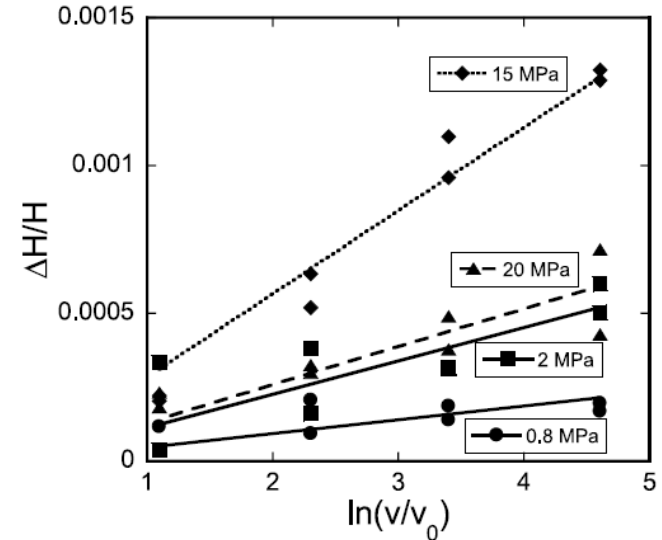


Rate-State Friction [2]

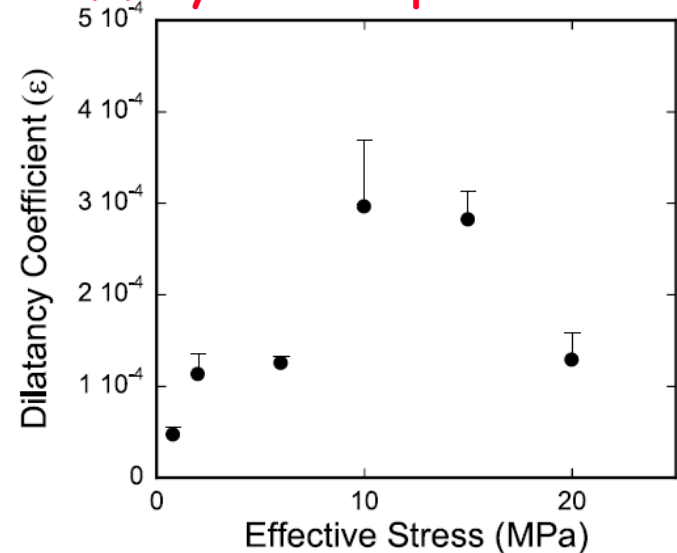
Concurrent Displacement and Fluid Measurements



Summary Data - Delta H



Summary Data - Epsilon



Porosity-Permeability Relationships

Single fracture versus bulk permeability

Single:
$$\bar{v}_i = \frac{k_i}{\mu} \frac{\partial p}{\partial x} = \frac{b^2}{12} \frac{1}{\mu} \frac{\partial p}{\partial x}$$

Bulk:
$$\bar{v}_b = \frac{b}{s} \bar{v}_i = \frac{b^3}{12s} \frac{1}{\mu} \frac{\partial p}{\partial x} = \frac{k_b}{\mu} \frac{\partial p}{\partial x}$$

Bulk permeability

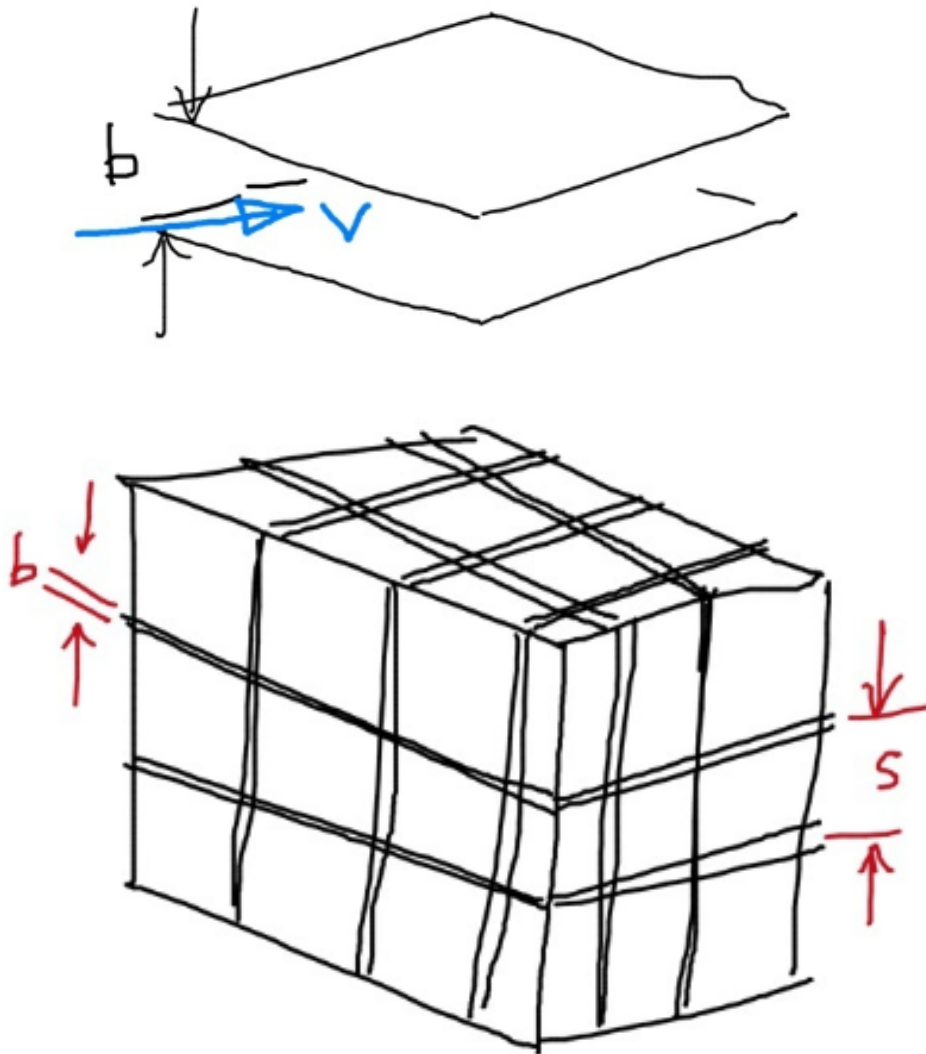
$$k = \frac{b^3}{12s}; \text{ therefore } k_0 = \frac{b_0^3}{12s}$$

Initial fracture aperture (b_0)

$$b_0 = \sqrt[3]{k_0 12s}$$

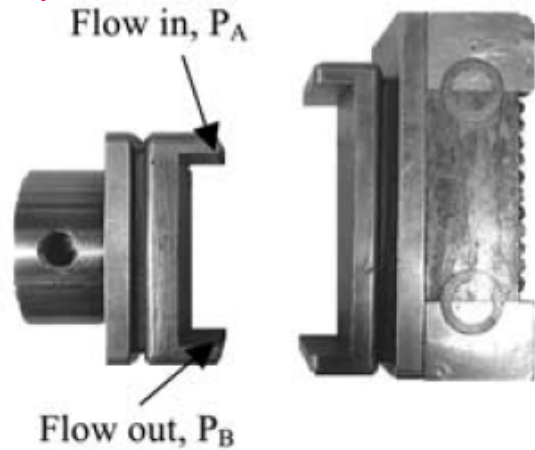
Change to new permeability (k)

$$\frac{k}{k_0} = \left(1 + \frac{\Delta b}{b_0}\right)^3$$

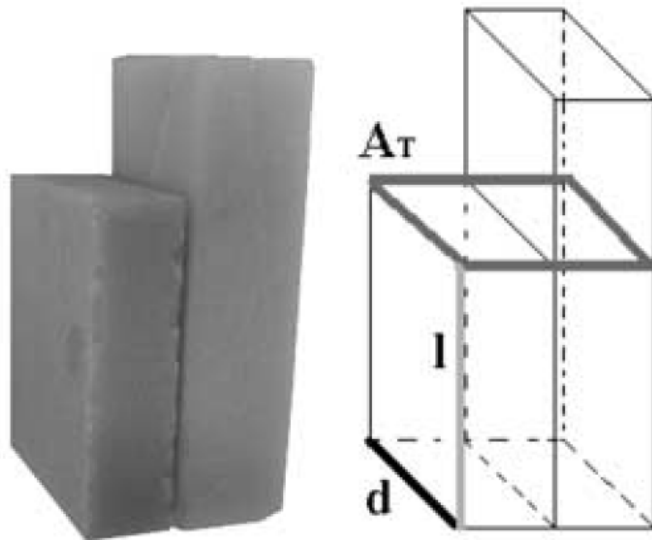


Role of Wear Products

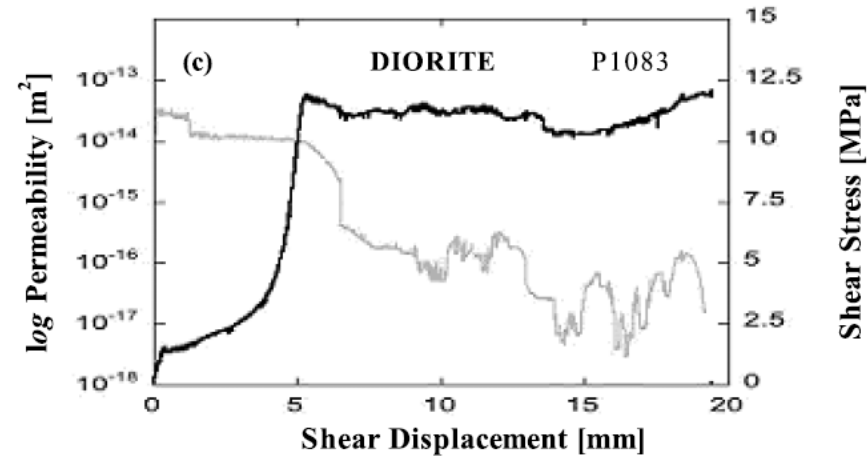
Sample Holder



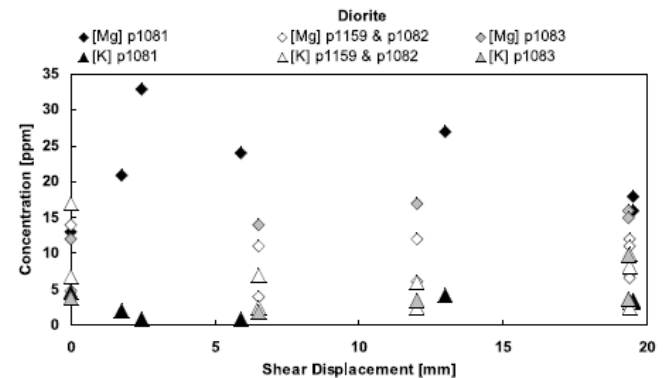
Sample



Shear-Permeability Evolution



Dissolution Products



Reactive Flow and Permeability Dynamics

Derek Elsworth, Penn State

Basic Observations of Permeability Evolution - Lab-to-field

Impacts on Permeability

Mechanical effects (pore pressure and thermal effects)

Controls on effective stress

Stress-porosity linkages for fractures

Compaction

Dilation

Rate-state models

Porosity-permeability linkages to fracture dilation

Other mechanical effects (wear)

Reactive chemical effects

Laboratory observations

Linkages among porosity/permeability/dissolution/precipitation

Mechanistic models for chemical-mechanical effects

In situ observations/characterizations of chemical-mechanical effects

Forward/reverse feedbacks on stress-permeability

Reservoir-Scale Evolution of Permeability

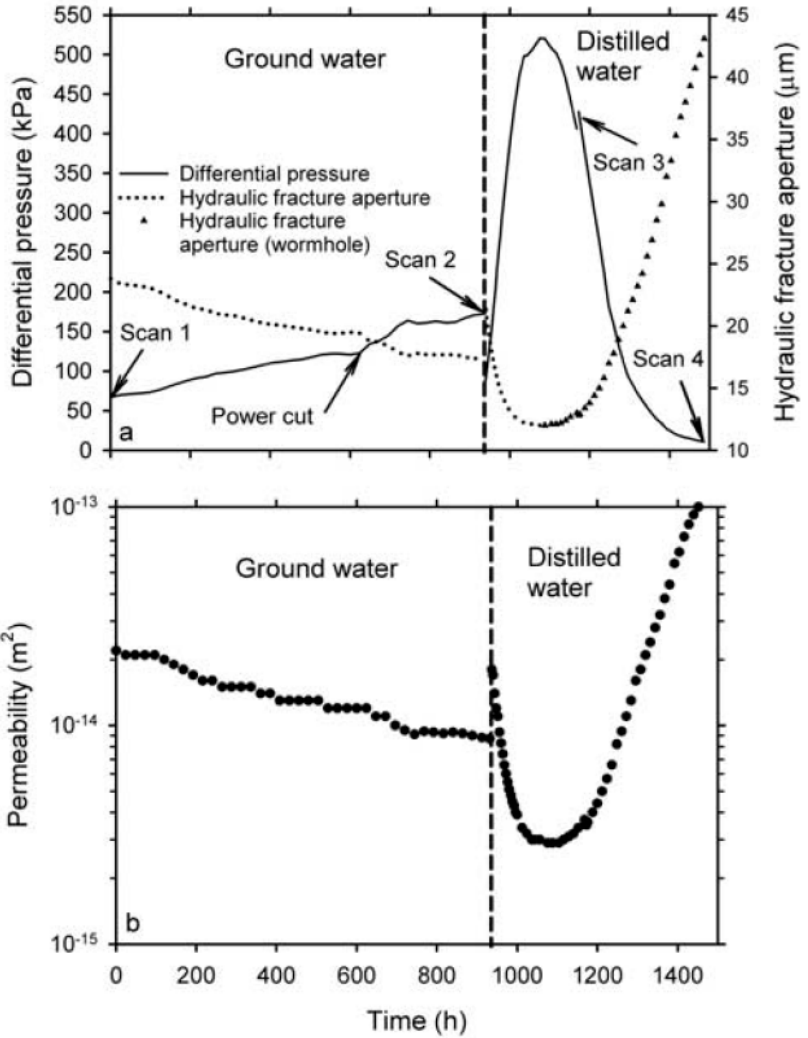
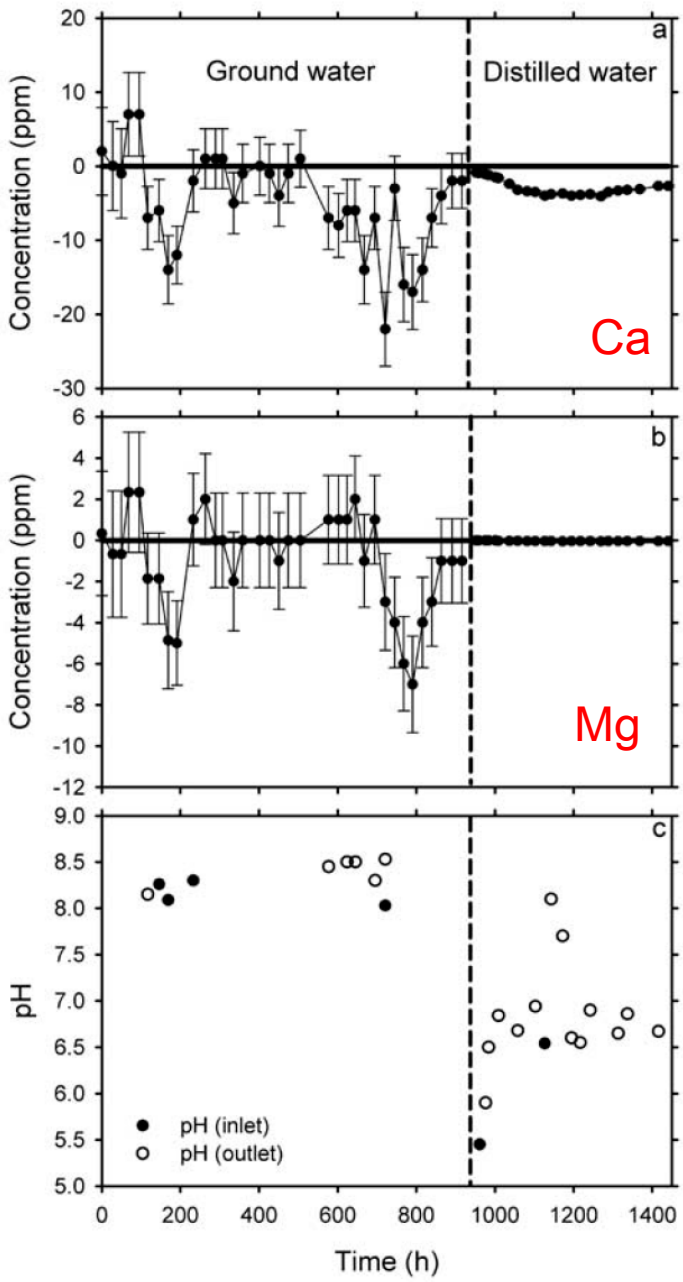
Spatial distribution

Timing

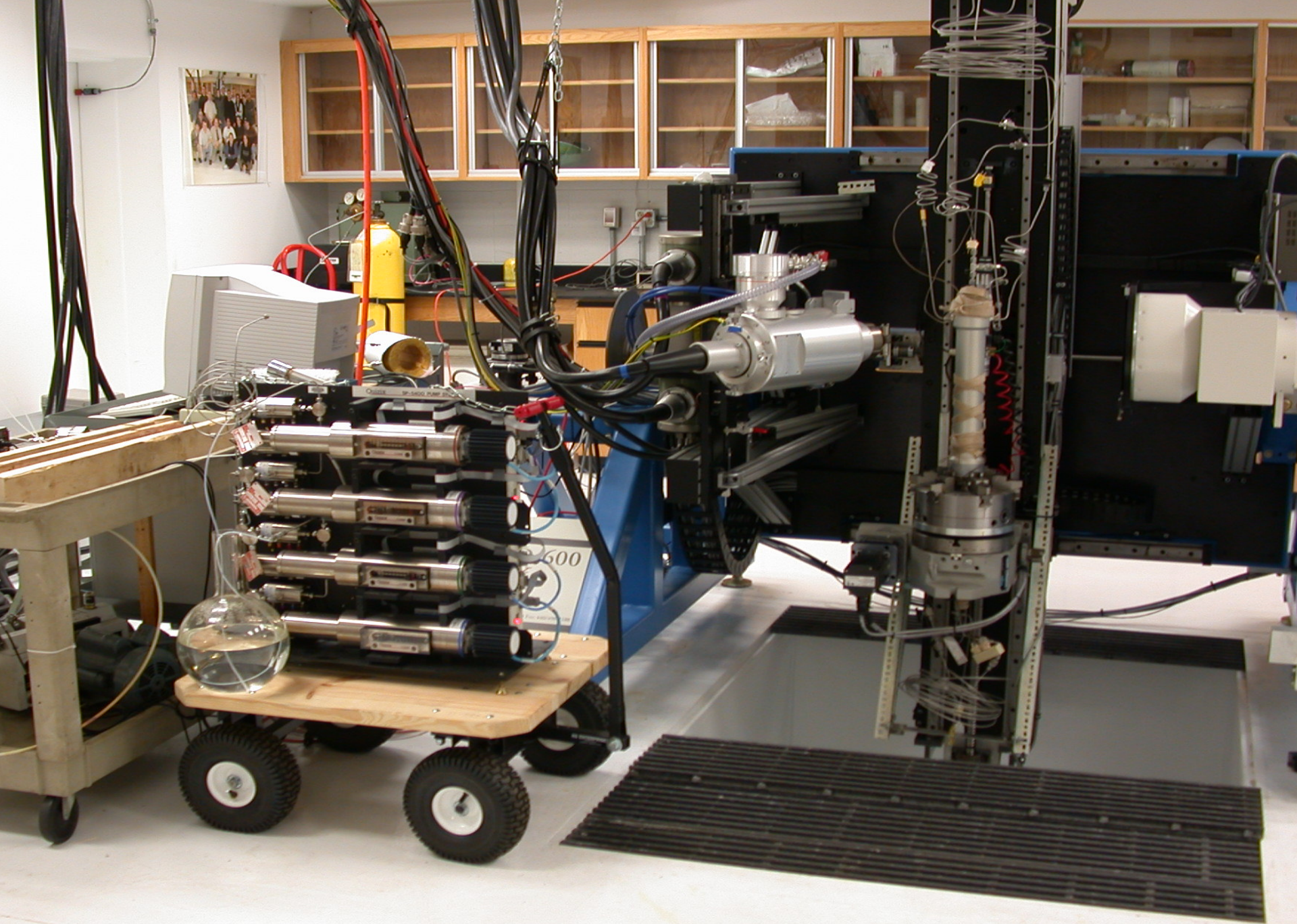
Seismicity as an indicator

Summary

Fractured Limestone – Features of Response

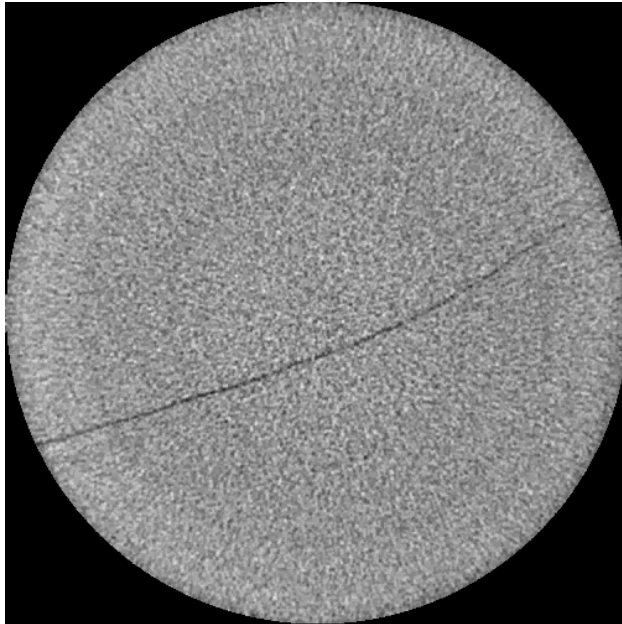


[Polak et al., WRR, 2004]

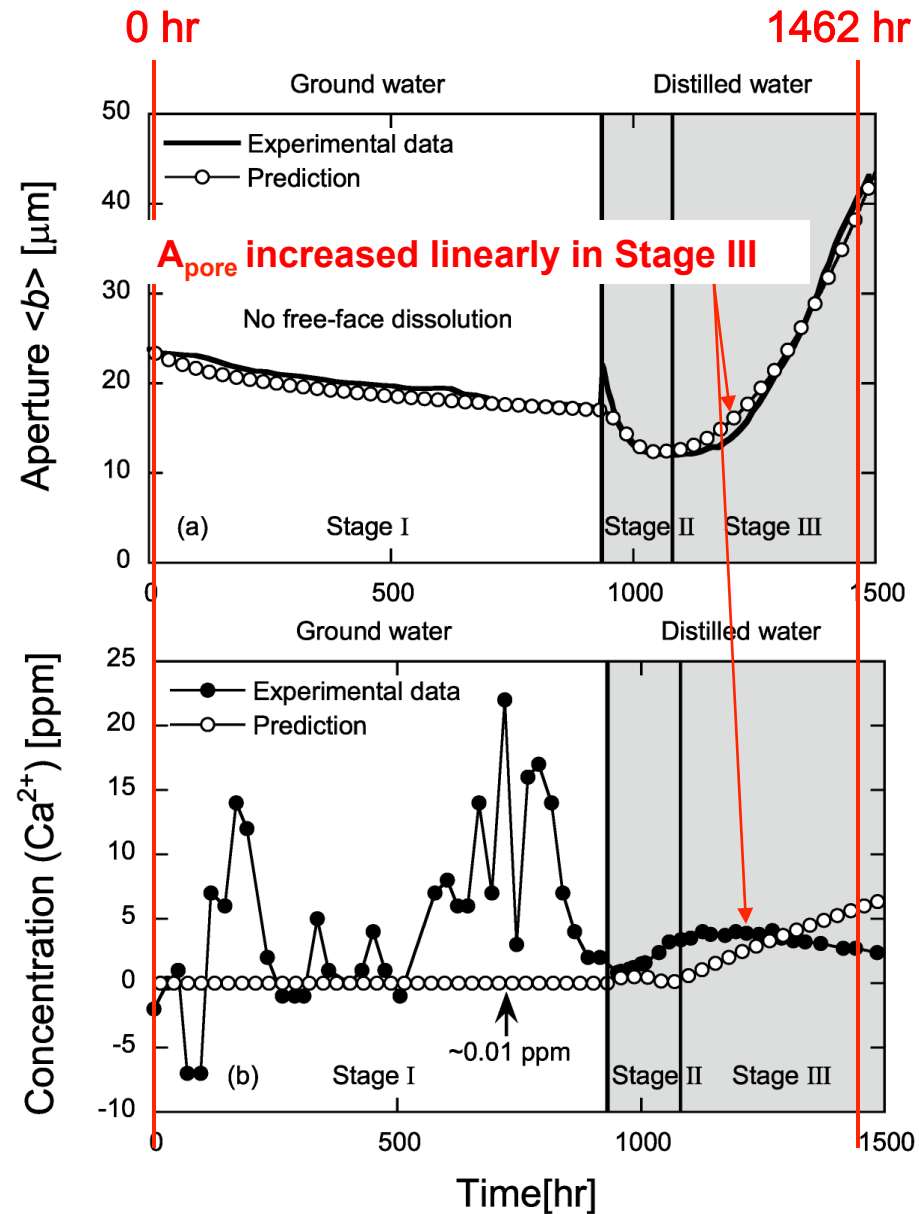
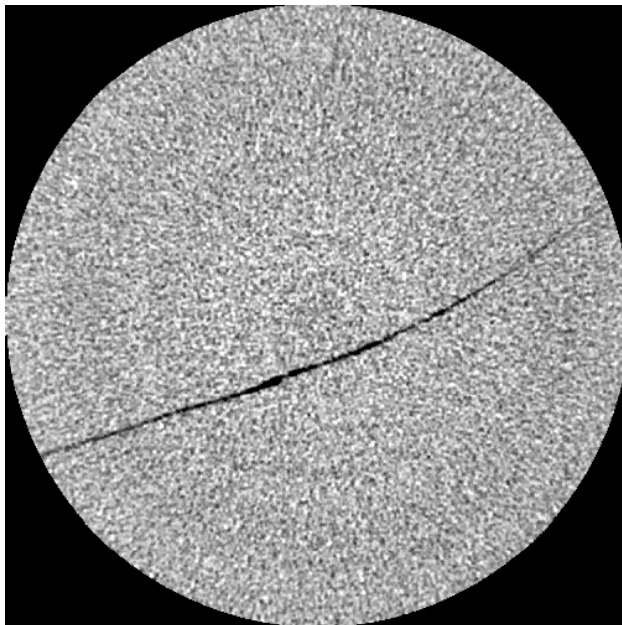


Fractured Limestone – Features of Response

0 hr



1462 hr



Reactive - Hydrodynamic Controls

Peclet No. (Pe)

$$Pe = \frac{\text{Advective flux}}{\text{Dispersive flux}} = \frac{\langle q \rangle}{D_m} = \frac{vb_0}{D_m}$$

Pe < 1 Dispersion dominated –
Perturbations damped

Pe > 1 Advection dominated –
Perturbations enhanced

Damkohler No. (Da)

$$Da = \frac{\text{Reactive flux}}{\text{Advective flux}} = \frac{2k_+L}{\langle q \rangle} = \frac{2k_+L}{vb_0}$$

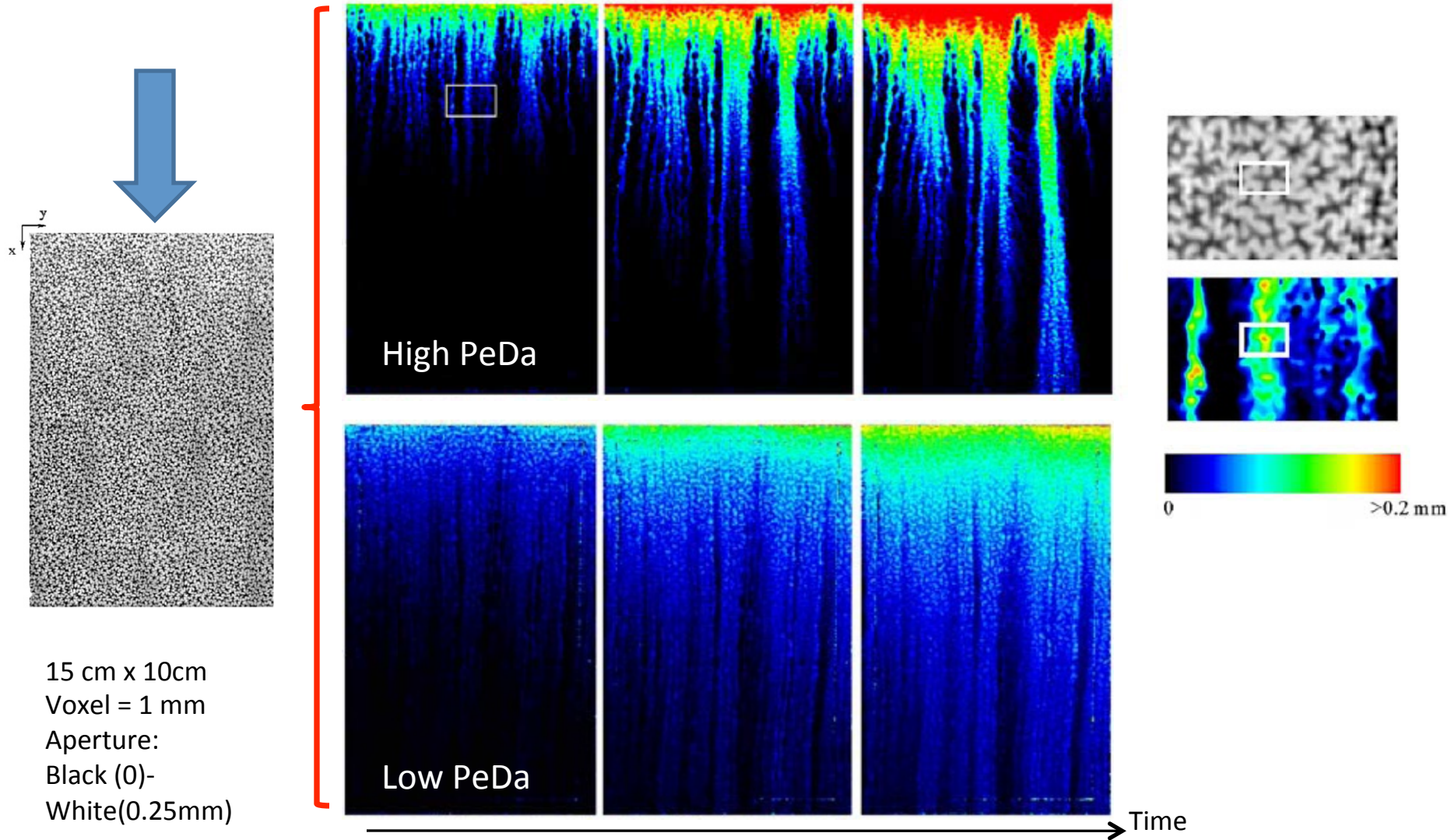
Da << 1 Reaction slow -
Undersaturated along fracture –
Perturbations damped

Da larger << 1 – Reaction faster
Saturated along fracture –
Perturbations enhanced

PeDa No. (Removes <q>)

$$Pe.Da = \frac{\text{Reactive flux}}{\text{Dispersive flux}} = \frac{2k_+L}{D_m}$$

Reactive Hydrodynamics: Role of Damkohler Number (PeDa)



Reactive - Mechanical Controls

Stress-Assisted Dissolution (PS)

$$\frac{dM_{diss}^{PS}}{dt} = \frac{3\pi V_m^2 (\sigma_a - \sigma_c) k_+ \rho_g d_c^2}{4RT}$$

Free-Face Effects (FF)

Dissolution (diss)

$$\frac{dM_{diss}^{FF}}{dt} = k_+ A_{pore} \rho_g V_m \left(1 - \frac{C_{pore}}{C_{eq}} \right)^n$$

Precipitation (prec)

$$\frac{dM_{prec}}{dt} = k_- A_{pore} \rho_g V_m \left(\frac{C_{pore}}{C_{eq}} - 1 \right)^n$$

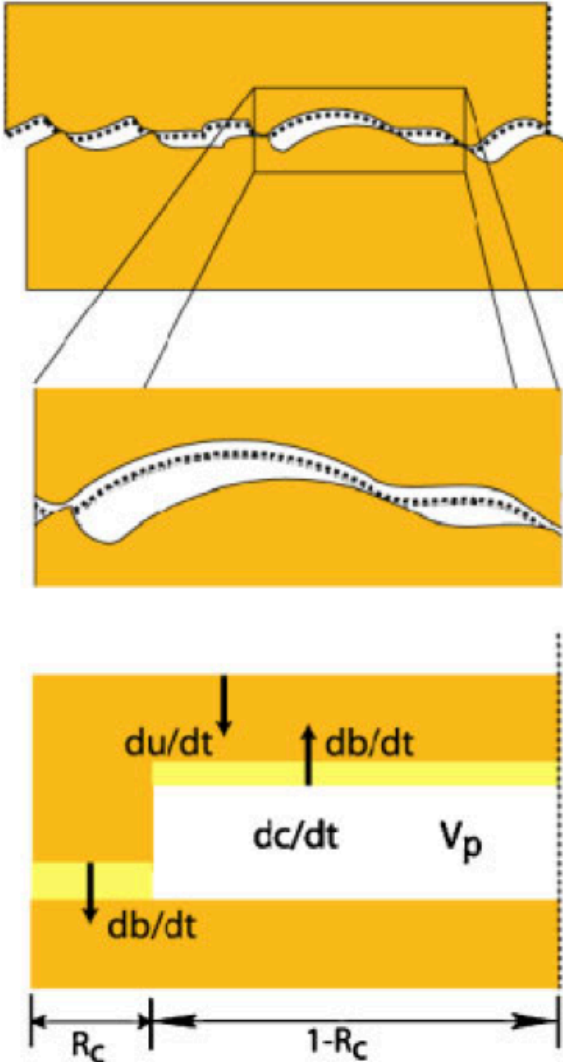
Mass-Flux Ratio

$$\chi = \frac{\text{Stress-Driven Flux}}{\text{Dissolution-Driven Flux}}$$

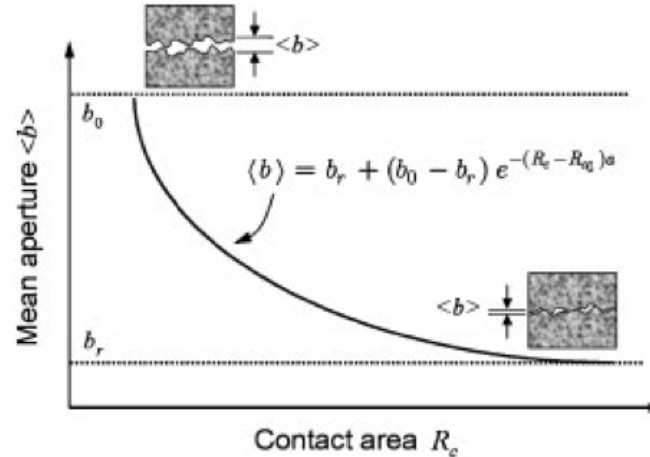
$$\chi = \left(\frac{\dot{M}^{PS}}{\dot{M}^{FF}} \right)_{diss} = \frac{3\pi}{4} \frac{d_c^2}{A_{pore}} \frac{V_m}{RT} \frac{(\sigma_a - \sigma_c)}{(1 - C_{pore}/C_{eq})^n}$$

Modes of Permeability Evolution

Fracture dilation and closure



Fracture closure



Change in aperture
(positive in dilation):

$$\Delta b = \frac{\partial b}{\partial t} \Delta t$$

Link aperture change
to fracture volume
(porosity) change:

$$\frac{\partial b}{\partial t} = -\frac{\partial V_{ps}}{\partial t} \frac{1}{R_c A_f} + \frac{\partial V_{ff}}{\partial t} \frac{1}{(1 - R_c) A_f}$$

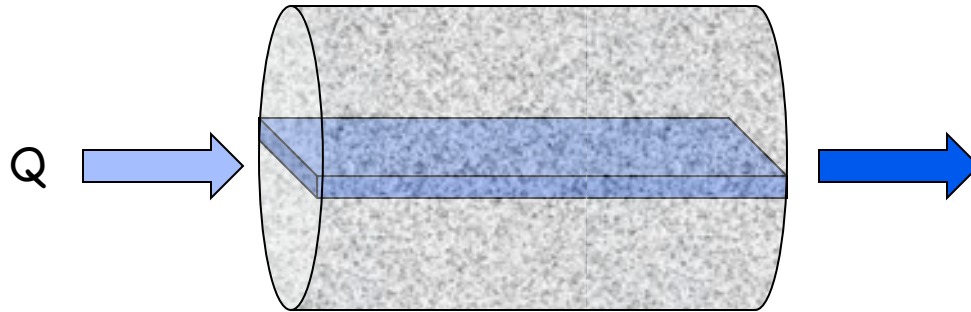
Link fracture volume
(porosity) change to fluid
concentration change:

$$\frac{\partial V_i}{\partial t} = \begin{cases} -\frac{\partial c_{ps}}{\partial t} \frac{V_p}{\rho} \\ + \frac{\partial c_{ff}}{\partial t} \frac{V_p}{\rho} \end{cases}$$

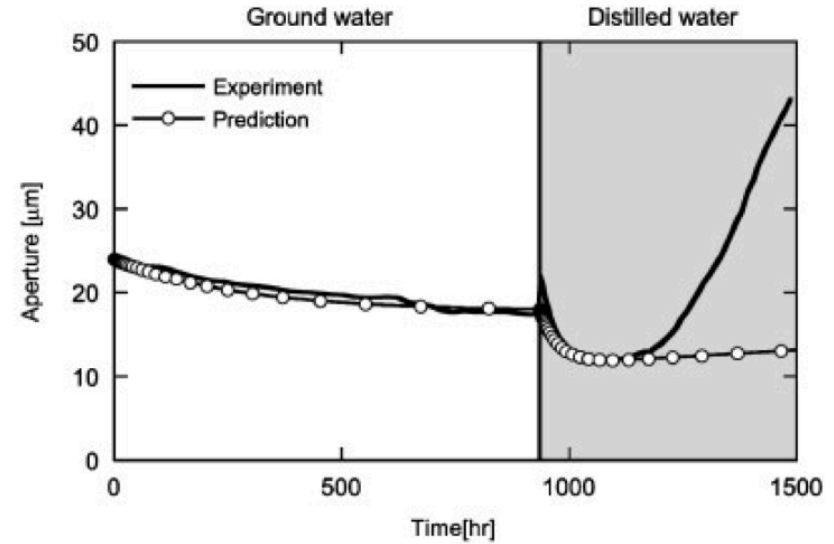
[Elsworth and Yasuhara, IJNAMG, 2009]

Modes of Lumped Parameter Permeability Evolution

Flow geometry

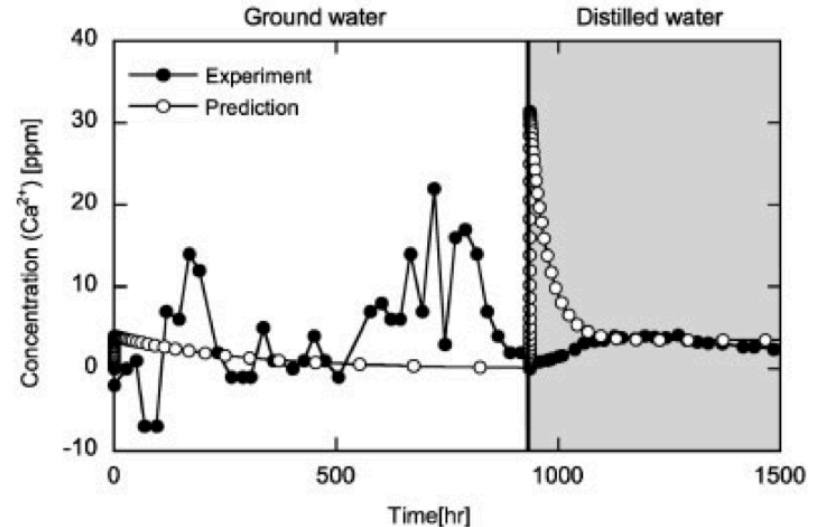


Isothermal response



Lumped mass balance equation

$$\frac{\partial c}{\partial t} - \underbrace{Ae^{-Ft}}_{-\partial c_{ps}/\partial t} + \underbrace{B(c - c_{eq})}_{-\partial c_{ff}/\partial t} + \underbrace{Q(c - c_{in})}_{-\partial c_Q/\partial t} = 0$$

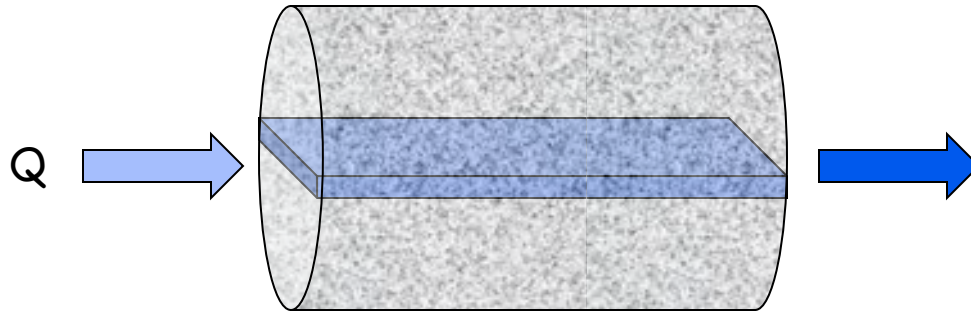


[Elsworth and Yasuhara, IJNAMG, 2009]

Modes of Lumped Parameter Permeability Evolution

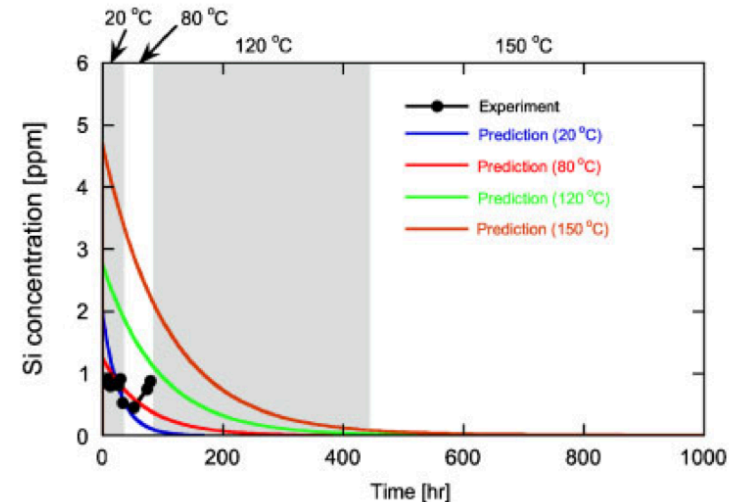
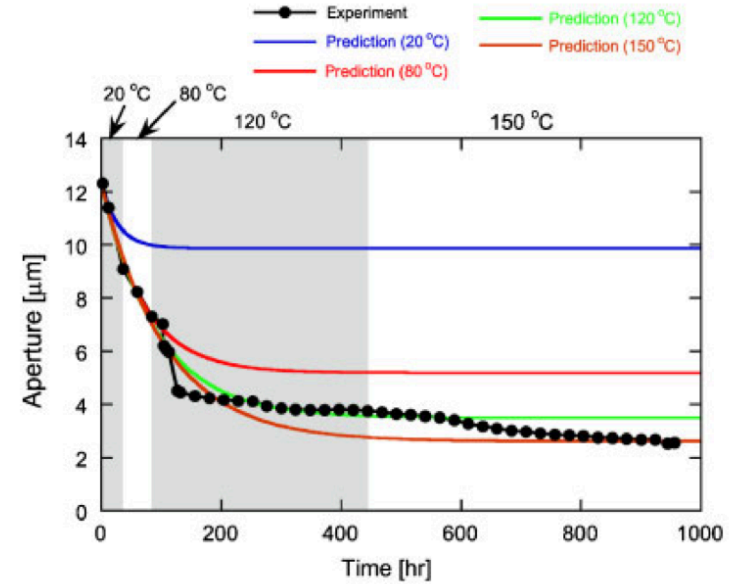
Non-isothermal response

Flow geometry



Lumped mass balance equation

$$\frac{\partial c}{\partial t} \underbrace{- A e^{-Ft}}_{-\partial c_{ps}/\partial t} + \underbrace{B(c - c_{eq})}_{-\partial c_{ff}/\partial t} + \underbrace{Q(c - c_{in})}_{-\partial c_Q/\partial t} = 0$$



[Elsworth and Yasuhara, IJNAMG, 2009]

Component Model

Interface Dissolution

$$\left. \begin{aligned} \frac{dM_{diss}}{dt} &\approx \dot{\epsilon}_{diss} \frac{d}{\omega} \rho_g \left(\frac{\pi}{4} d_c^2 \omega \right) \\ &= \frac{3\pi V_m^2 \sigma_{eff} k_+ \rho_g d_c^2}{4RT} \\ \frac{dM_{diss}}{dt} &= \frac{3\pi V_m^2 (\sigma_a - \sigma_c) k_+ \rho_g d_c^2}{4RT} \end{aligned} \right\} \sigma_c = \frac{E_m \left(1 - T/T_m \right)}{4V_m}$$

Interface Diffusion

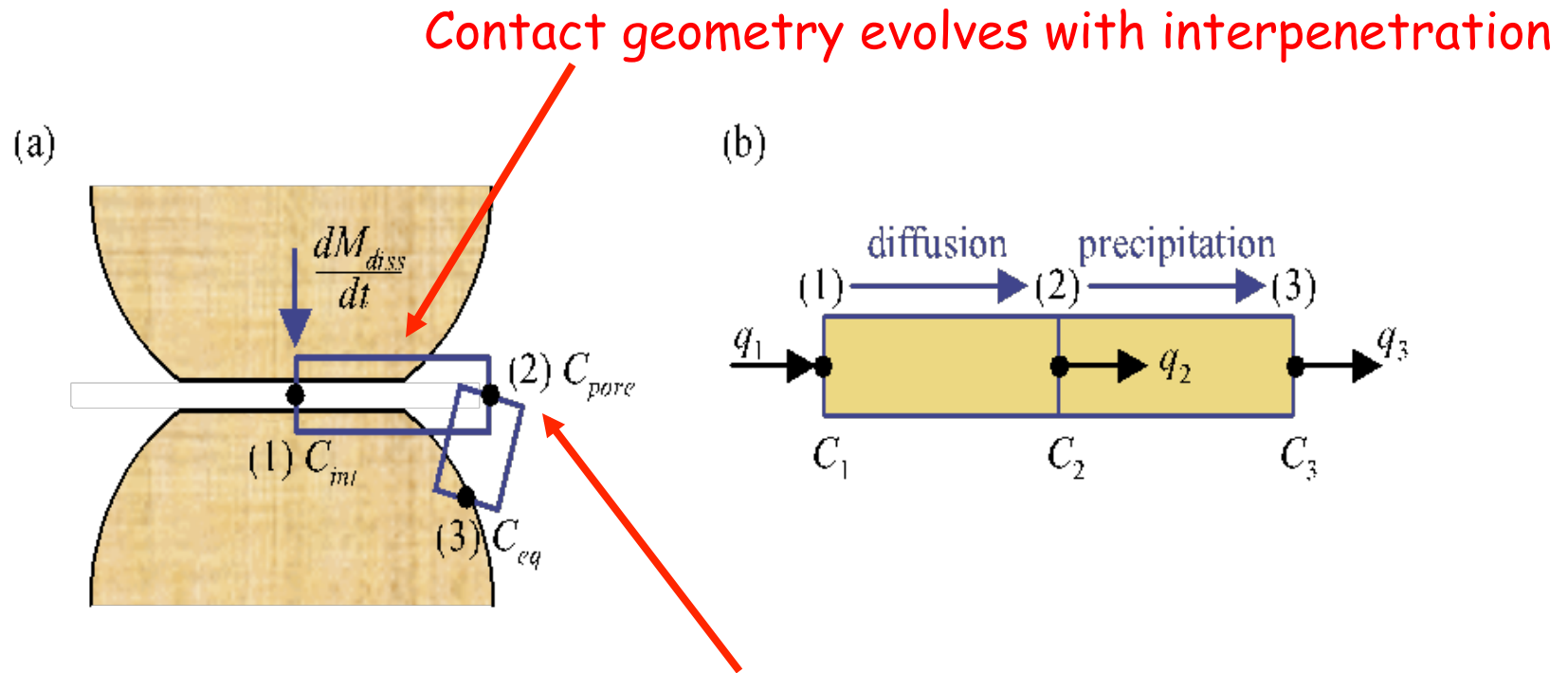
$$J = -D_b \frac{dC}{dx} \qquad J_m = -2\pi r \omega D_b \left(\frac{dC}{dr} \right)_{r=d_c}$$

$$J_m = \frac{dM_{diff}}{dt} = \frac{2\pi \omega D_b}{\ln(d_c/2a)} (C_{int} - C_{pore})$$

Pore Precipitation

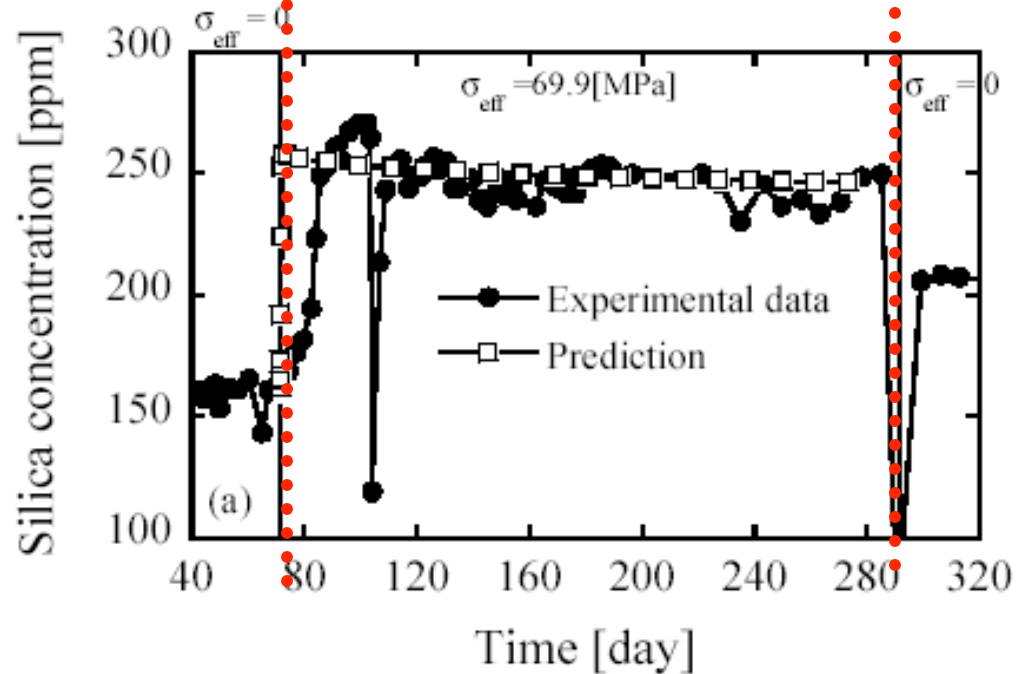
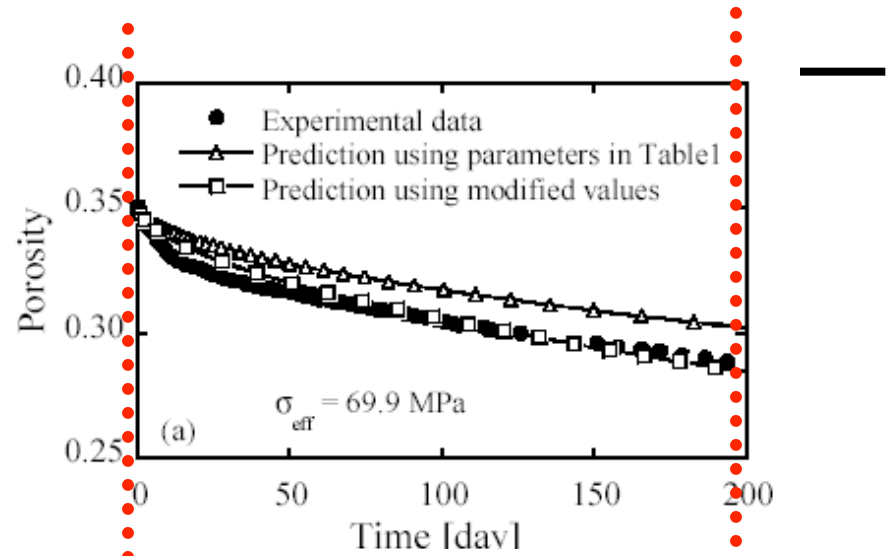
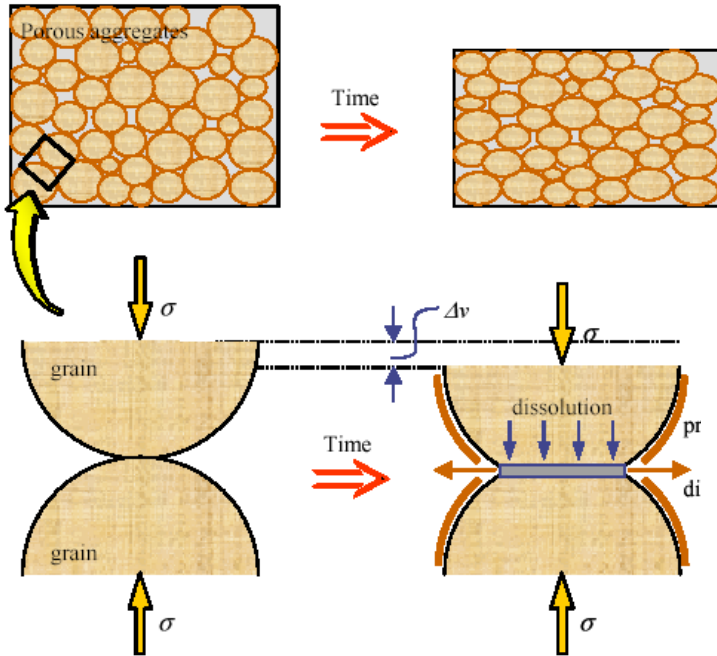
$$\frac{dM_{prec}}{dt} = V_{pore} \frac{A}{M} k_- (C_{pore} - C_{eq})$$

Mass Transfer Modes - Essential Components



Pore concentration allows mass balance for arbitrarily open or closed systems

Matching Compaction Data



[Experimental data from Elias and Hajash, 1992]

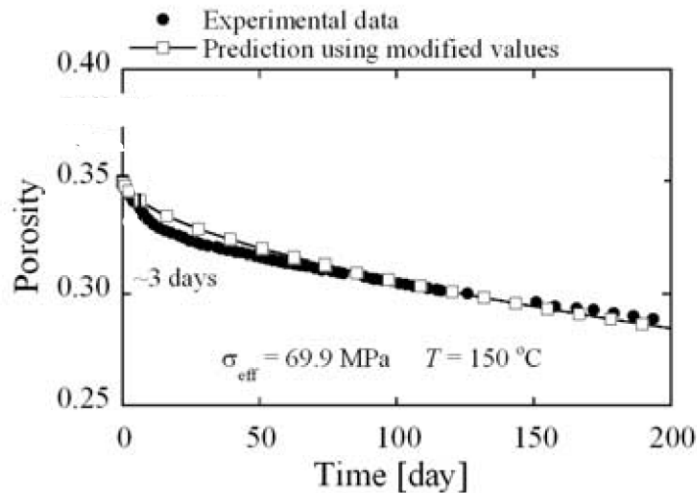
System Evolution at 35-70 MPa and 150°C

Observation

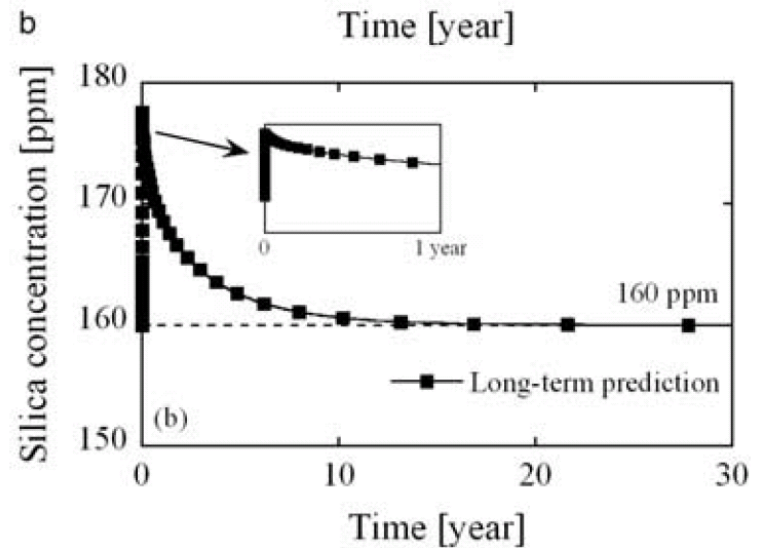
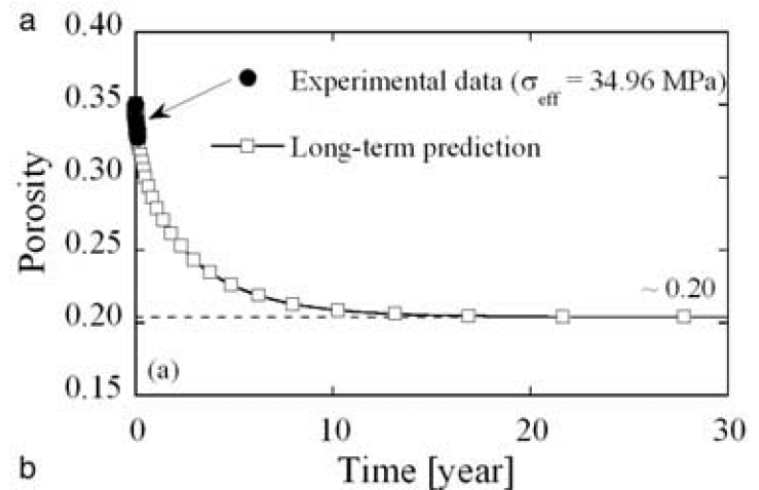
Extension



70 MPa and 150°C



35 MPa and 150°C

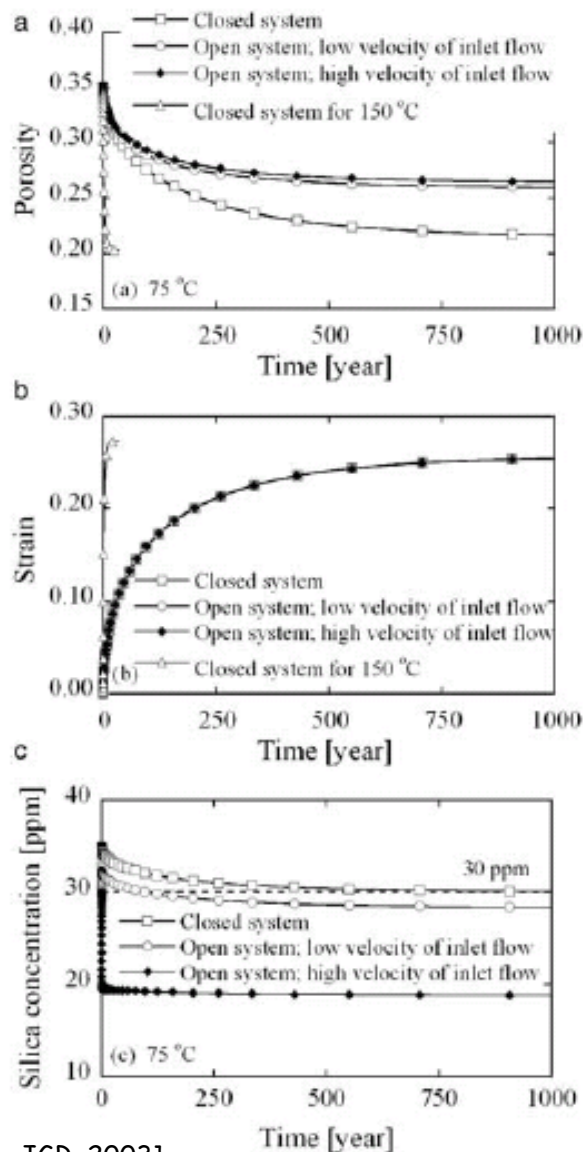


[Experimental data from Elias and Hajash, 1992]

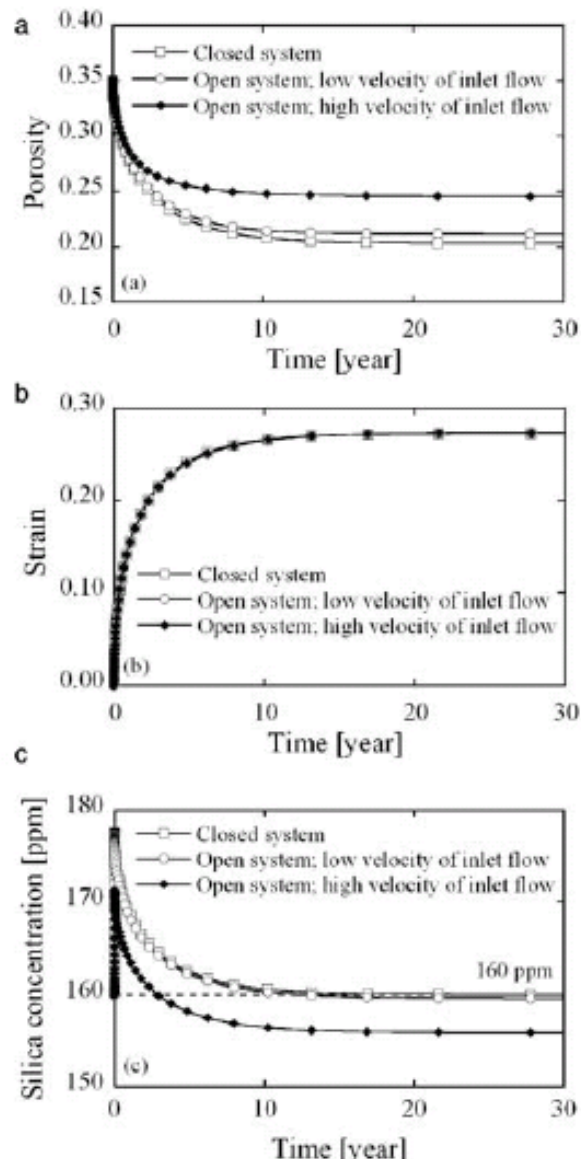
[Yasuhara et al., JGR, 2003]

Timescales of Evolution of Granular Systems at 35 MPa and 75-150°C

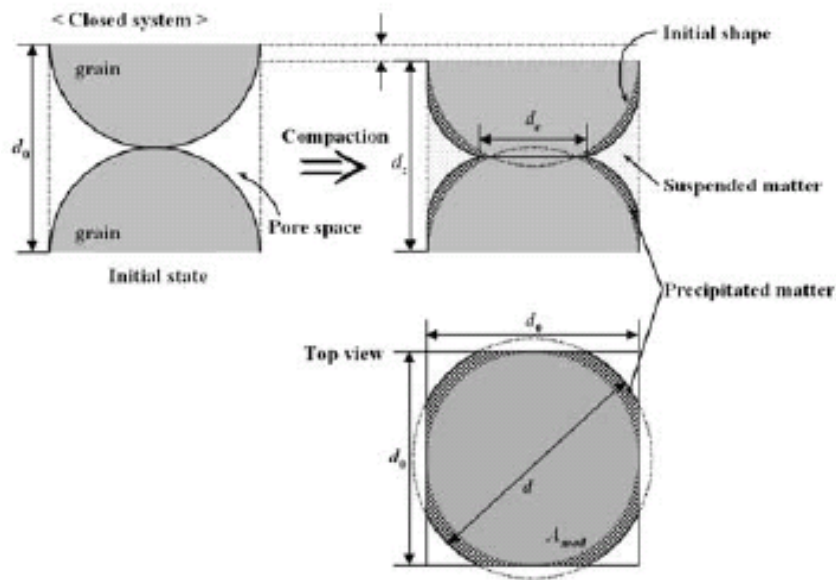
75°C



150°C



Permeability Evolution in Granular Systems at 35 MPa and 75-300°C

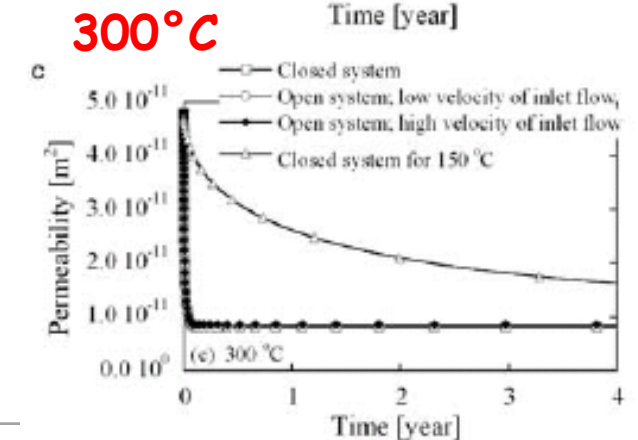
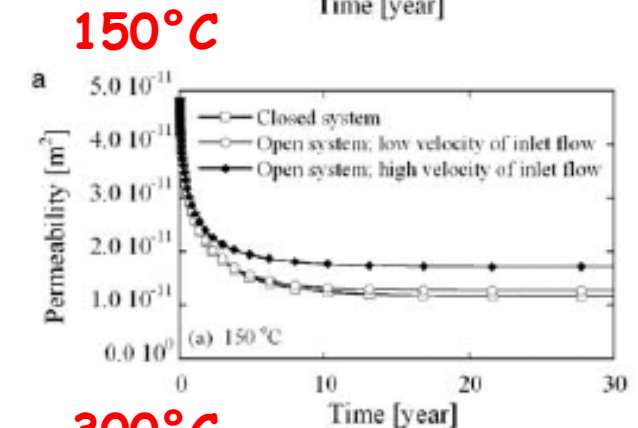
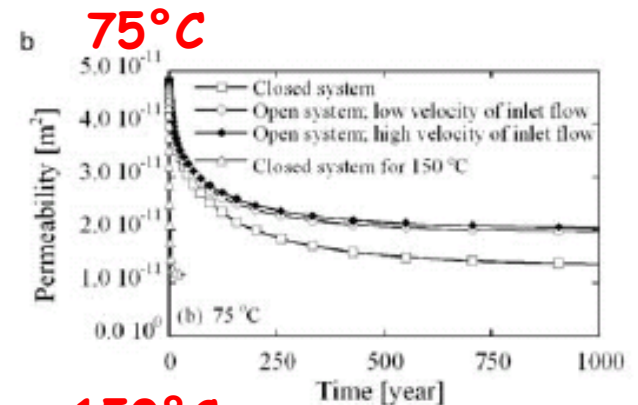


Capillary Model: $k = \frac{n\delta^2}{96}$

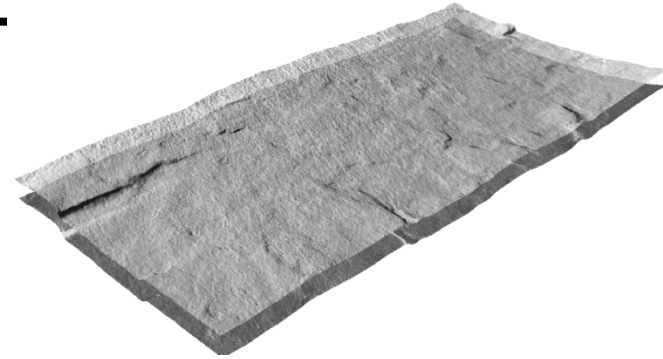
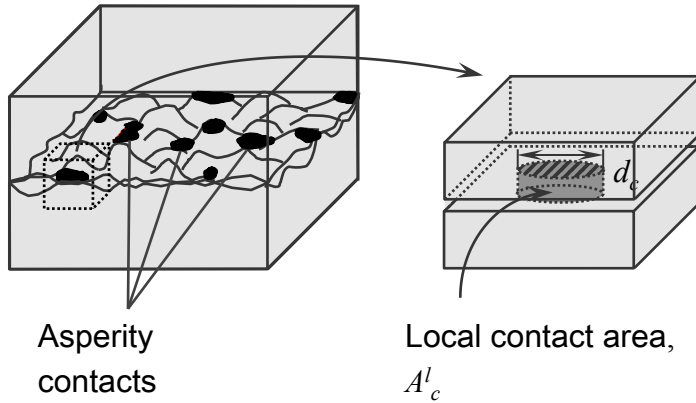
Pore Evolution: $V_p = (\pi/4)\delta^2 d_0$

Linked Permeability: $k \sim \frac{nV_p}{24\pi d_0}$

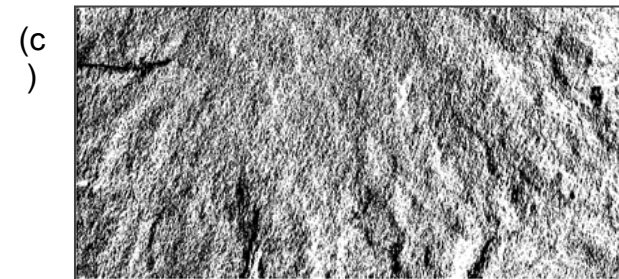
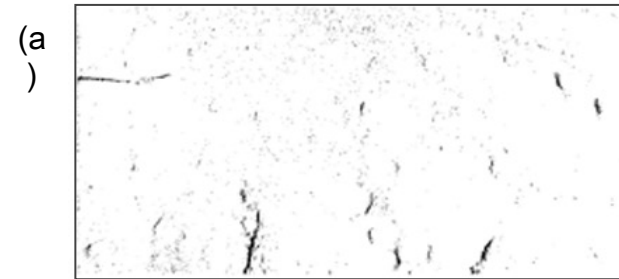
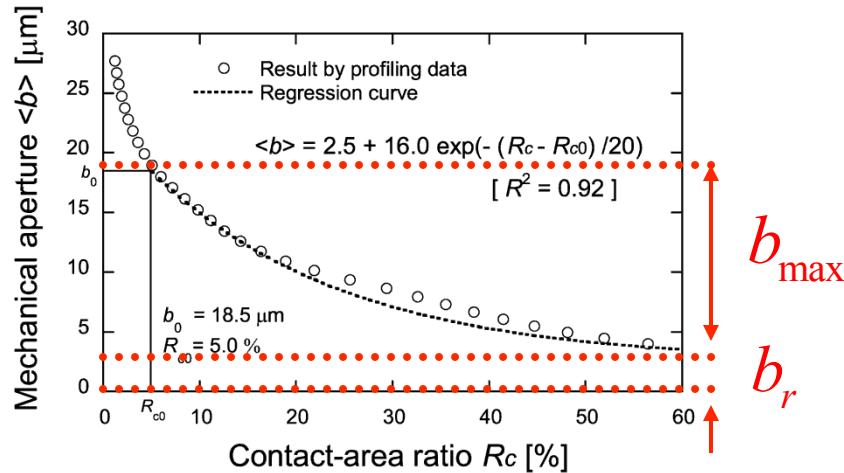
[Yasuhara et al., JGR, 2003]



Constraint on Fracture Apertures and Fluid Concentrations

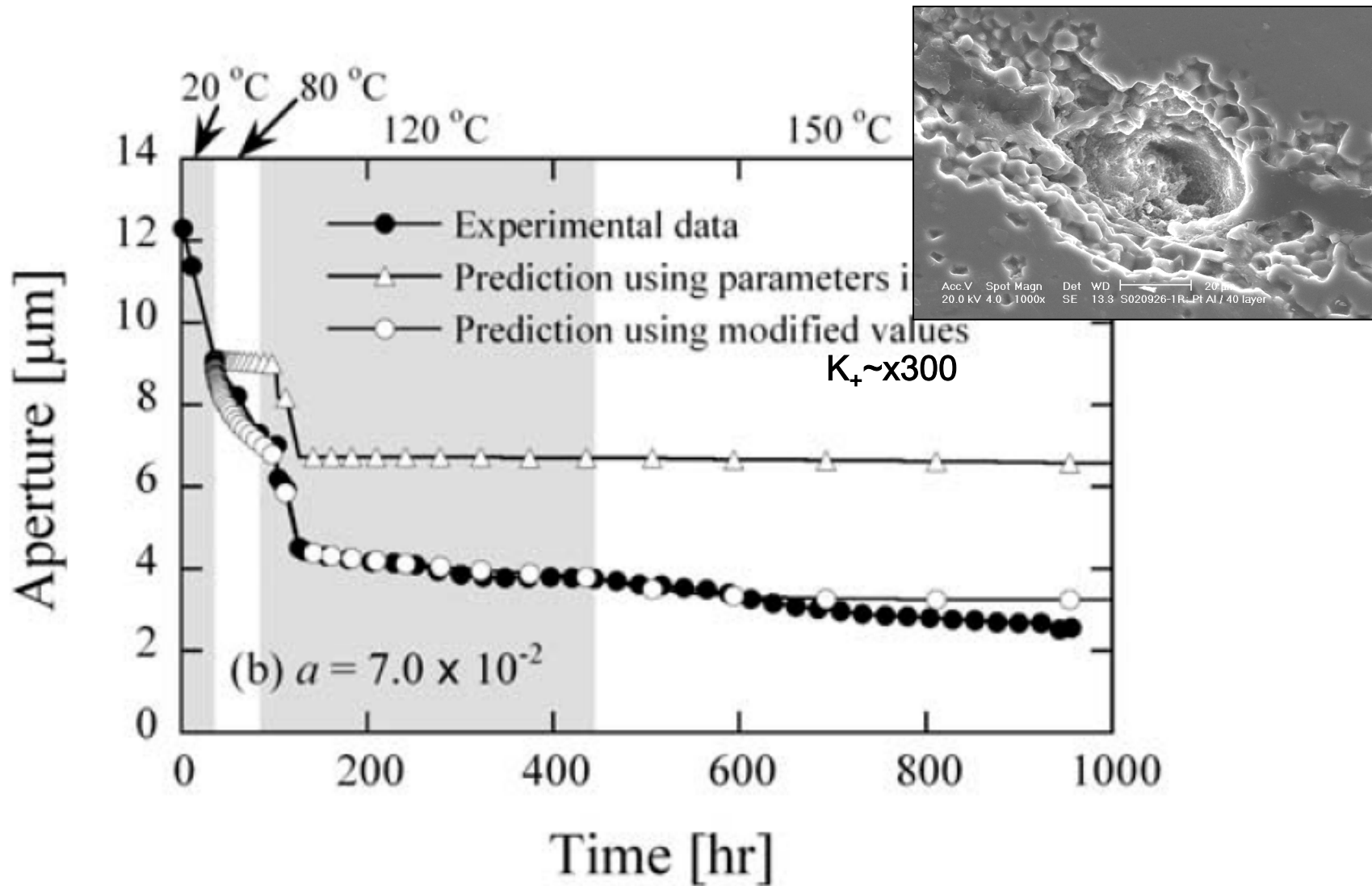


$$\langle b \rangle = b_r + b_{\max} \text{Exp}[(R_c - R_{c0}) / a]$$



Increasing fracture closure

Modeling Results - Novaculite

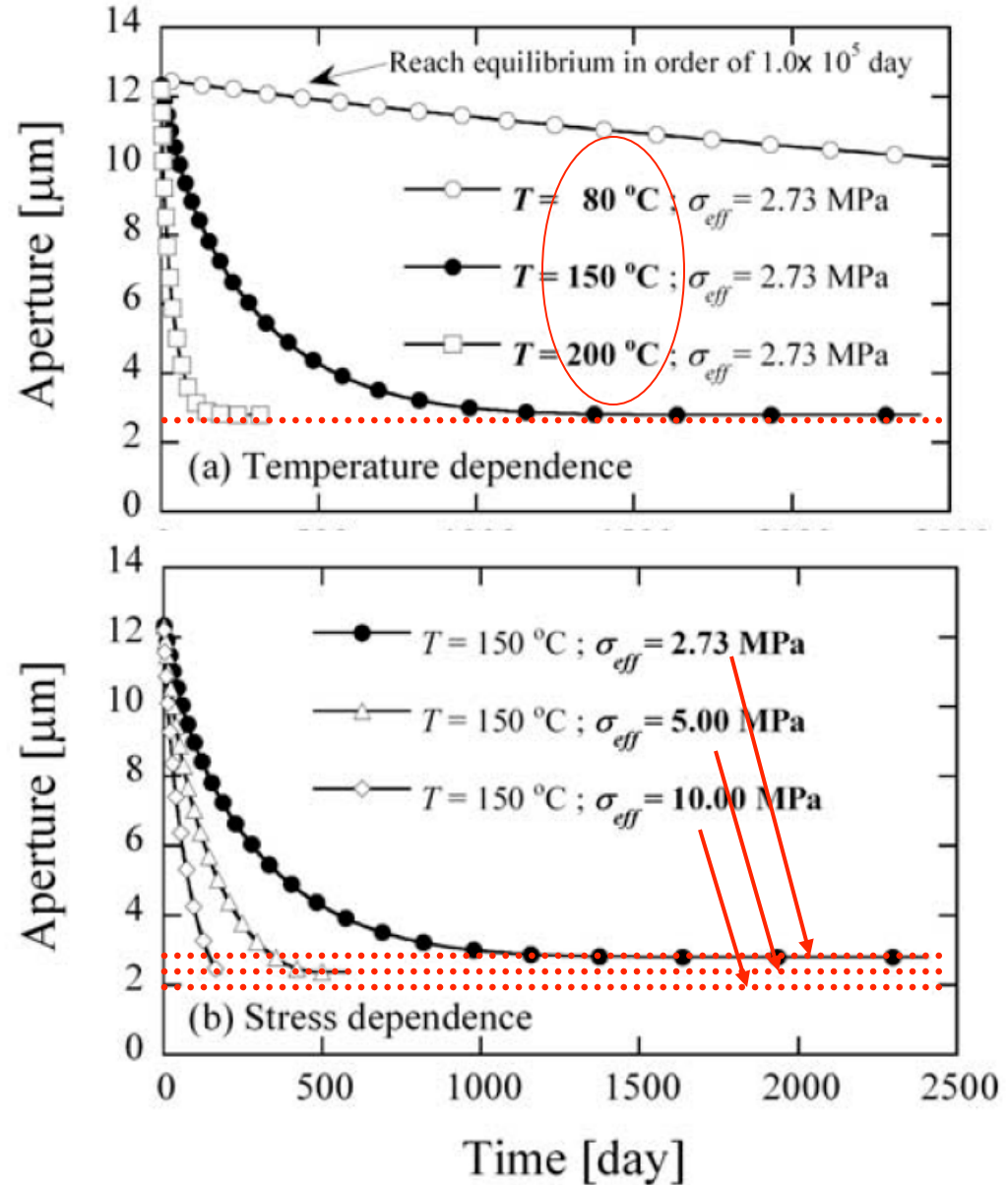


[Yasuhara et al., JGR, 2004]

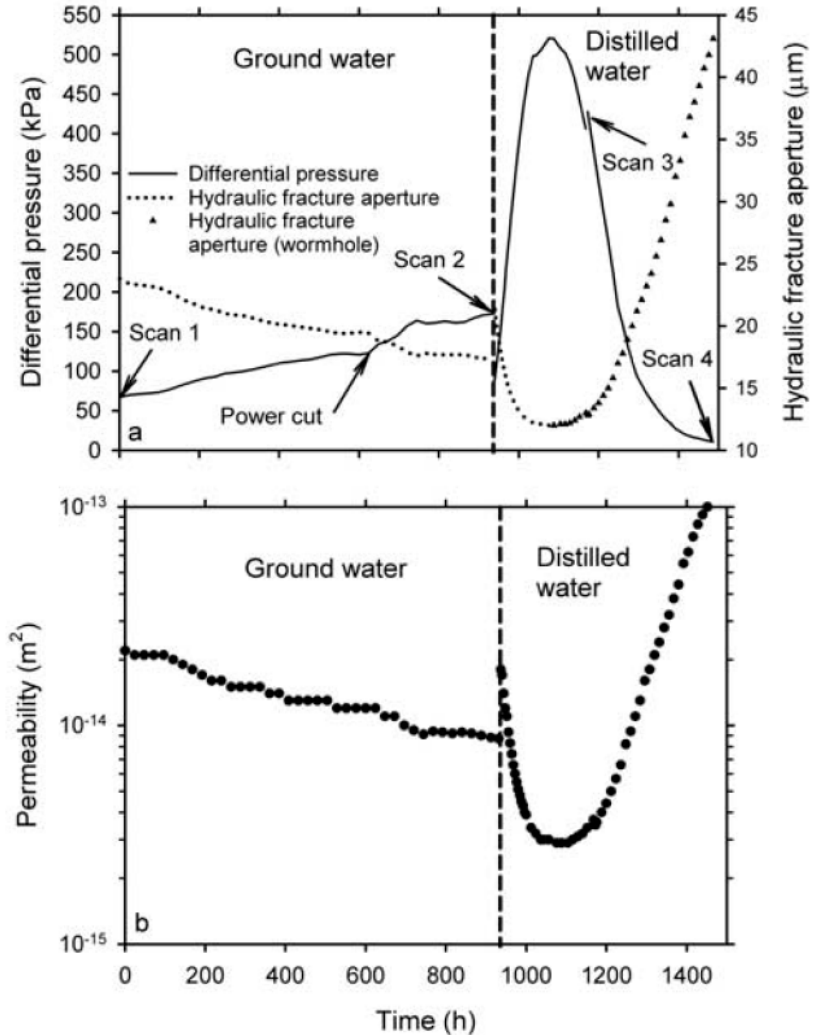
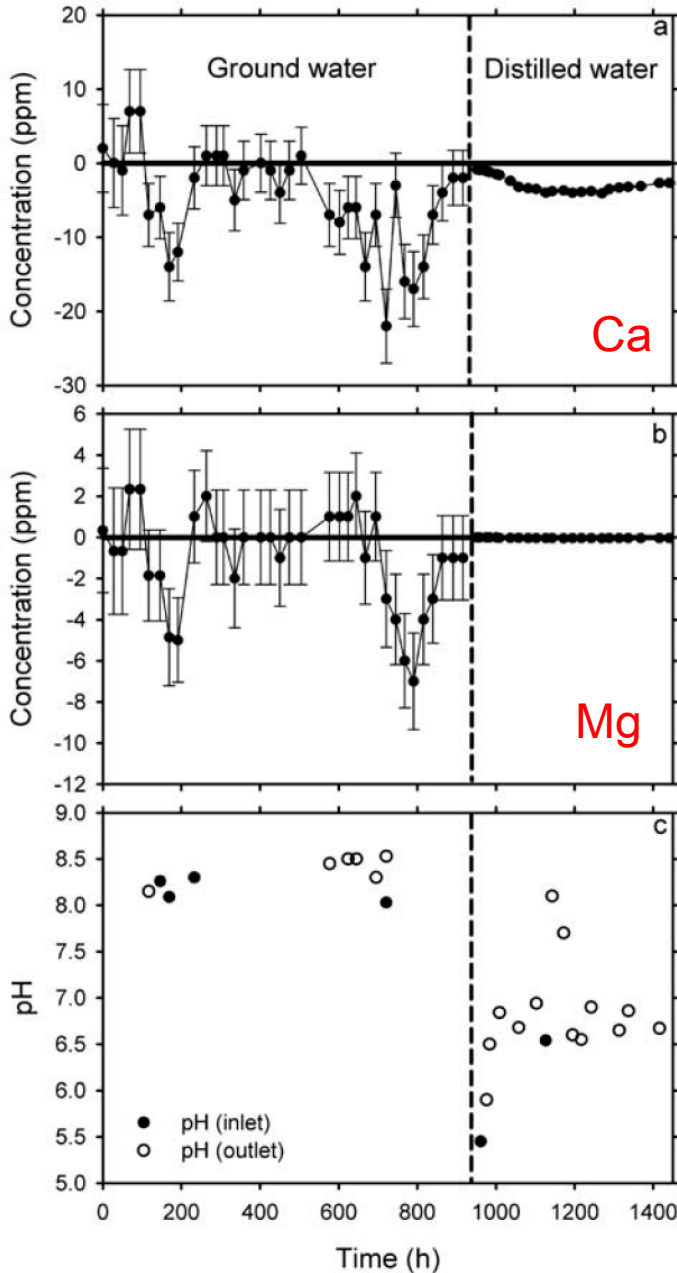
Projected Response of Fracture

Define projected behavior for varied **temperatures**

...and **mean stress** magnitudes



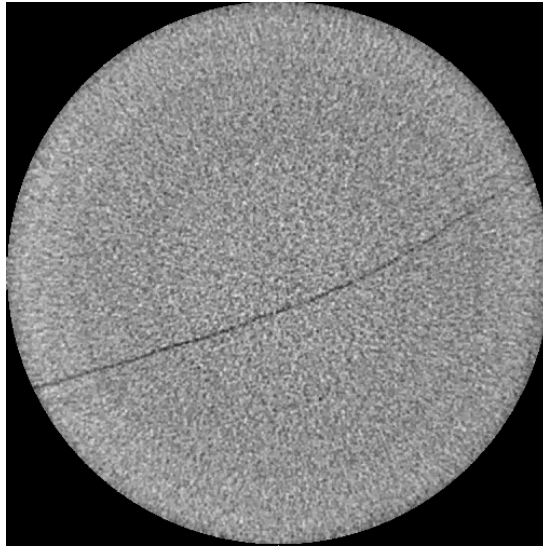
Fractured Limestone - Features of Response



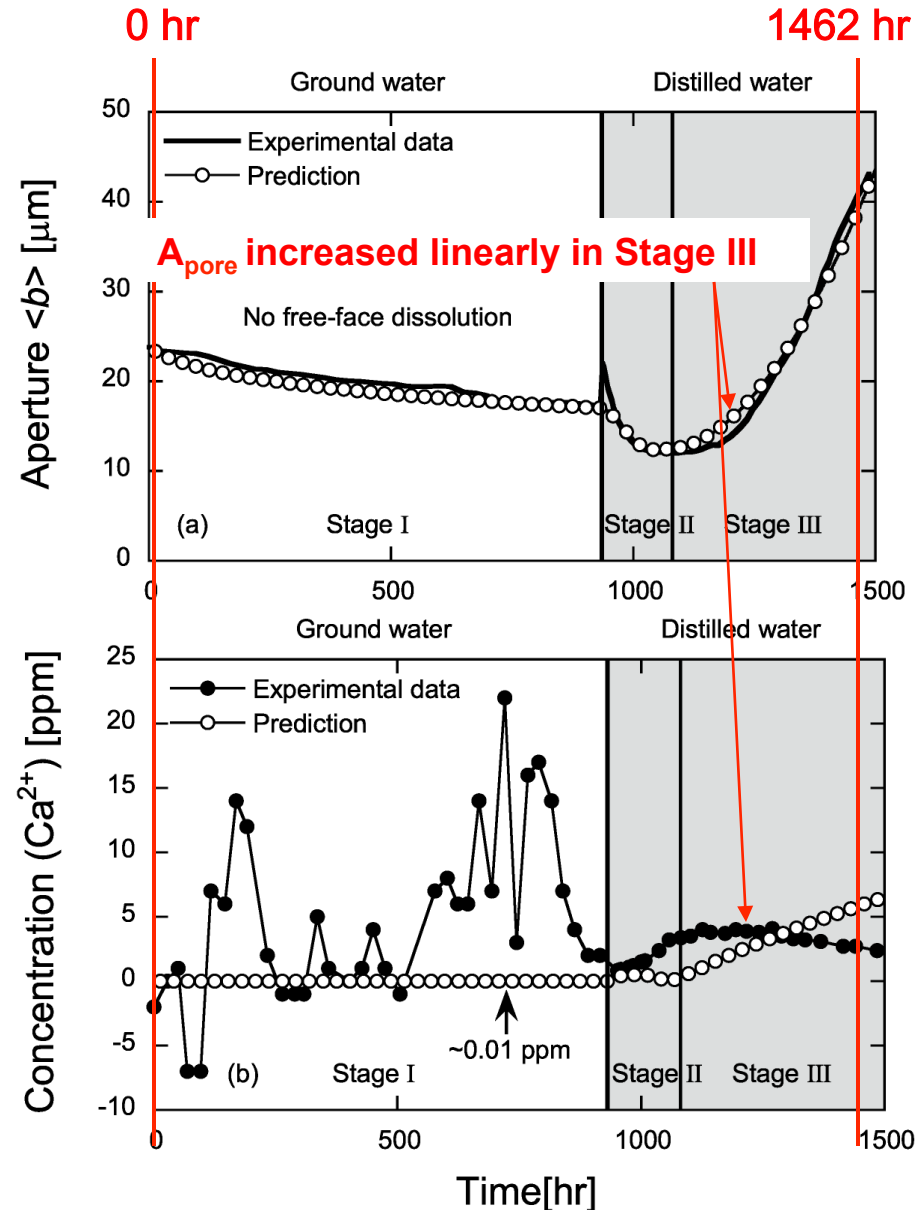
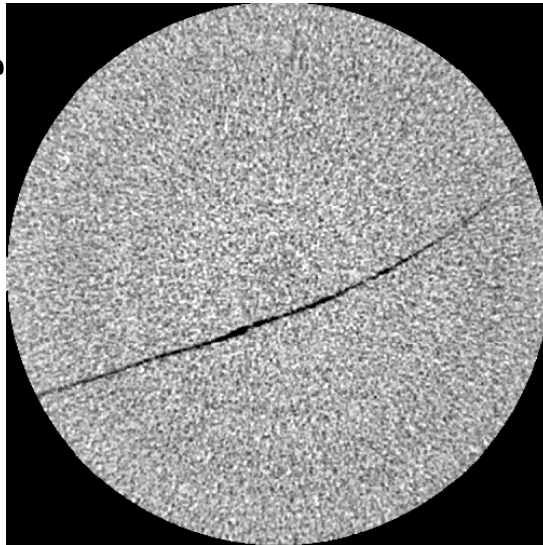
[Polak et al., WRR, 2004]

Fractured Limestone - Features of Response

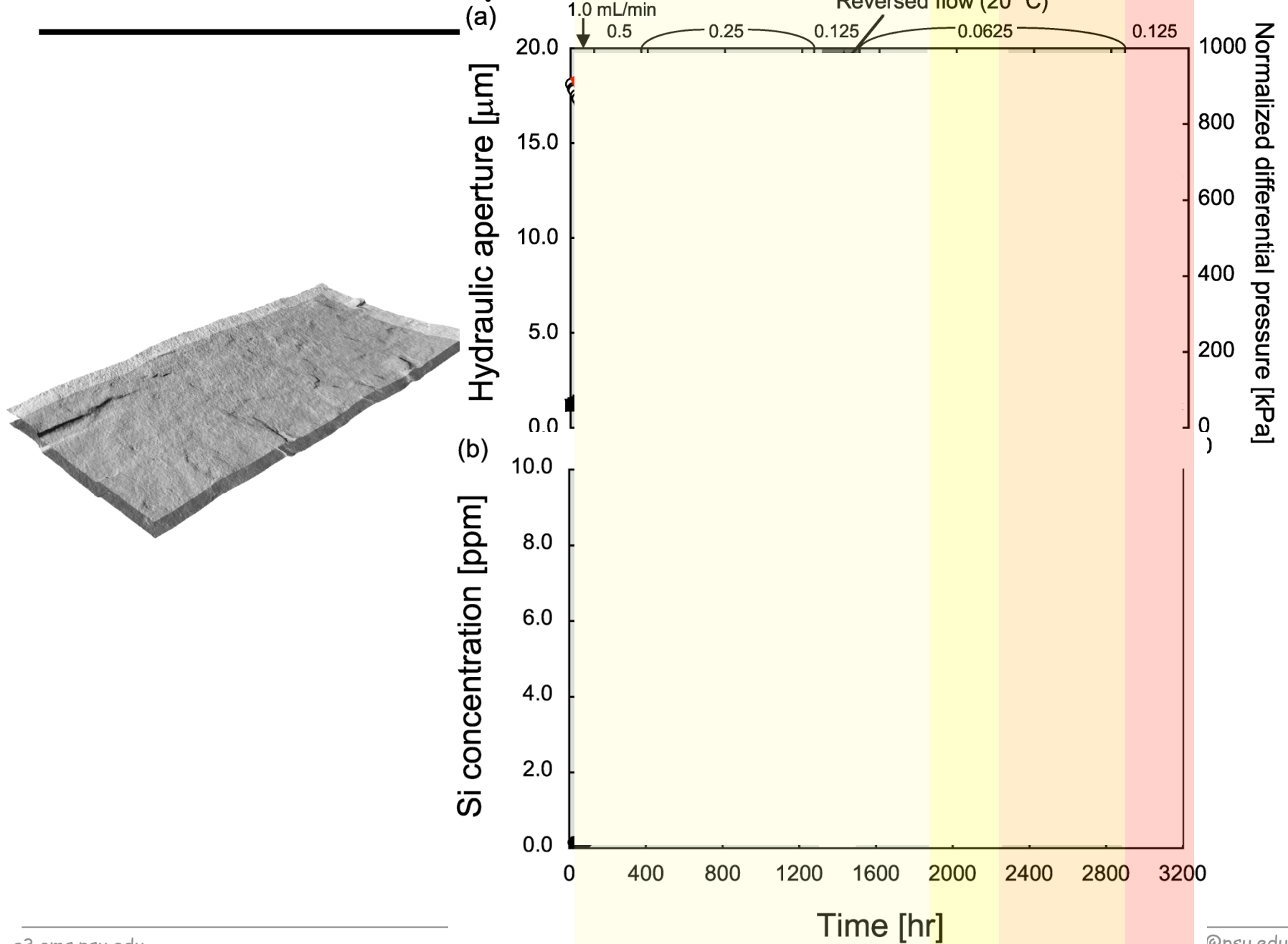
0 hr



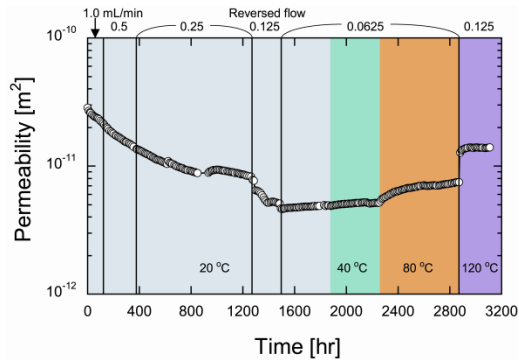
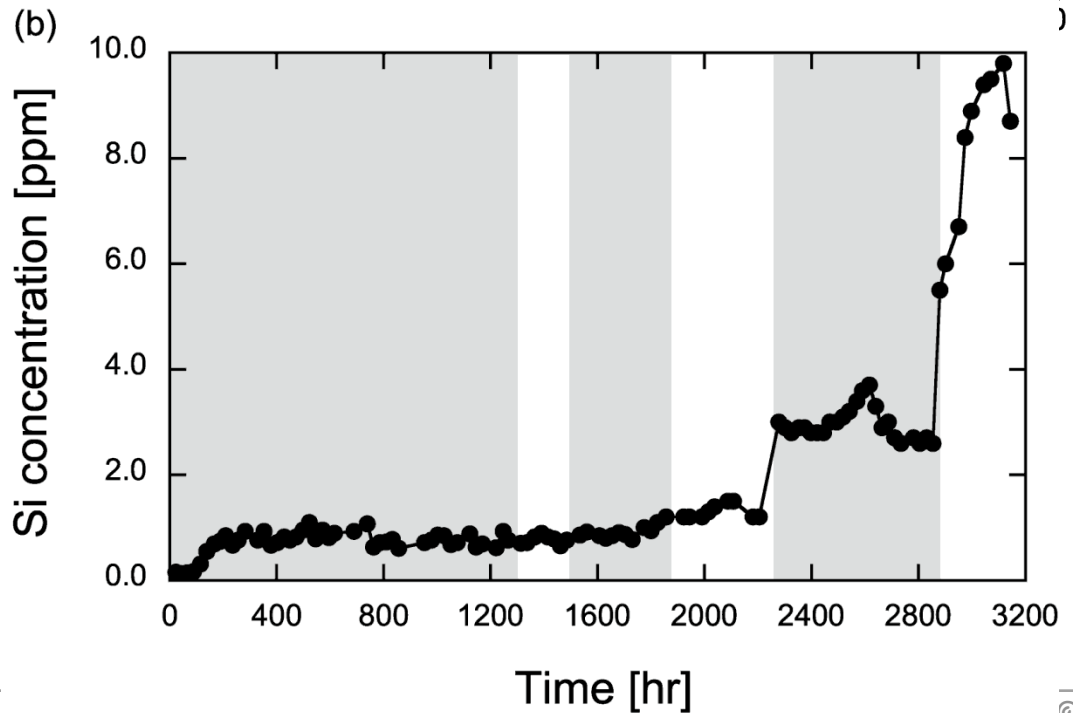
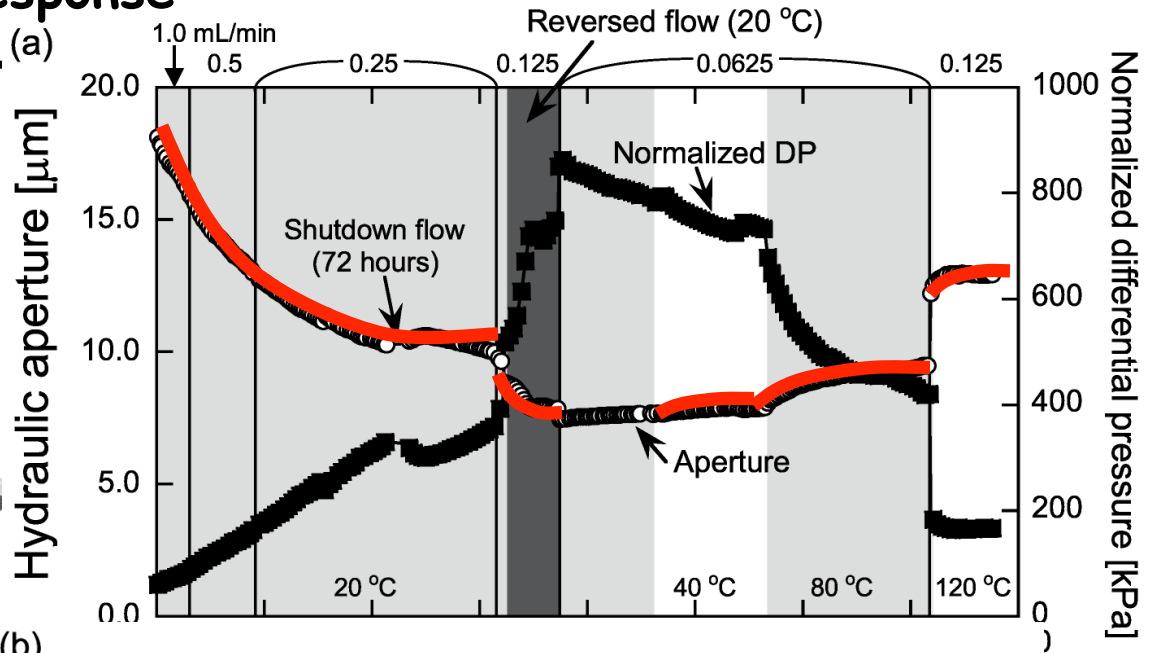
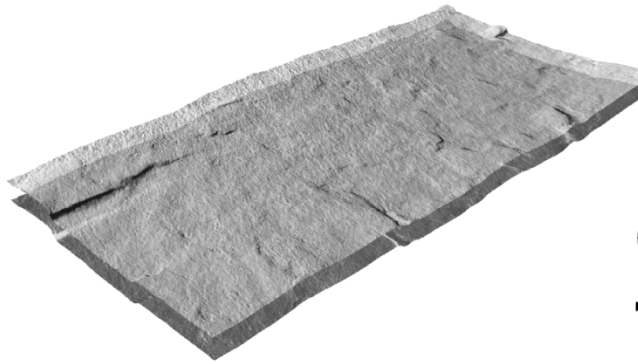
1462 hr



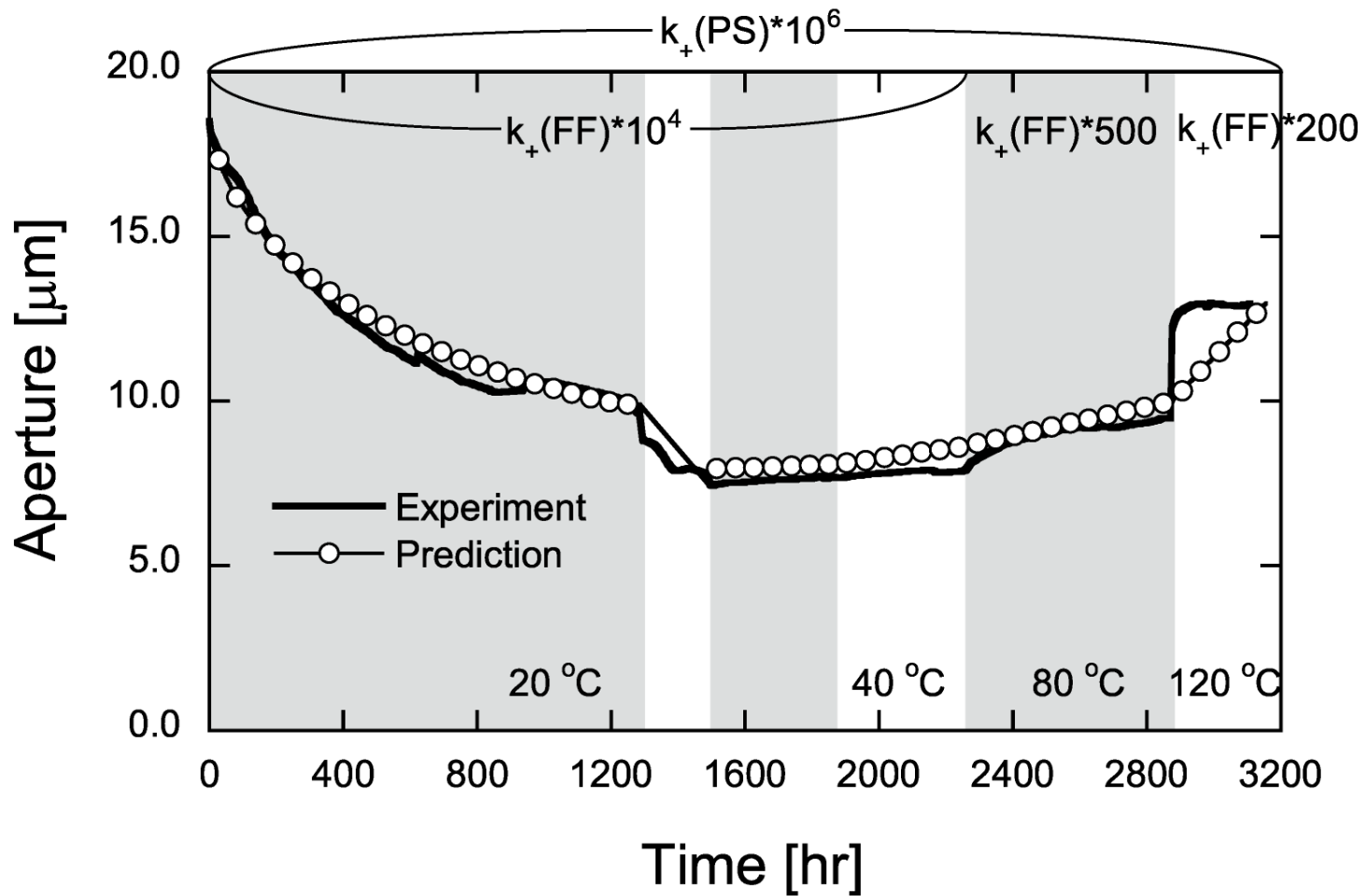
Novaculite - 20 week response



Novaculite - 20 week response

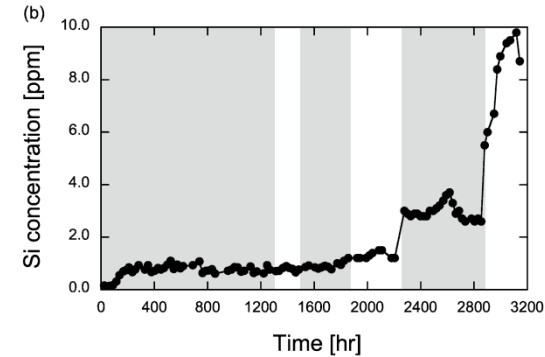
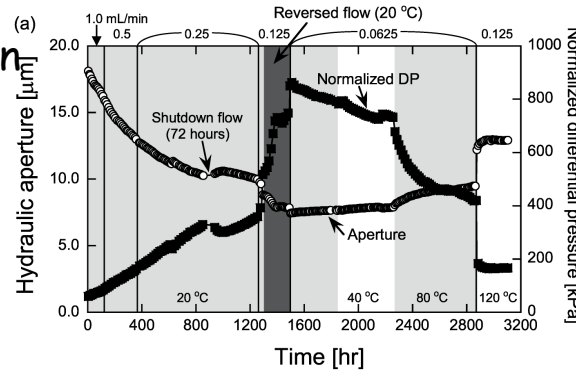
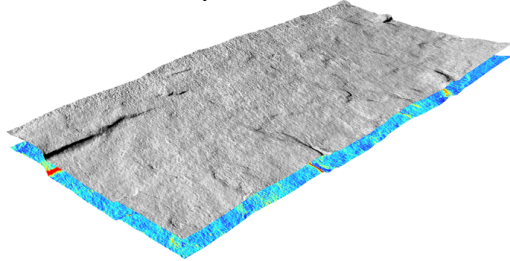


....and Lumped Parameter Prognostic Model for Novaculite ...



Distributed Parameter Models - Applied to Novaculite ...

1. Set initial aperture distribution



2. Apply I.C. and B.C.

→ Obtain velocity distr. in a fracture by solving Reynolds' equation $\nabla \left(\frac{b^3}{12\mu} \nabla p \right) = 0$

3. Dissolution at contact area and free-face (reaction)

→ Obtain concentration distribution + Modify aperture distribution due to dissolution

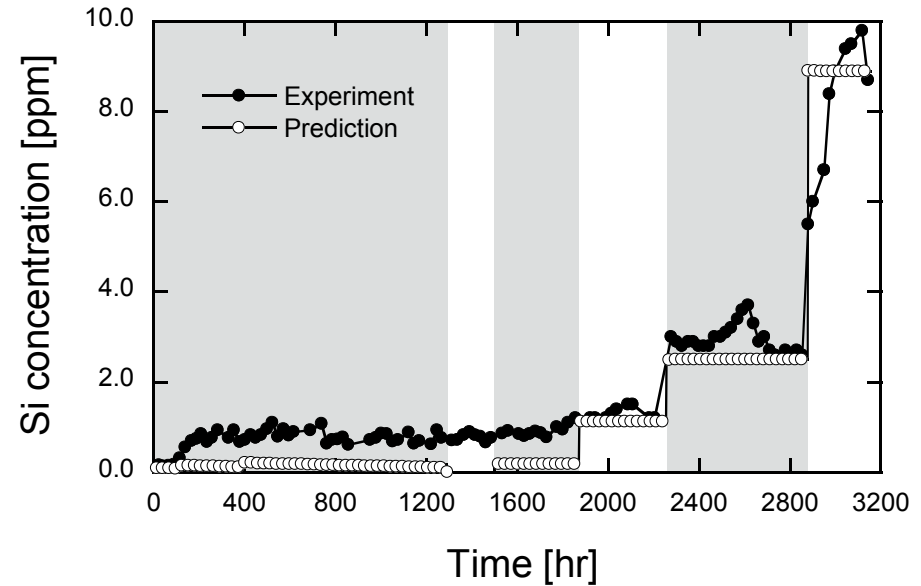
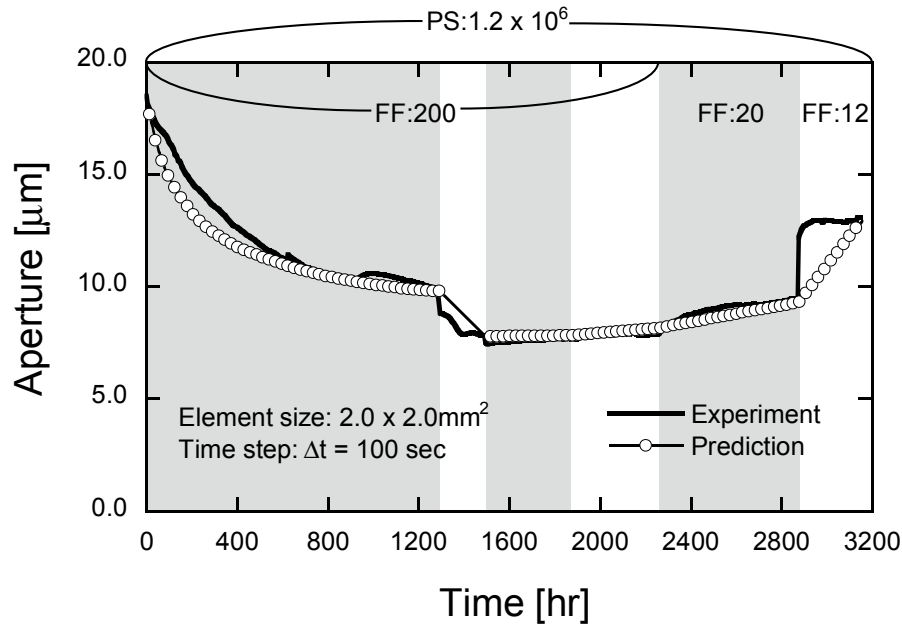
$$\frac{dM^{PS}}{dt} = \frac{3\pi V_m^2 \rho_g k_+ (\sigma_a - \sigma_c) A_e}{4RT}; \quad \frac{dM^{FF}}{dt} = 2A_e k_+ \frac{C_{eq} - C_i}{C_{eq}}$$

4. Lagrangian-Eulerian method (Advection-diffusion)

→ Obtain concentration distribution within and out of domain

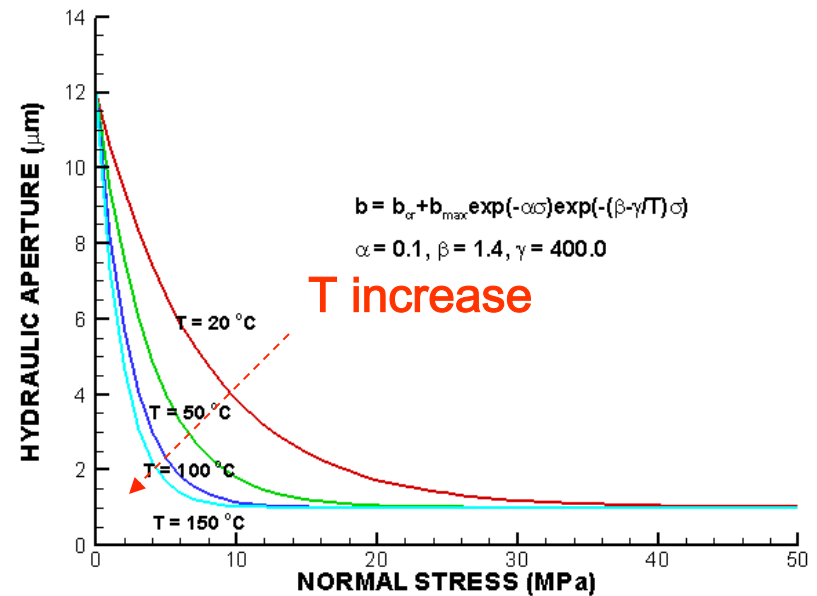
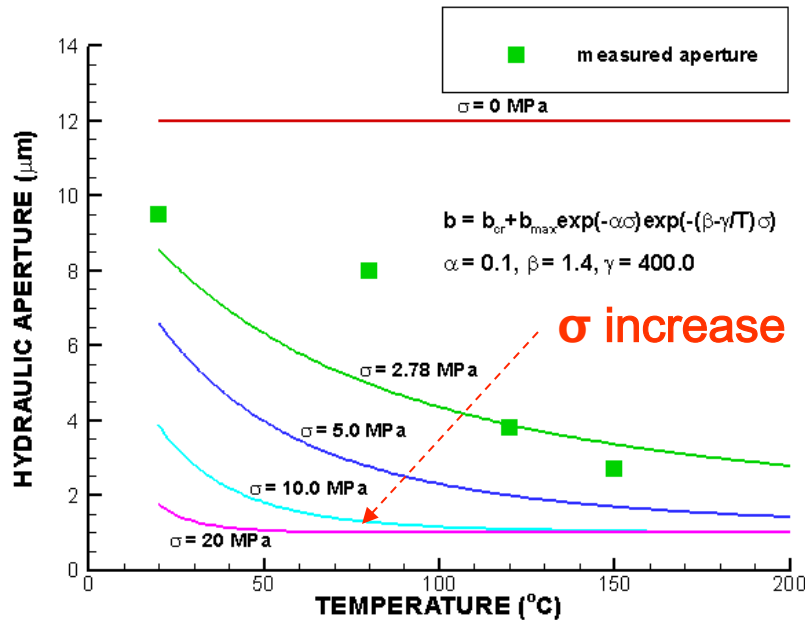
Iteration

Distributed Parameter Model - Results for Novaculite ...



- Numerical model is capable of better replicating experiment – multiplier on k_+ is greatly reduced over lumped parameter case.

TMC-Induced Aperture Change - Stress Control



$$b = b_{cr} + \underbrace{\{b_{mc} + b_{max} \exp(-\alpha\sigma')\}}_{M \& TM \text{ induced change}} \underbrace{\exp\left\{-\left(\beta - \frac{\gamma}{T}\right)\sigma'\right\}}_{MC \& TC \text{ induced change}}$$

M & TM induced change

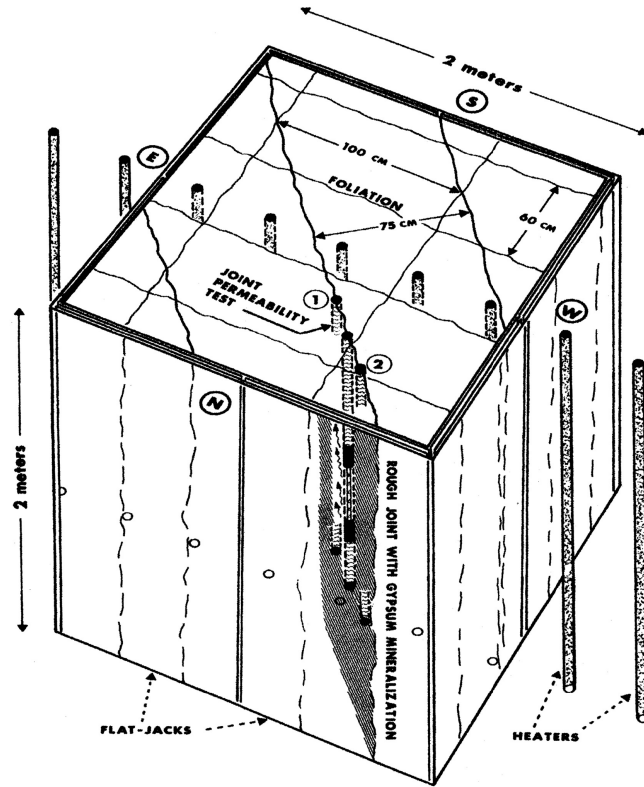
MC & TC induced change

Application to novaculite (laboratory) data under stress control

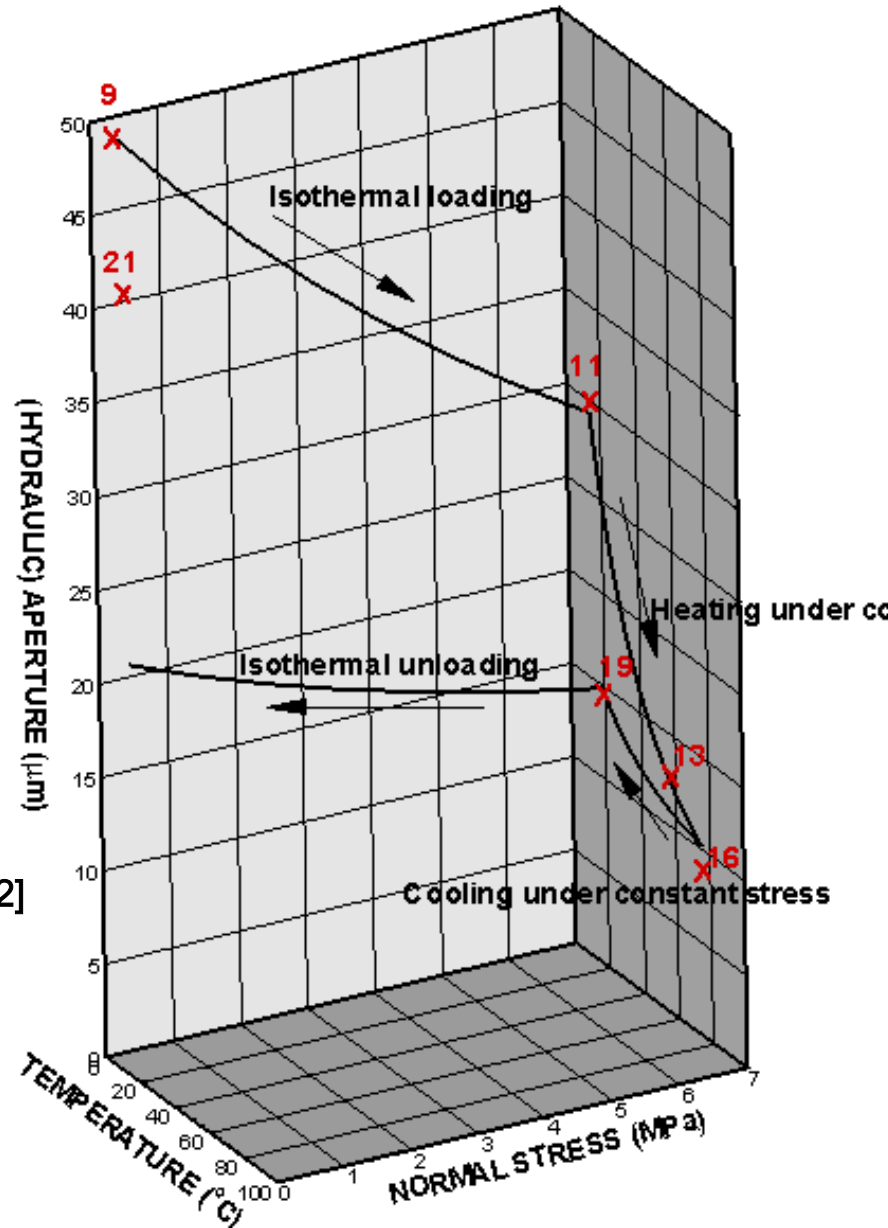
Sparse data but available data conform to the expected response based on micro-mechanical arguments

Experimental data needed at a variety of scales

TMC-Induced Aperture Change - Stress Control



[Handin et al., 1982]

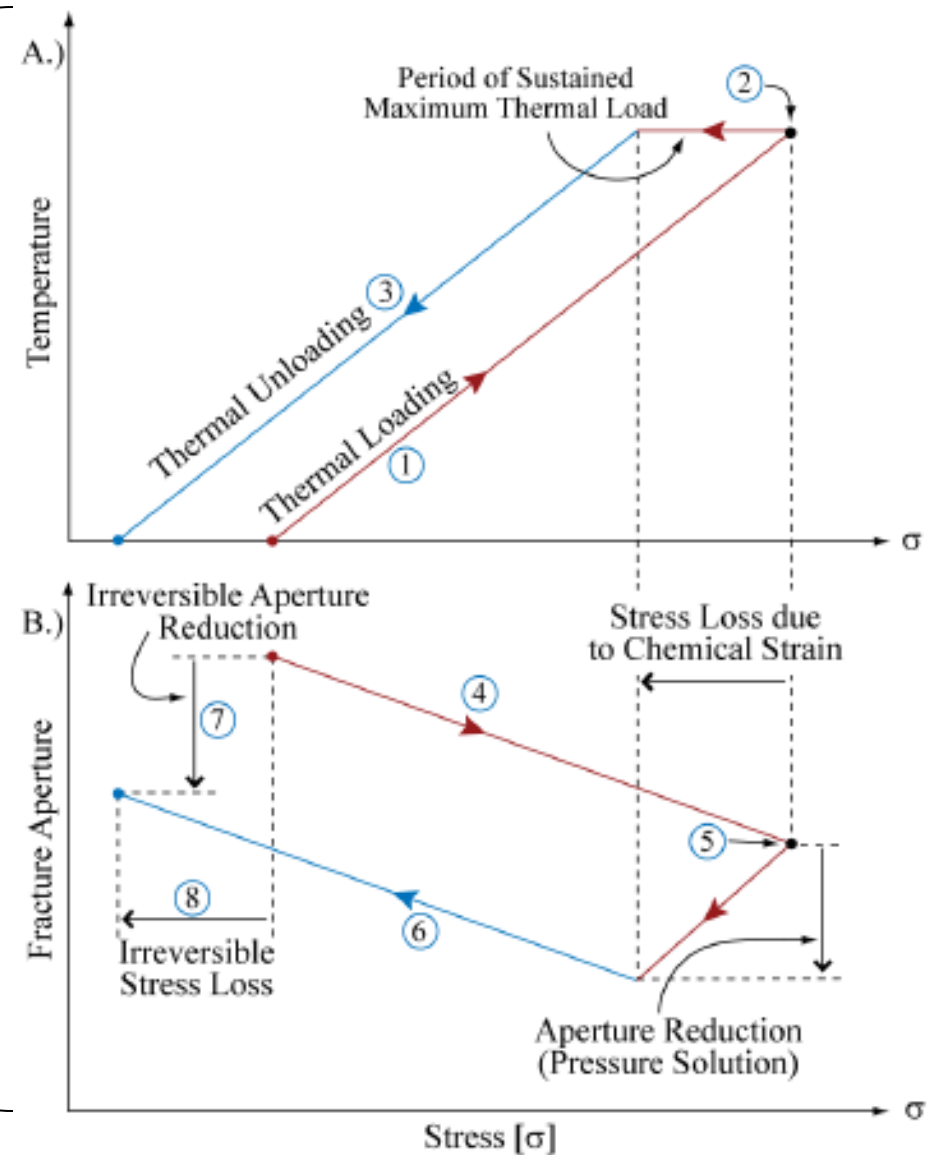
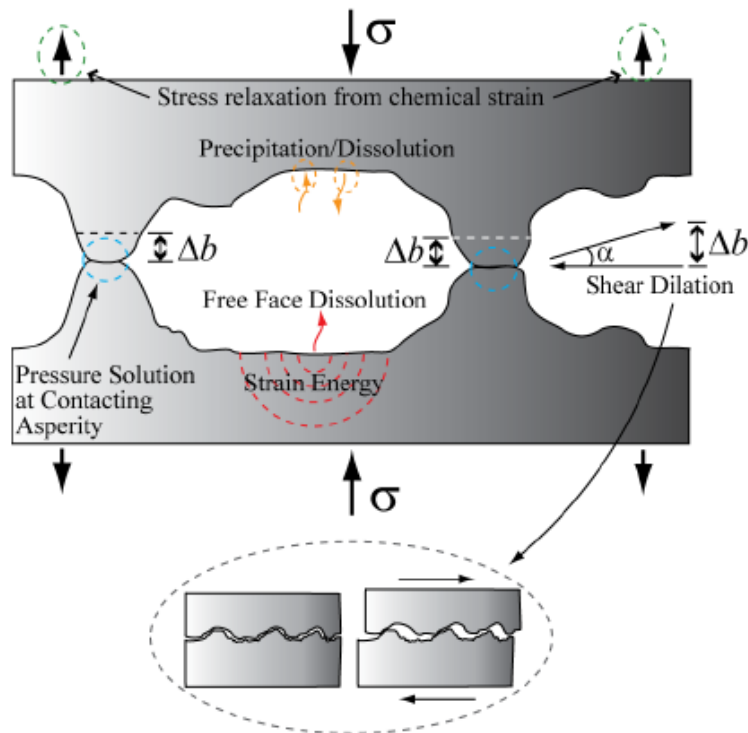


Application to granodiorite data (field) under stress control

Replicates most features on curve

Experimental data needed at a variety of scales

The Role of Irreversible “Chemical” Strains on Mechanical and Transport Properties



Reactive Flow and Permeability Dynamics

Derek Elsworth, Penn State

Basic Observations of Permeability Evolution - Lab-to-field

Impacts on Permeability

Mechanical effects (pore pressure and thermal effects)

Controls on effective stress

Stress-porosity linkages for fractures

Compaction

Dilation

Rate-state models

Porosity-permeability linkages to fracture dilation

Other mechanical effects (wear)

Reactive chemical effects

Laboratory observations

Linkages among porosity/permeability/dissolution/precipitation

Mechanistic models for chemical-mechanical effects

In situ observations/characterizations of chemical-mechanical effects

Forward/reverse feedbacks on stress-permeability

Reservoir-Scale Evolution of Permeability

Spatial distribution

Timing

Seismicity as an indicator

Summary

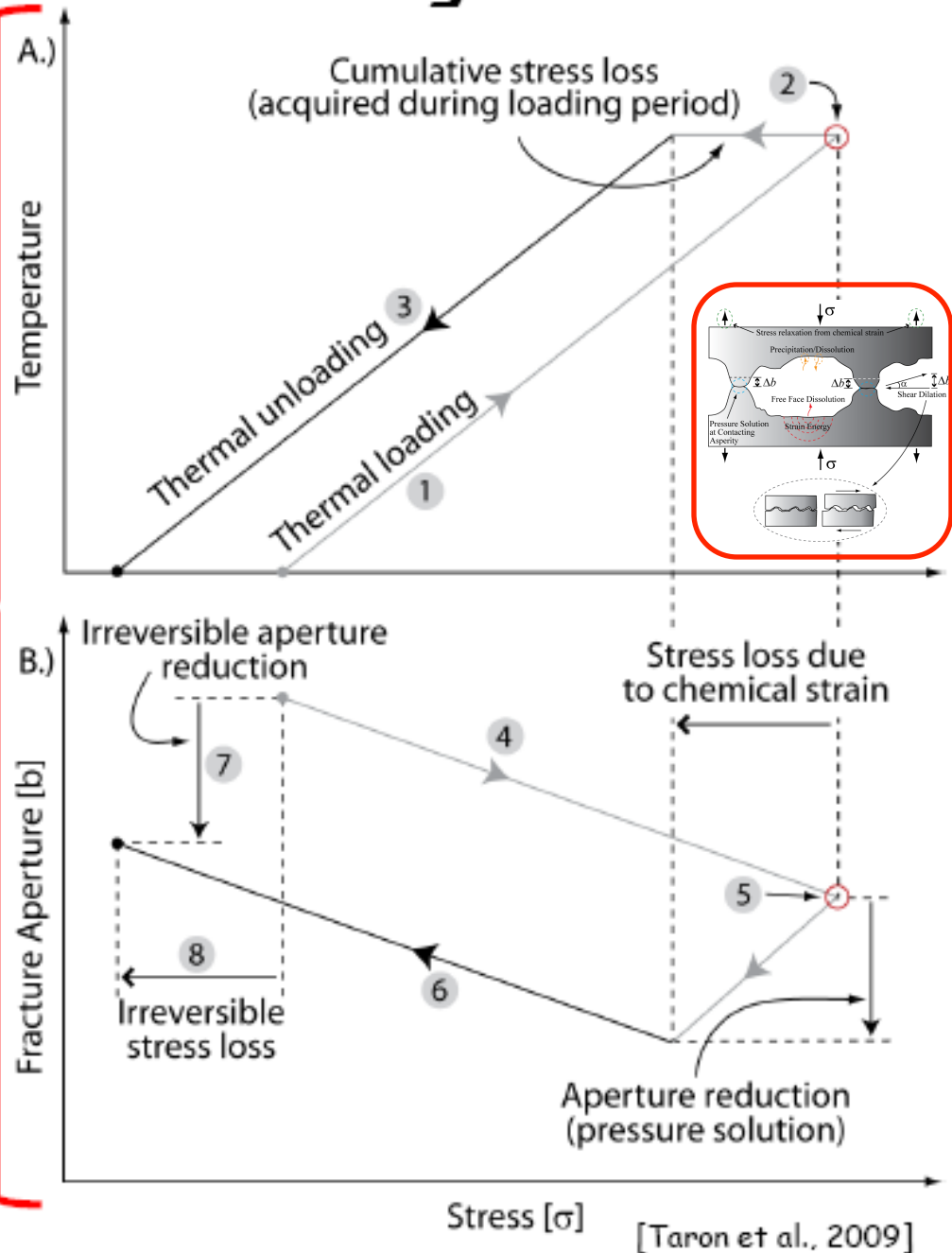
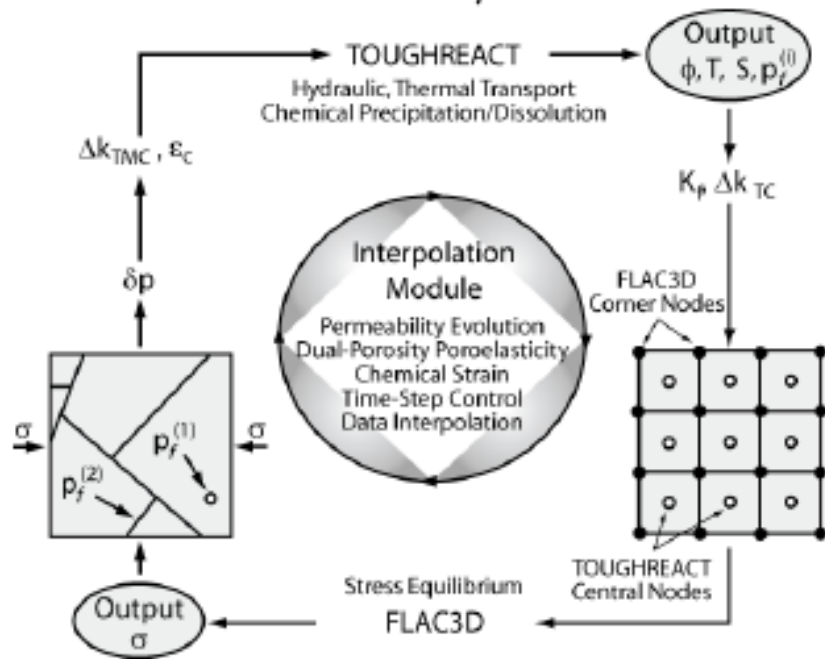
Coupled THMC Modeling

- TOUGHREACT (THC)** - Accommodates non-isothermal, multi-component phase equilibria, pressure diffusion, multi-phase hydrologic transport, and chemical precipitation/dissolution (transient mass/energy balance)

$$\frac{\partial M}{\partial t} = -\nabla \cdot \mathbf{F} + q$$

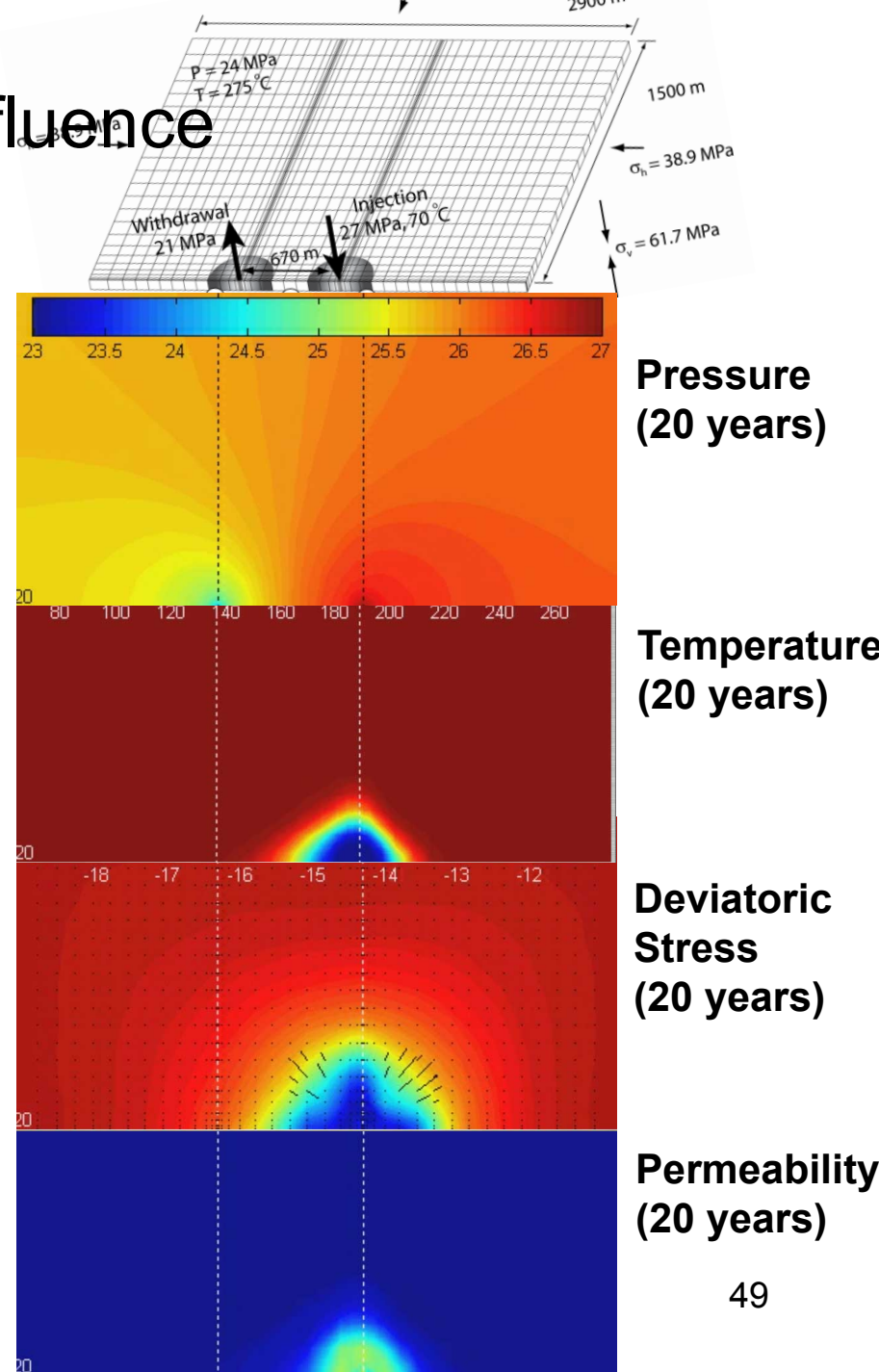
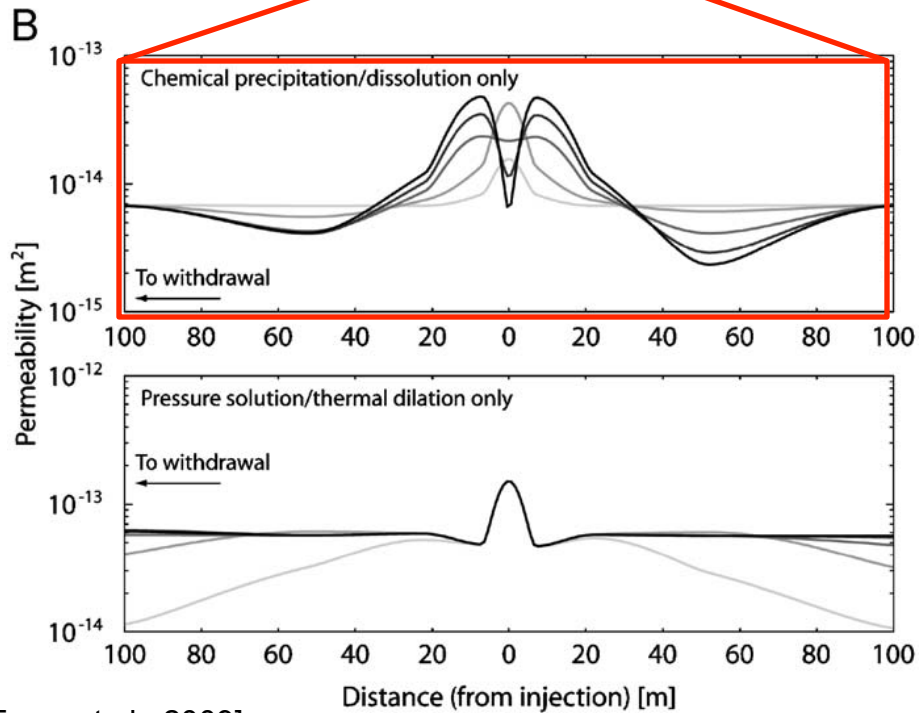
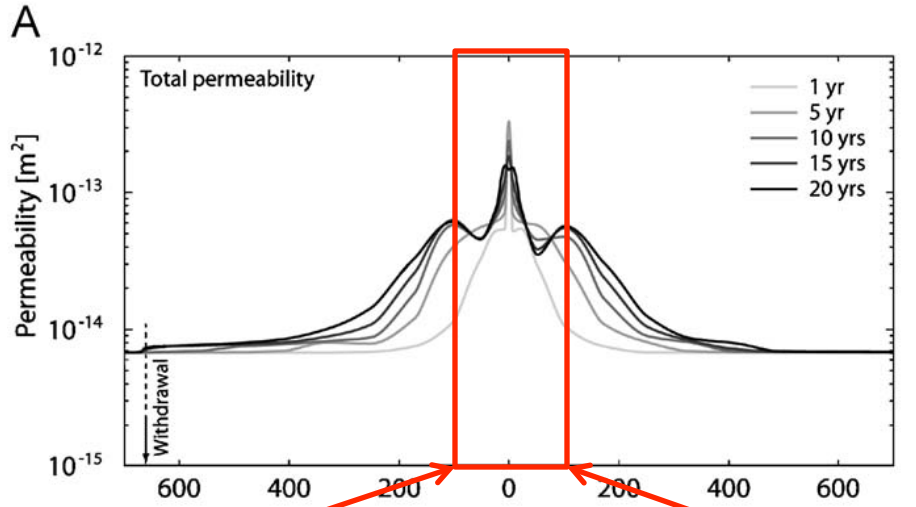
- FLAC3D (M)** - Mechanical constitutive relations (force equilibrium, capable of THM)

$$\nabla \cdot \boldsymbol{\sigma}^T = -\rho \mathbf{b}$$

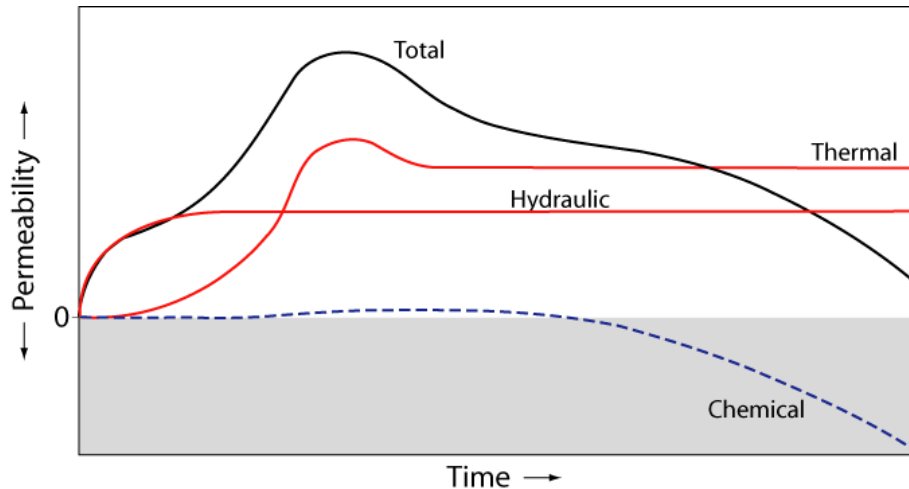


Coupled THMC Modeling

Chemical –vs- Mechanical Influence



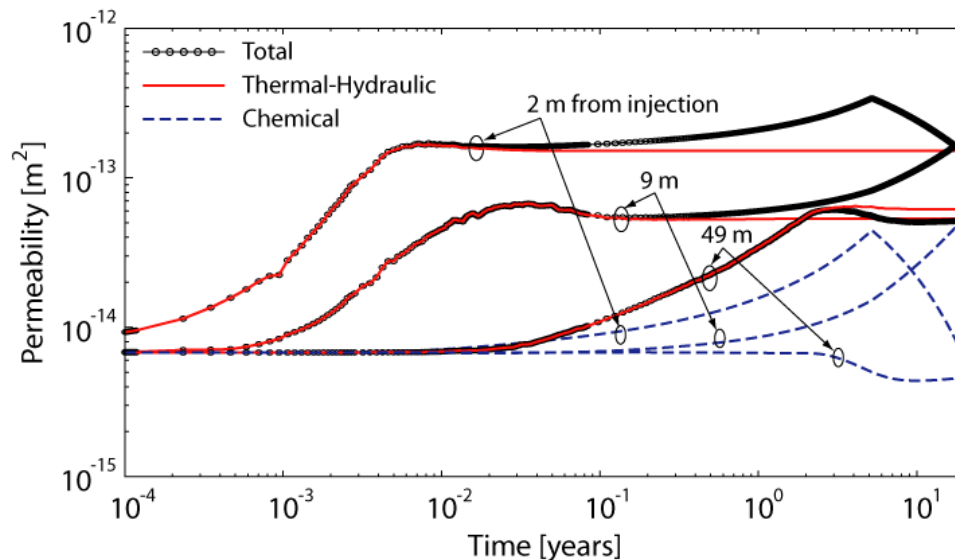
Timescales and Characteristic Times



Thermo-hydraulic processes combined in this model.

Onset of chemical permeability change a longer time-scale process.

Sharp onset of chemical change due to complete dissolution of all calcite in veins.



Triggered Seismicity - Key Questions

Principal trigger - change in (effective) stress regime:

- Fluid pressure
- Thermal stress
- Chemical creep

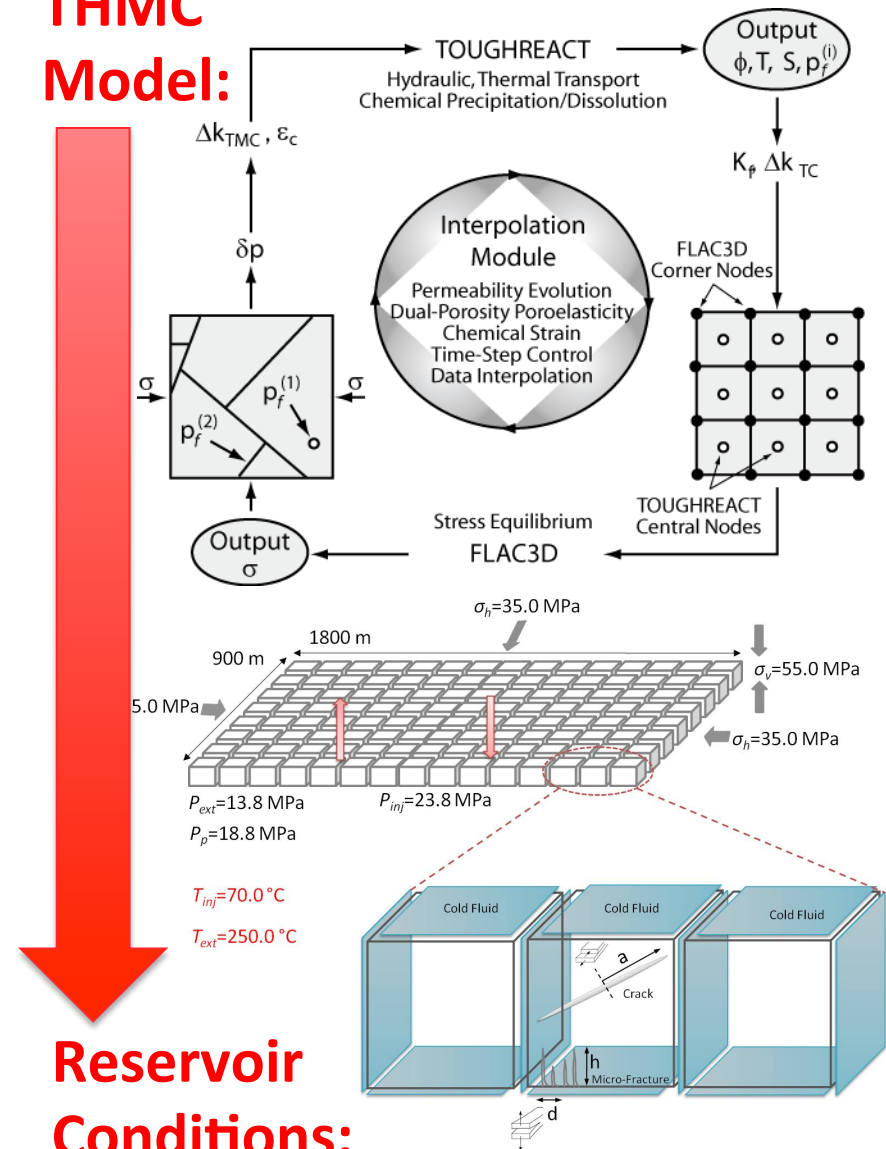
How do these processes contribute to:

- Rates and event size (frequency-magnitude)
- Spatial distribution
- Time history (migration)

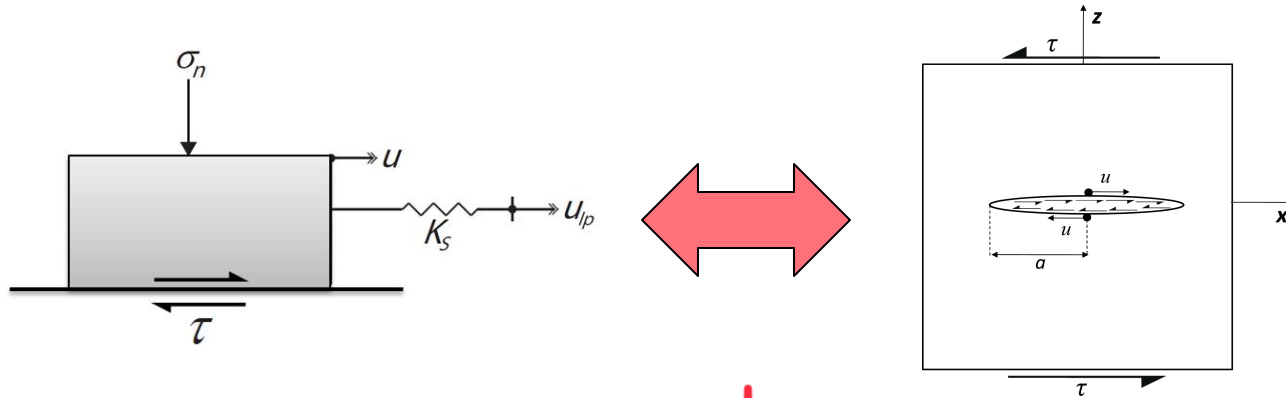
How can this information be used to:

- Evaluate seismicity
- Manage/manipulate seismicity
- Link seismicity to permeability evolution

THMC Model:

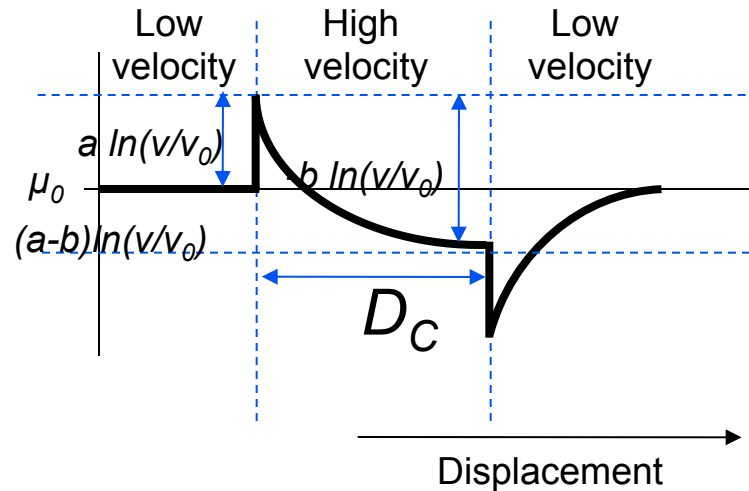


Approaches - Rate-State versus Brittle Behavior

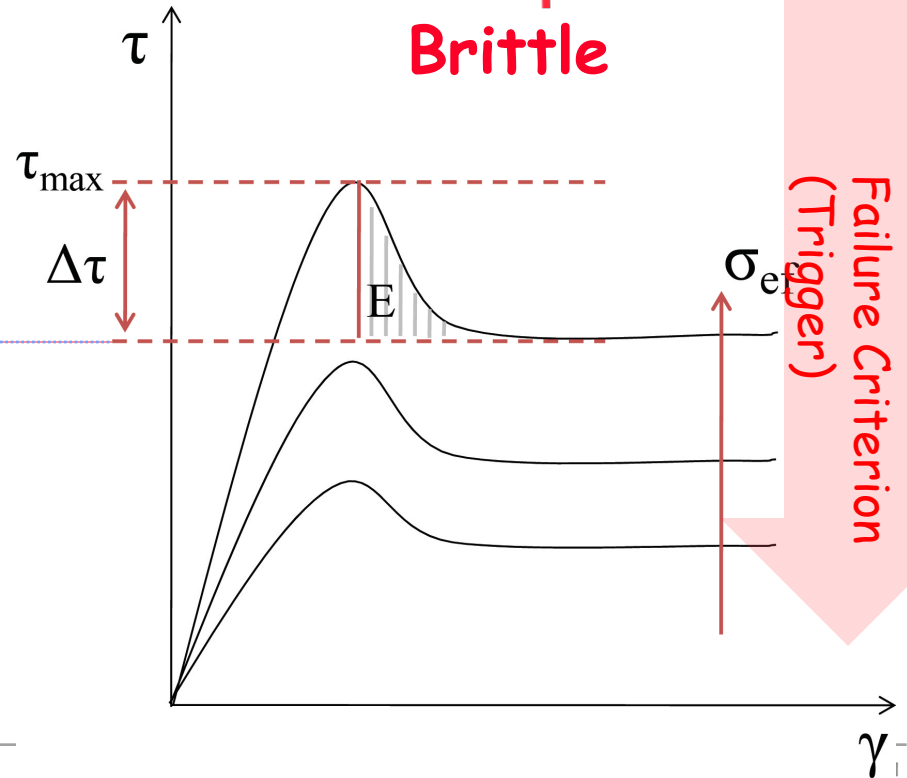


Coefficient of friction

Rate-State



Brittle

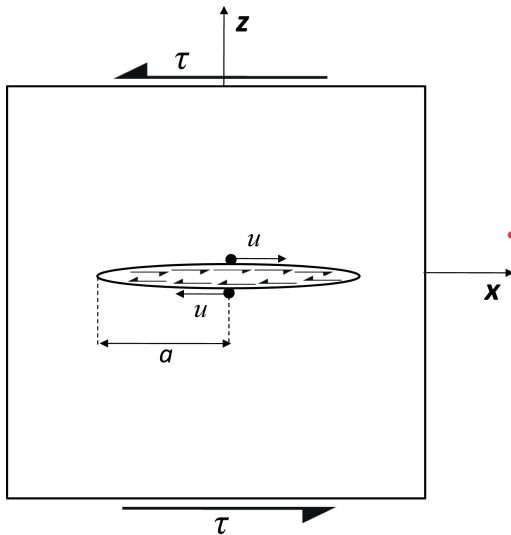


System Stiffness
(Stored Energy)

Failure Criterion
(Trigger)

Component Behavior - Reservoir stiffness

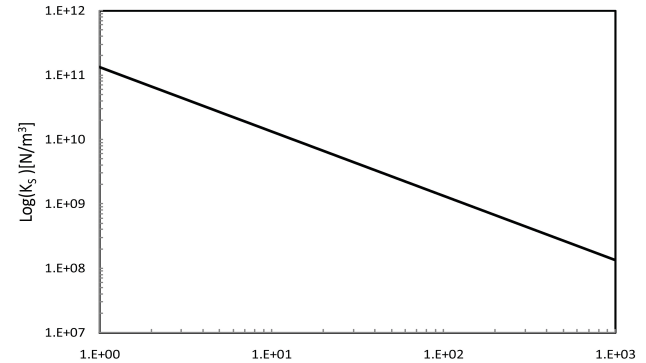
Penny-shaped Crack



Stiffness:

$$K_s = \frac{\tau}{u_m} = \frac{3G\pi(3\lambda + 4G)}{8(\lambda + 2G)} \frac{1}{a} = \frac{3G\pi(2-\nu)}{8(1-\nu)} \frac{1}{a}$$

$$K_s = \frac{4G}{3a}$$



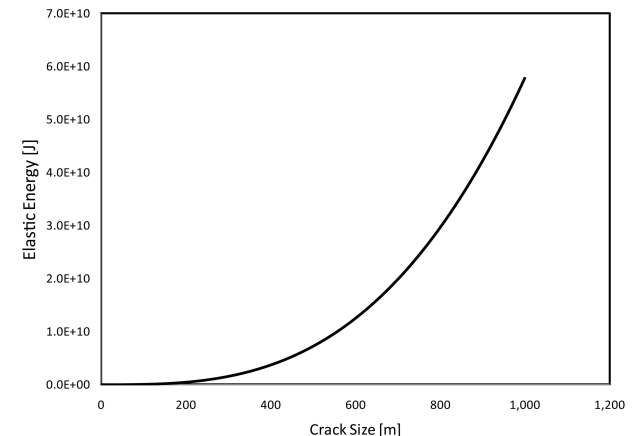
Energy:

$$E = \frac{1}{2} \int_{2A} \tau u dA = \frac{8(\lambda + 2G)}{3G(3\lambda + 4G)} = \frac{2\tau^2 a^3}{3G}$$

$$E_p = \frac{2\tau^2 a^3}{3G}$$

Magnitude:

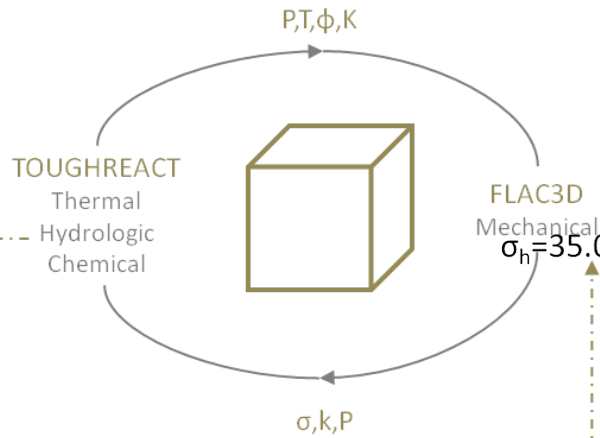
$$\log E_p = 1.5M_s + 9.1$$



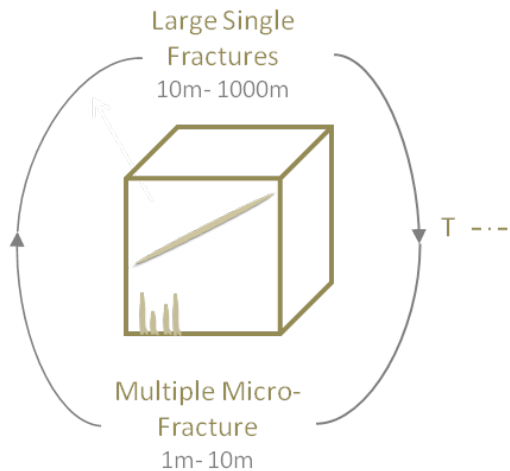
Continuum THMC Model

Model:

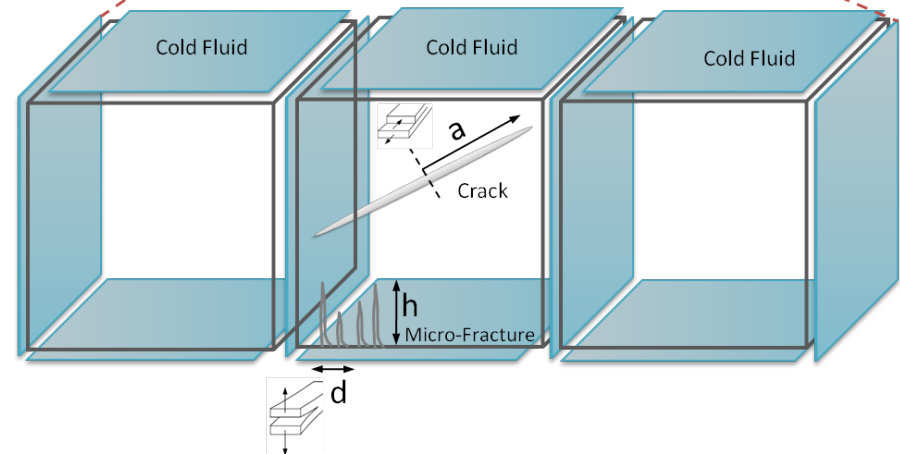
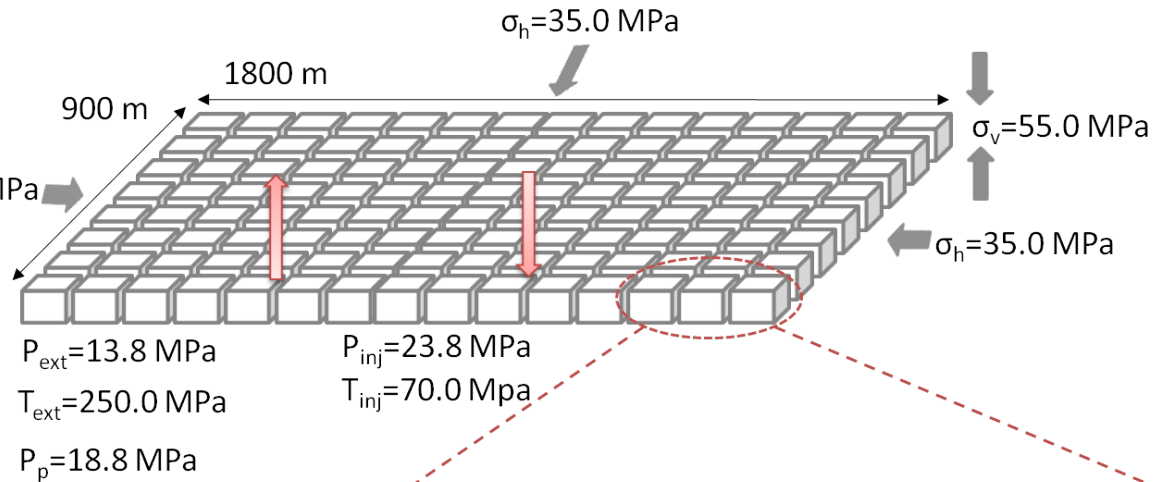
THMC Simulator



Numerical Model

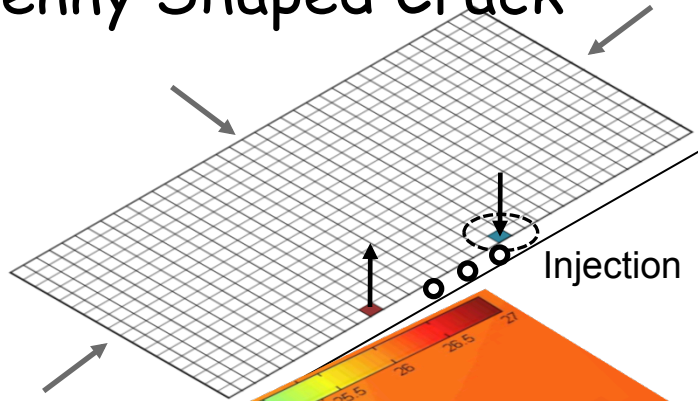


Reservoir Conditions:



Large Fracture Geometry

Penny Shaped Crack

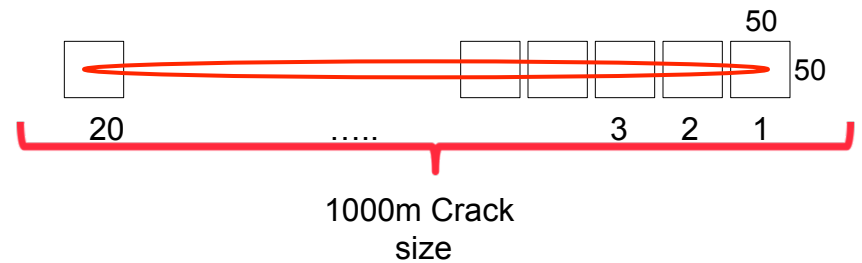
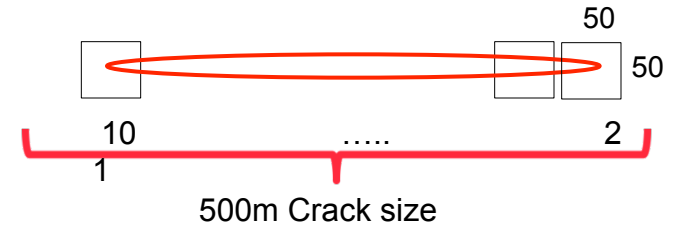
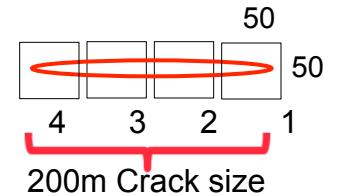
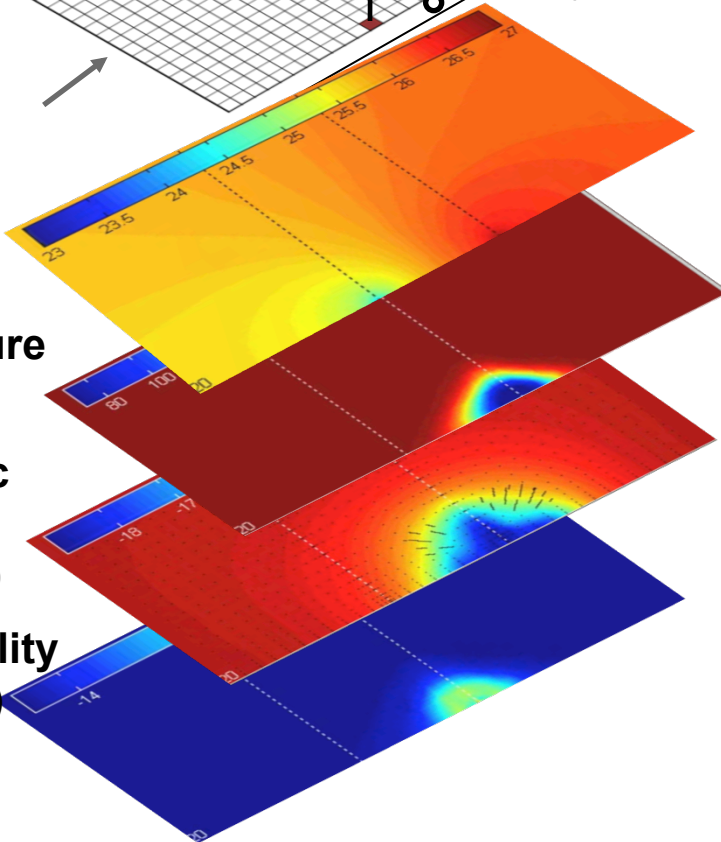


Pressure
(20 years)

Temperature
(20 years)

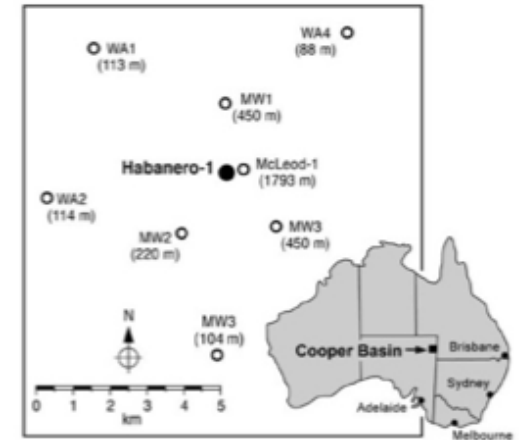
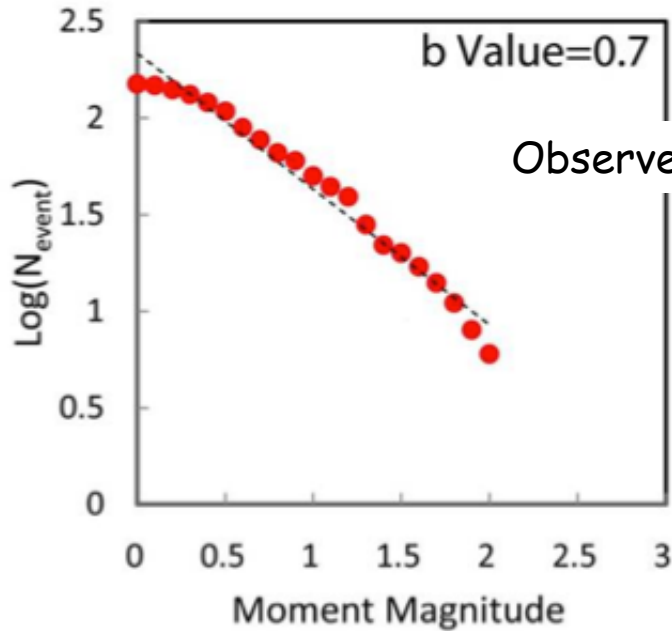
Deviatoric
Stress
(20 years)

Permeability
(20 years)

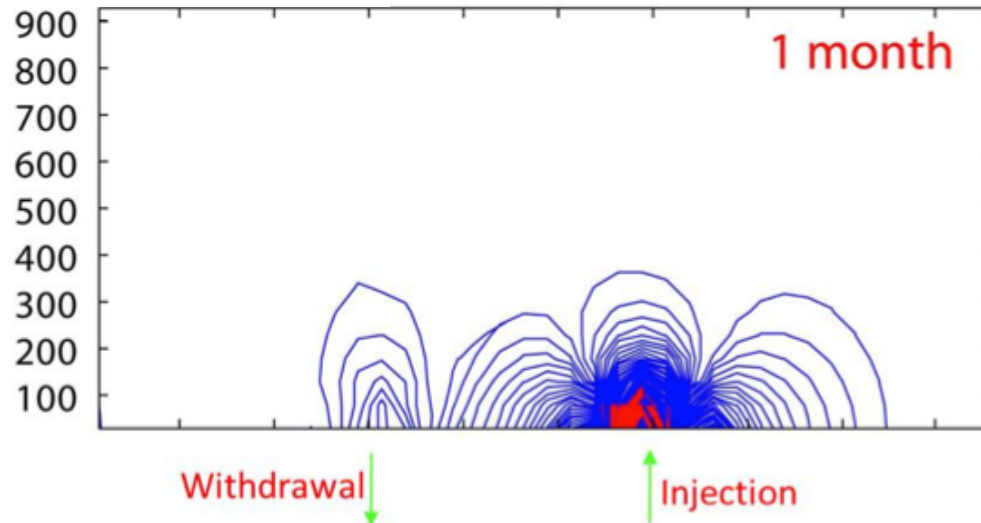


Short-term Validation

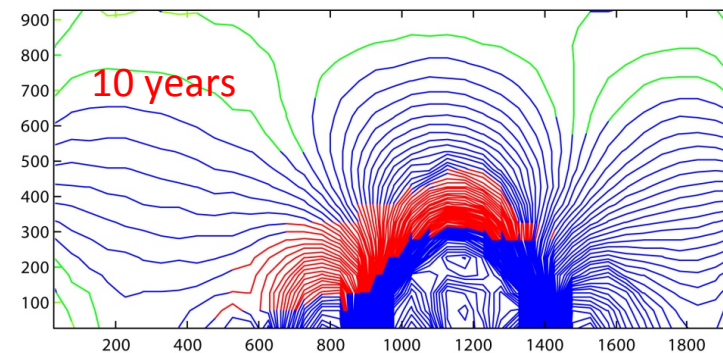
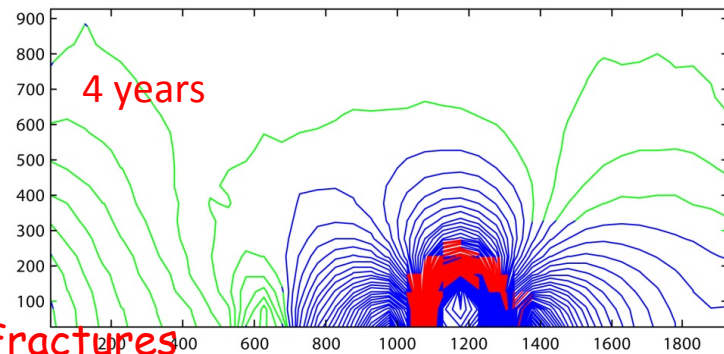
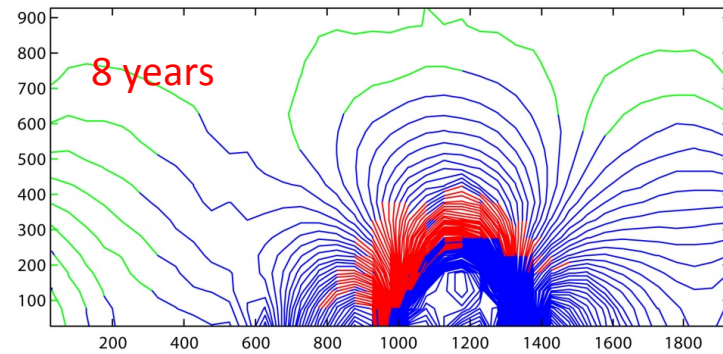
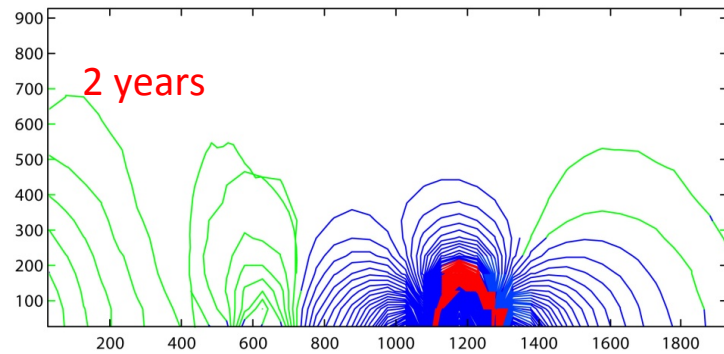
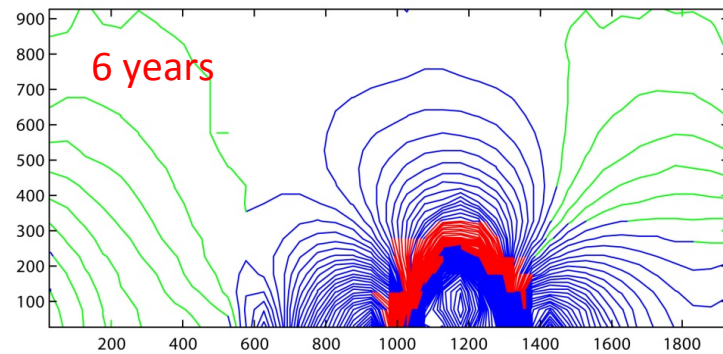
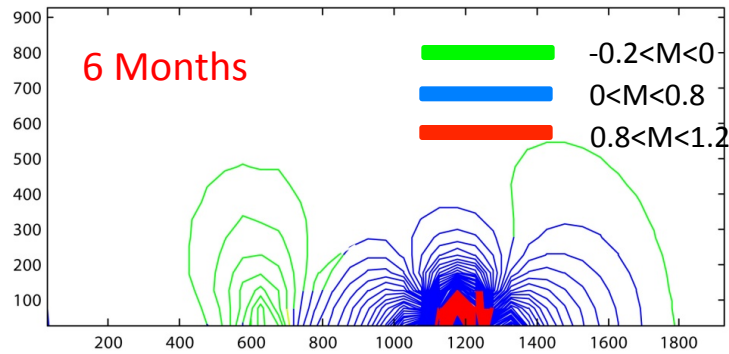
Model Results:



Map of Cooper Basin Geothermal Field, Australia

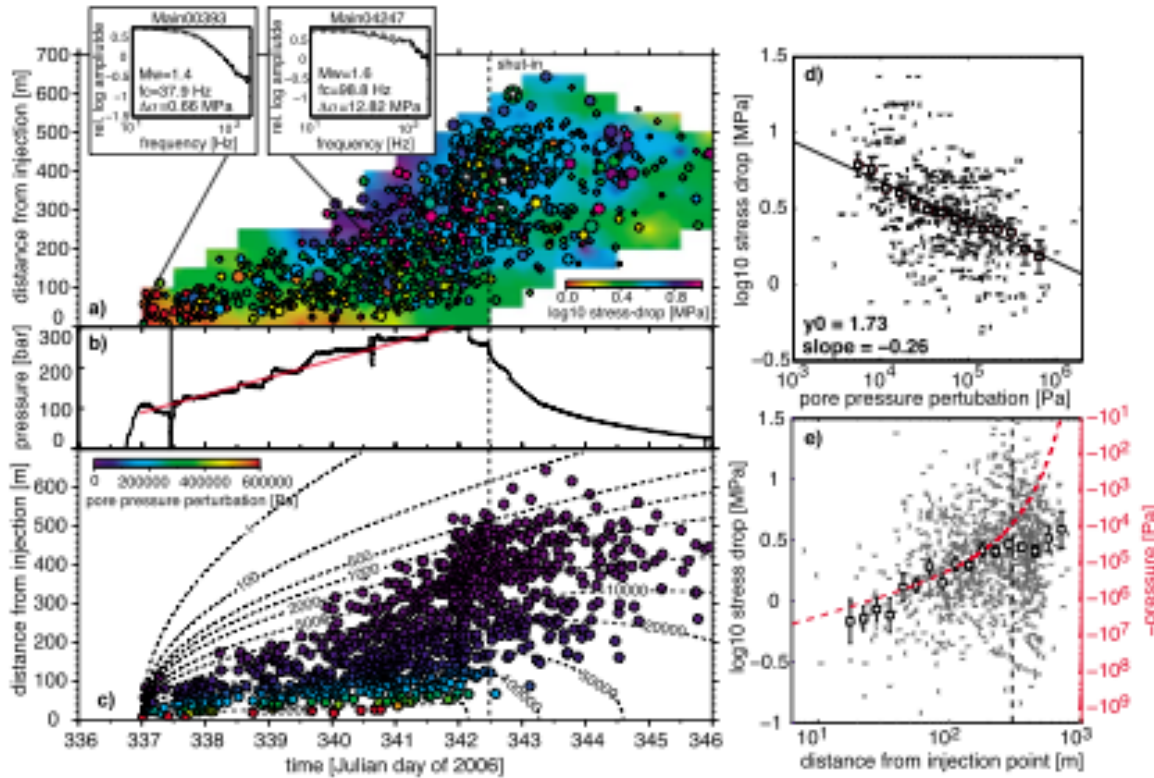


Migration of Triggered Seismicity

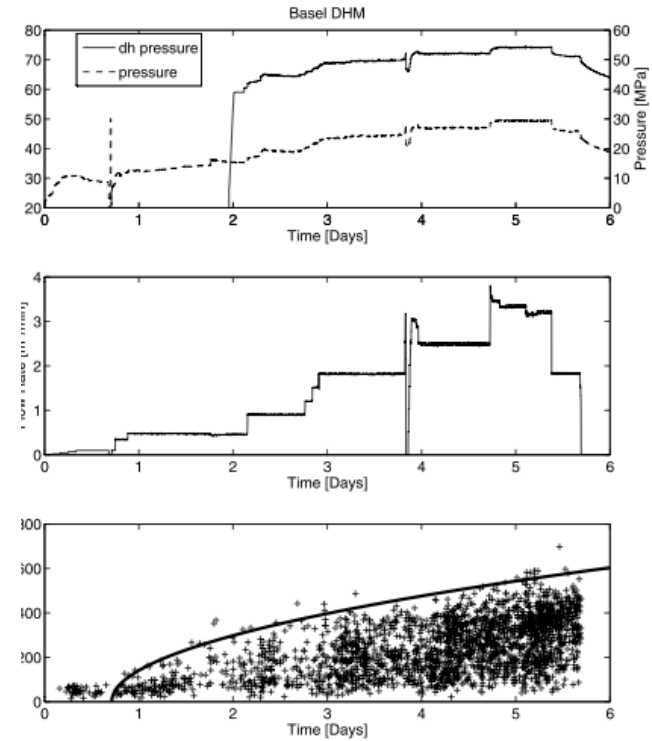


200 m Fractures

Observations of Induced Seismicity (Basel)



[Goertz-Allmann et al, 2011]



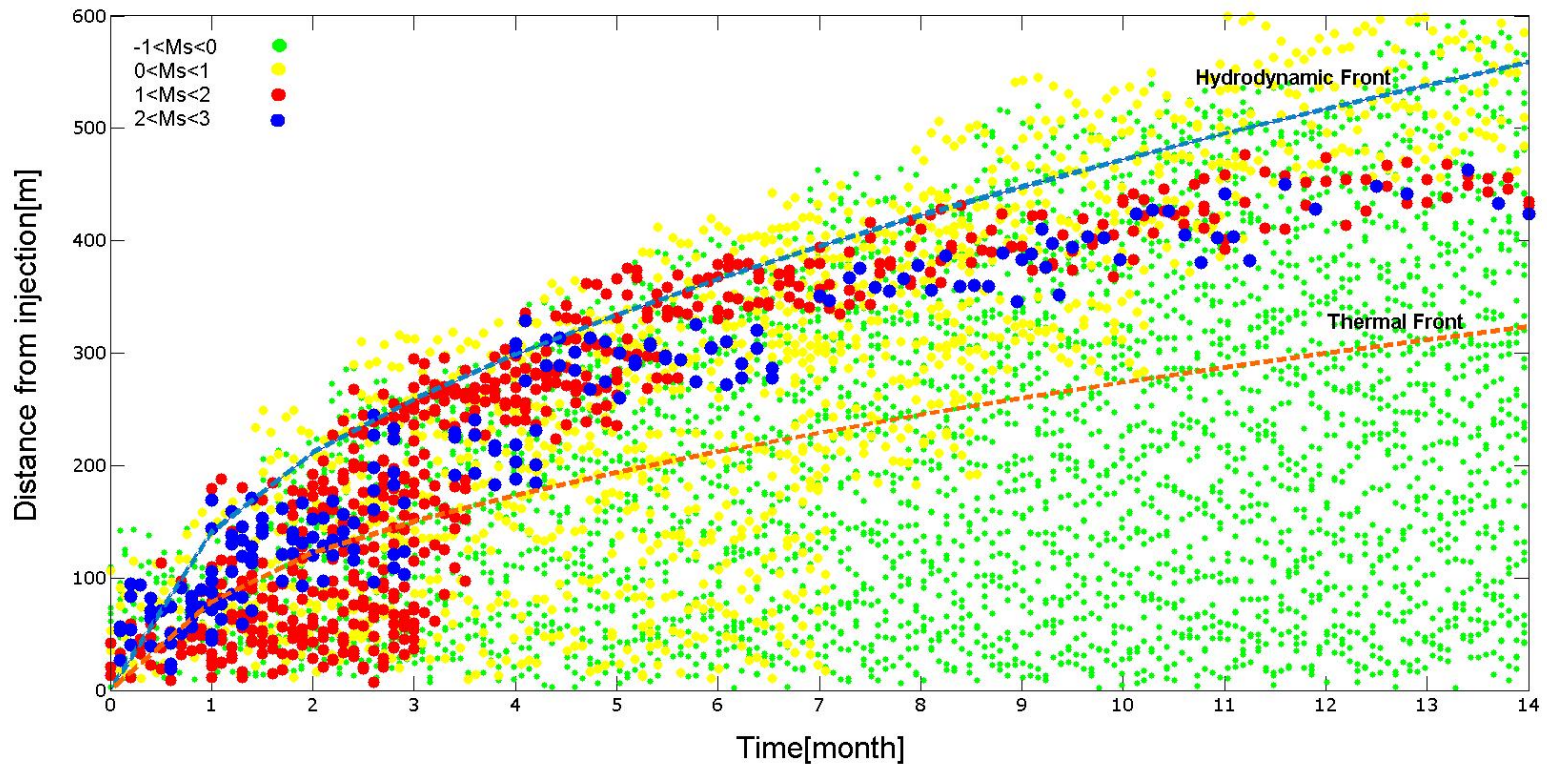
[Shapiro and Dinske, 2009]

r-t Plot - Fluid and Thermal Fronts and Induced Seismicity

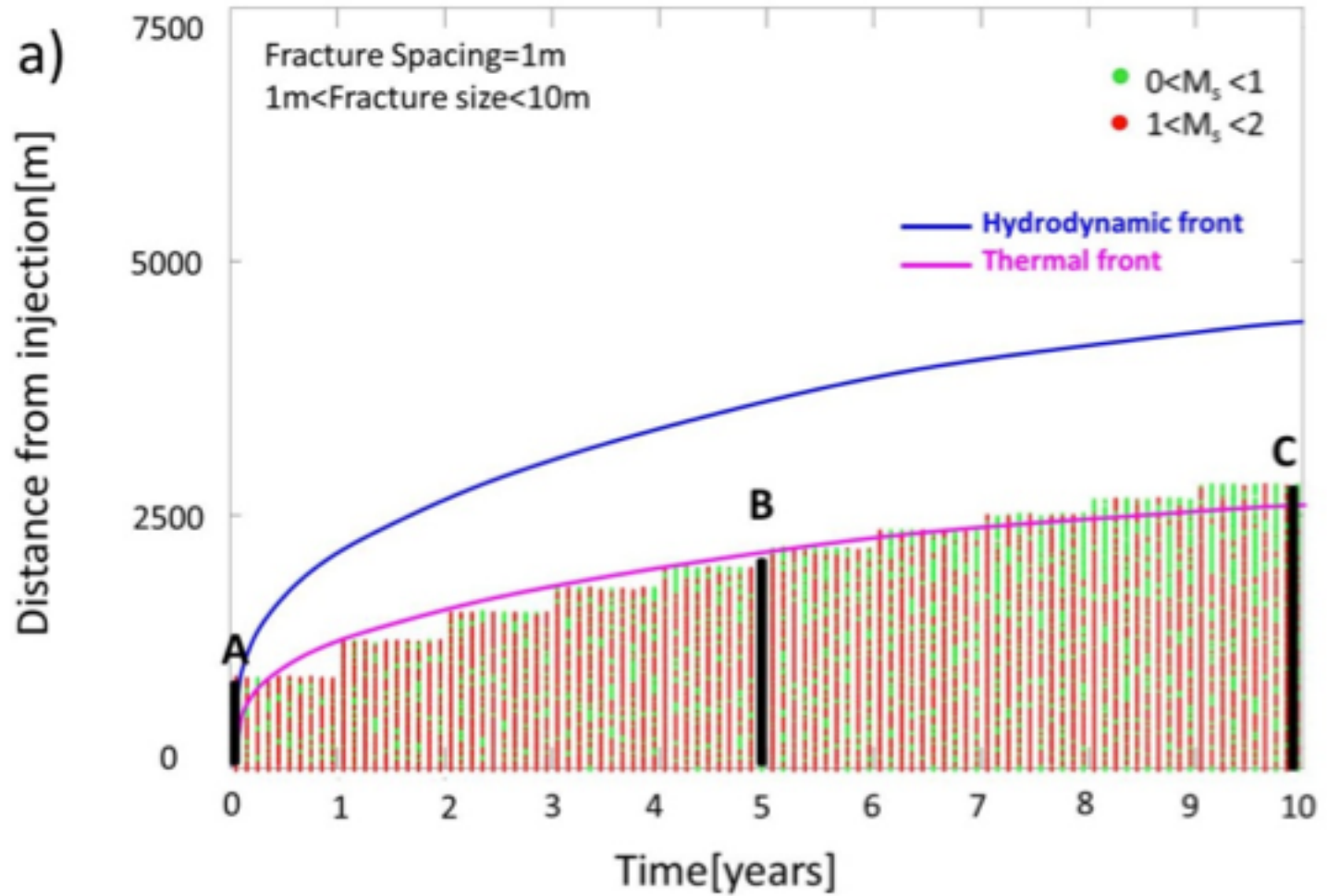
- Q: Flow rate
- t: Time
- h: Thickness
- φ: Porosity
- b: Aperture

$$r = \sqrt{\frac{2Qt}{\pi h \phi}}, \quad k_0 = \frac{b^3}{12S}$$

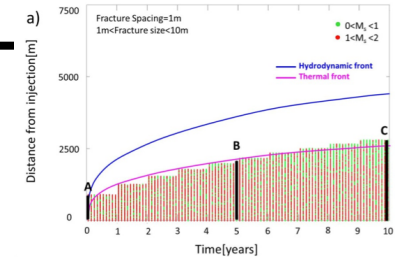
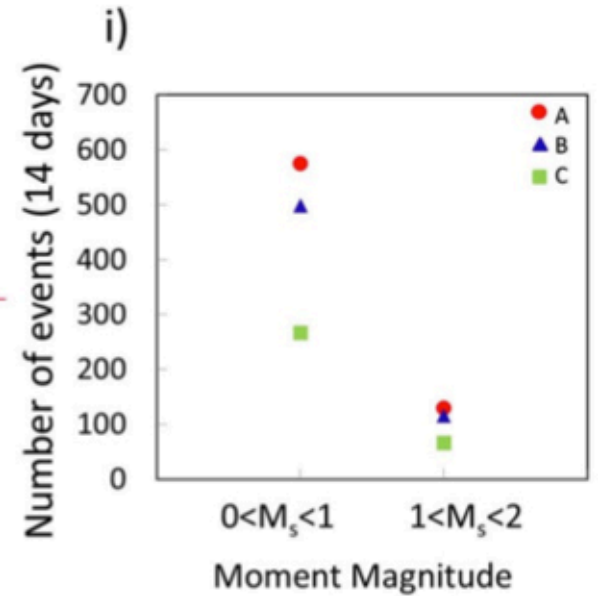
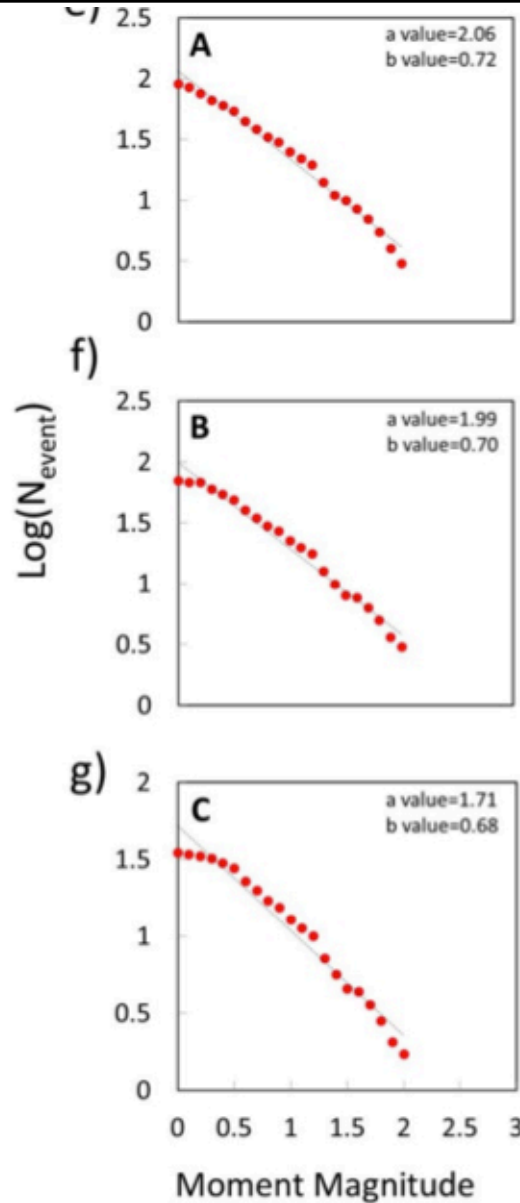
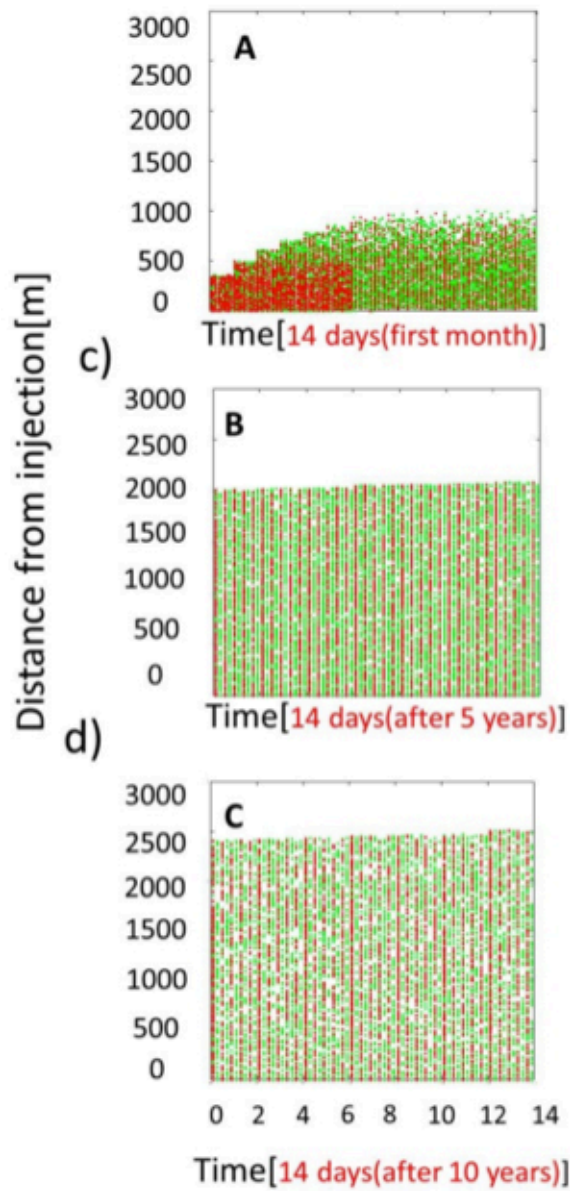
Parameters utilized in simulation		
k_0	Permeability[m ²]	10 ⁻¹⁷
P_p	Pore Pressure[Mpa]	14.8
P_{inj}	Fluid Pressure[Mpa]	17.8
T_{res}	Reservoir Temperature[°c]	250
T_{inj}	Fluid Temperature[°c]	70
S	Fracture Spacing[m]	10 to 500



Long-Term Projection

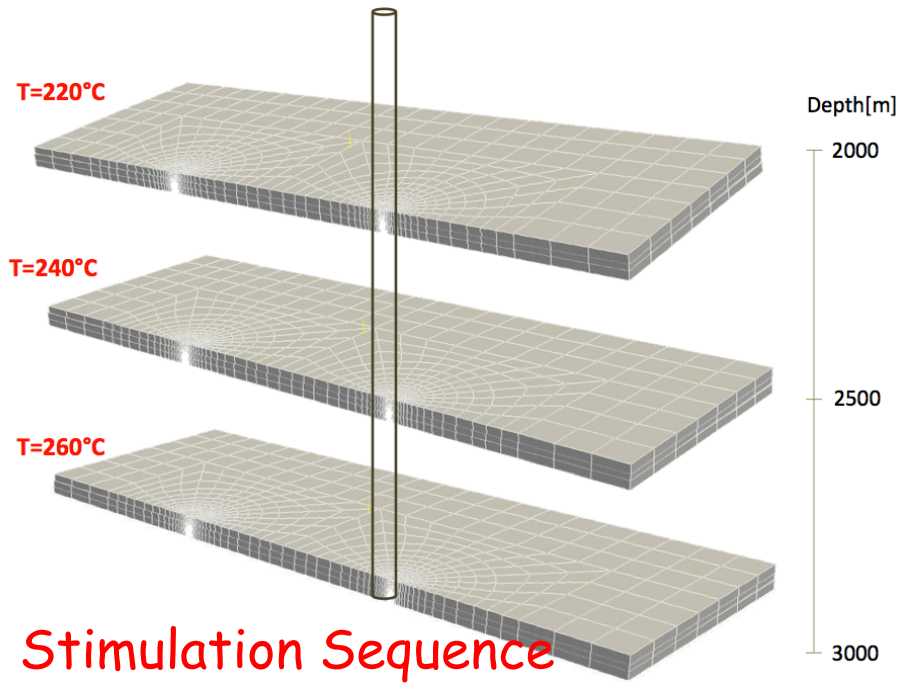


Long-Term Projection

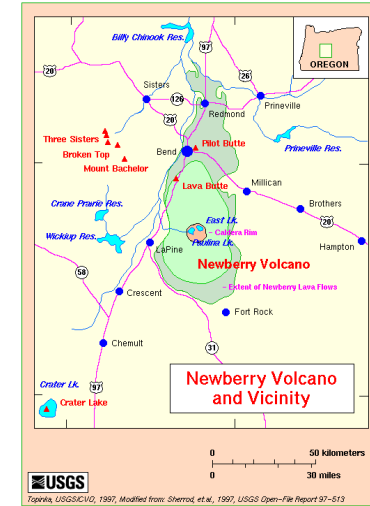


Newberry Stimulation

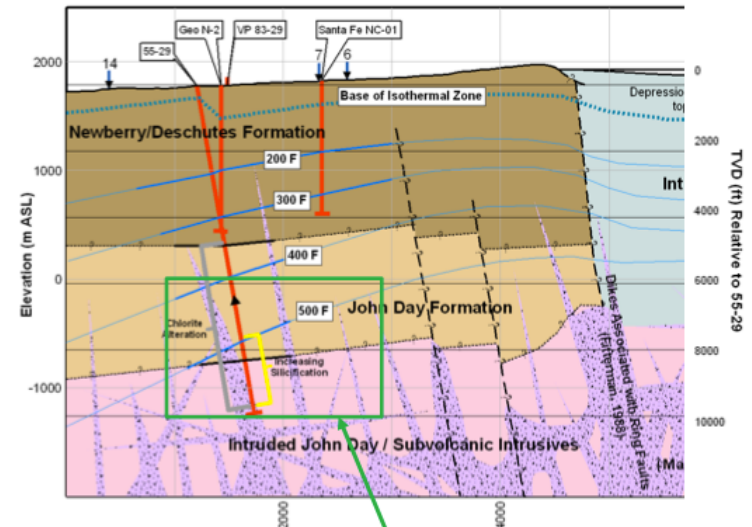
Stacked Reservoir Model



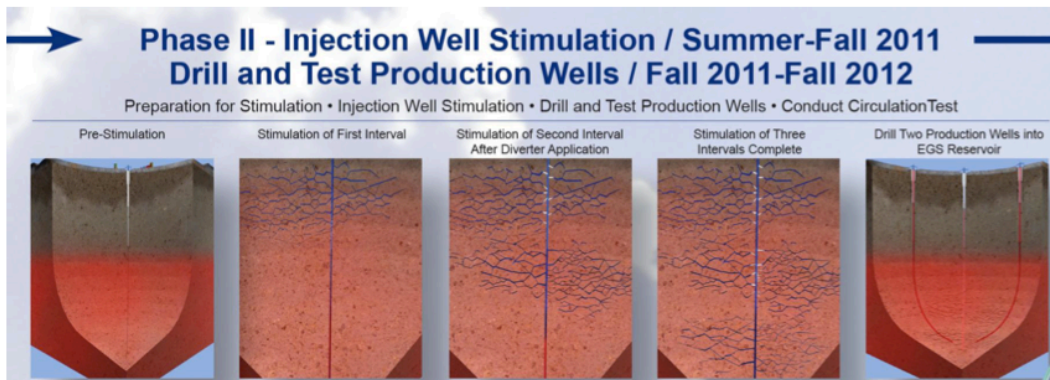
Location



Volcanic stratigraphy

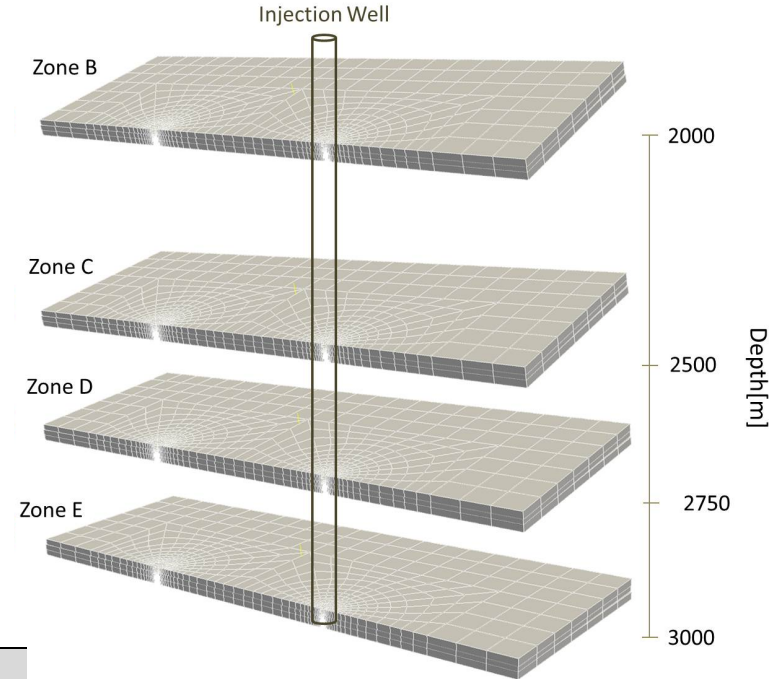
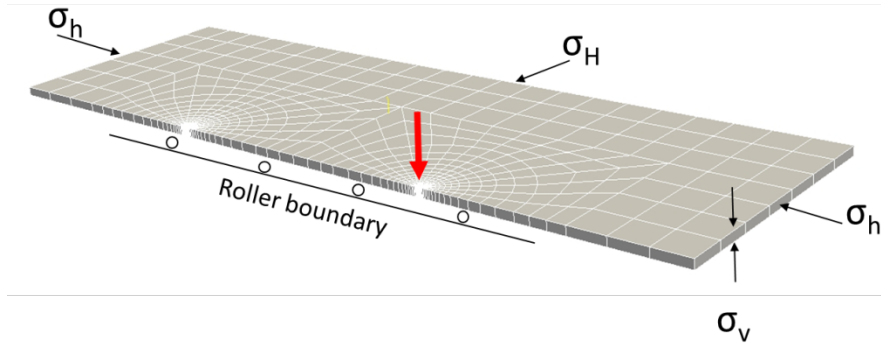


Stimulation Sequence



Zone Characteristics

Stimulation zones



Parameters	Unit	Depth[m]			
		2000	2500	2750	3000
		Zone B	Zone C	Zone D	Zone E
S_{hmin}	MPa	36	45	50	54
S_{Hmax}	MPa	48	58	64	70
S_v	MPa	48	60	66	72
$P_{injection}$	MPa	29	33	35	37
$P_{reservoir}$	MPa	24	28	30	32
$P_{production}$	MPa	19	23	25	27
Peak Strength	MPa	25	30	35	38
T_{rock}	°c	230	280	290	310
$T_{injection}$	°c	20	20	20	20

$$S_{hmin} = 0.75 S_v$$

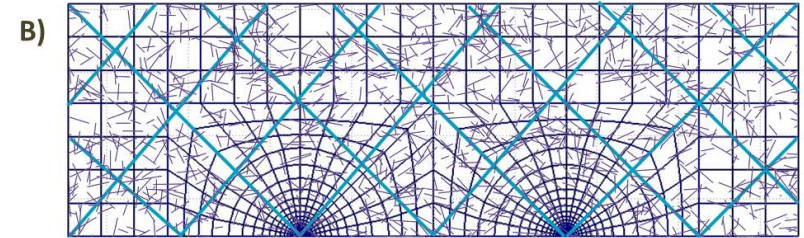
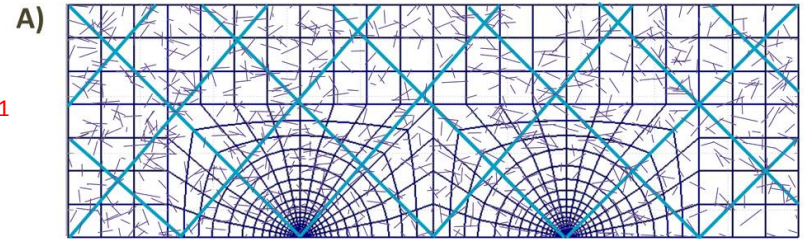
$$\Delta p = 5 \text{ MPa}$$

Zone Characteristics

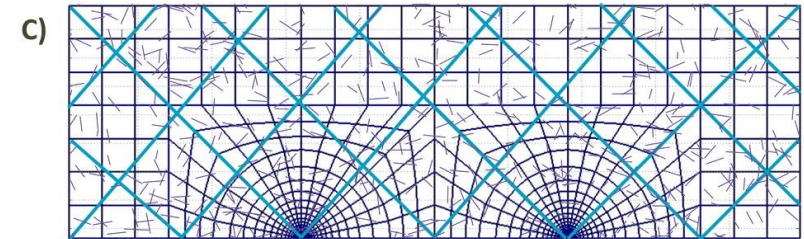
Fracture Network Characterization

Fracture density is 0.5 m^{-1}

Large fractures: density of 0.003 m^{-1} - spacing 300 m



0.9 m^{-1}



0.26 m^{-1}

$200 < \text{Large Fracture} < 1200 \text{m}$

$10 < \text{Small Fracture} < 200 \text{m}$

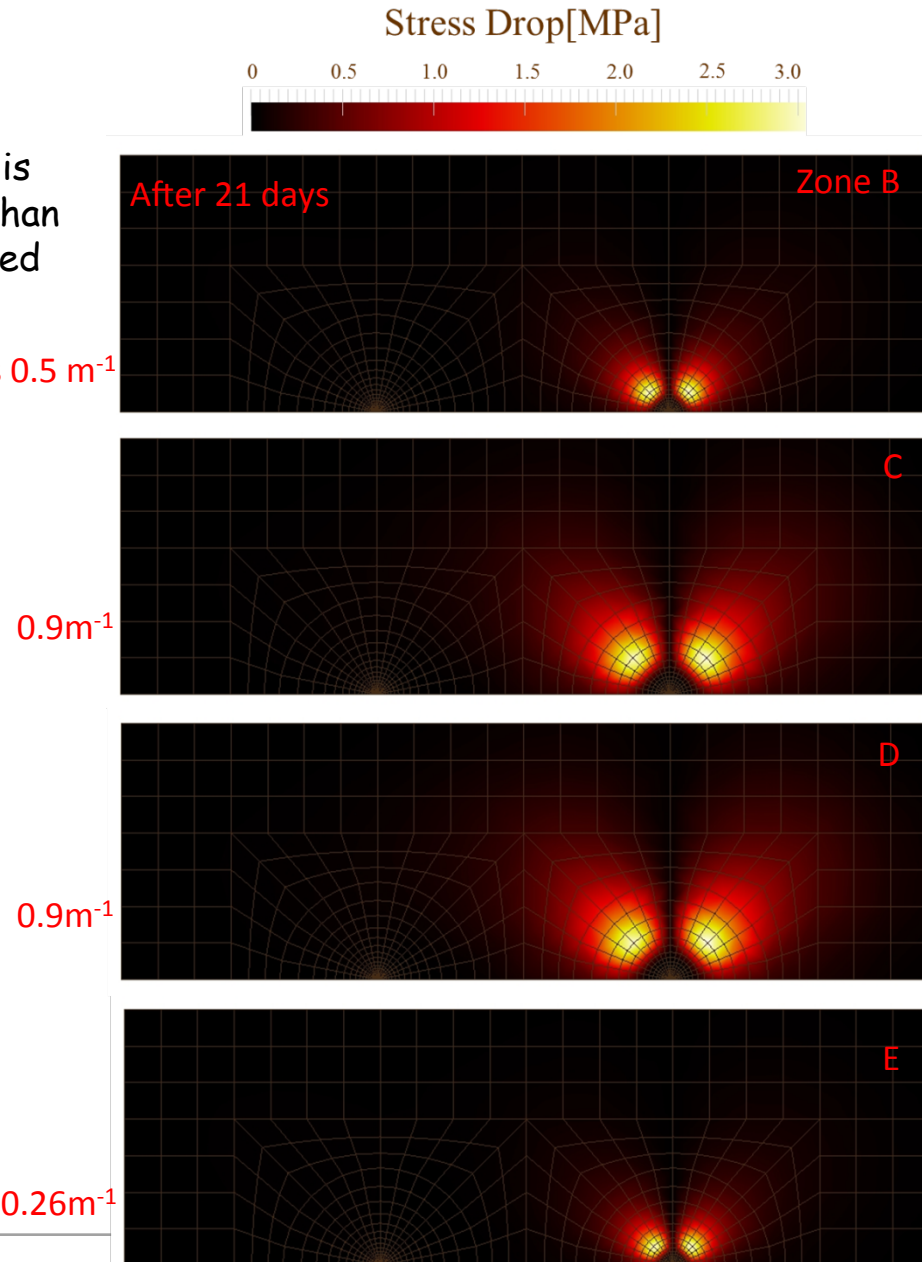
Fracture Characterization	Unit	Depth[m]			
		2000	2500	2750	3000
		Zone B	Zone C	Zone D	Zone E
Density	m^{-1}	15/30m	27/30m	27/30m	8/30m
Number of seeded fractures	-	1000	1800	1800	600
Fracture size	m	10-1200	10-1200	10-1200	10-1200
Fracture spacing	m	1-300	1-300	1-300	1-300
Standard deviation($\bar{\sigma}$)	-	19	19	19	19
Mean($\bar{\mu}$)	-	360	360	360	360

Cumulative Stress Drop

Models with various fracture densities:

The mean stress drop is limited to be smaller than the maximum prescribed stress drop.

Fracture density is 0.5 m^{-1}



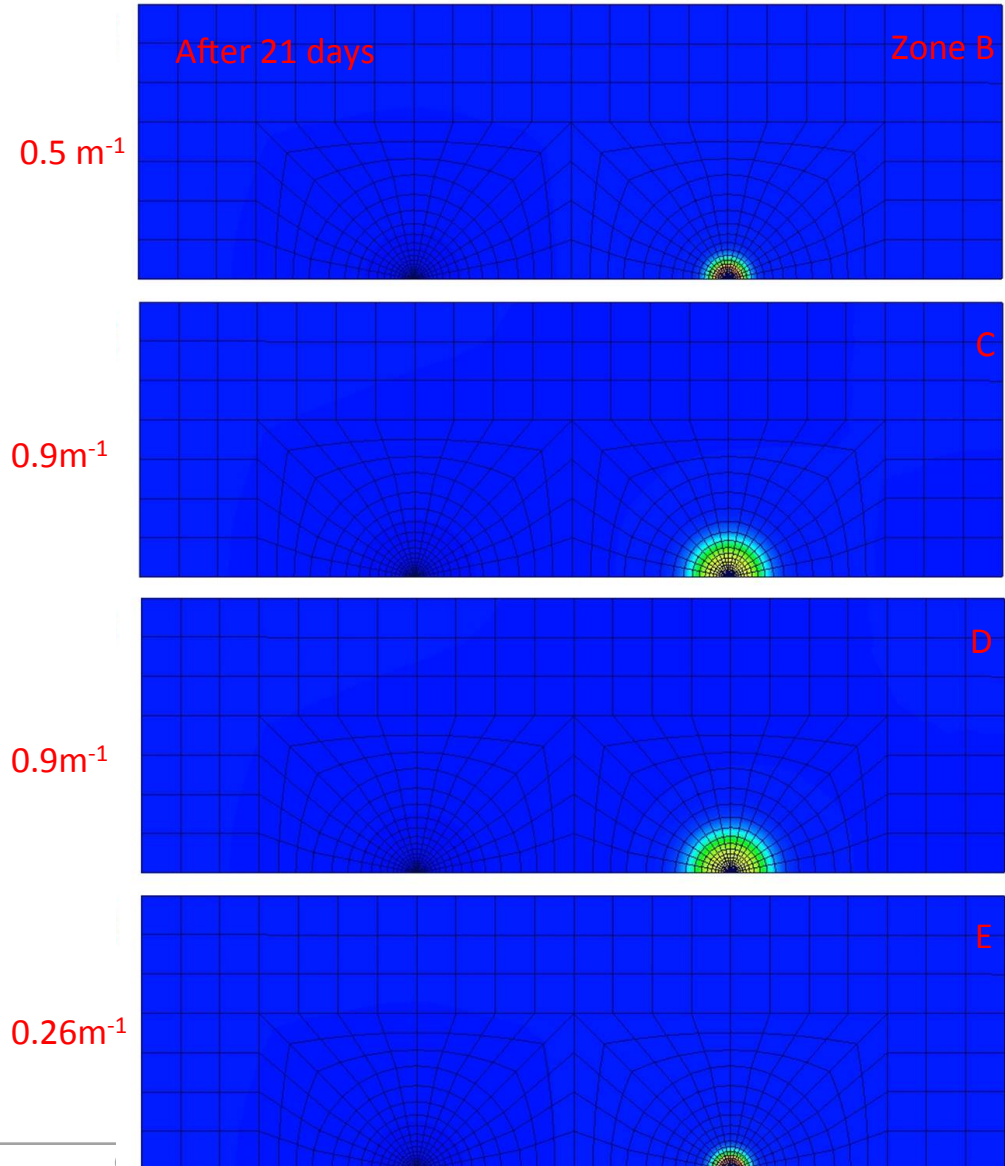
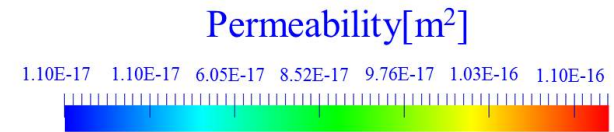
Development of stress drop begins earlier, reaches further from injection in a given time (~21 days) and is completed fastest for zones C and D.

Permeability

Comparison of average radial permeability changes for different fracture structures:

The mechanical shearing effect (dilation angle is 10°) occurs due to the change in effective stress driven by fluid and thermal effects and their influence on reservoir shear failure.

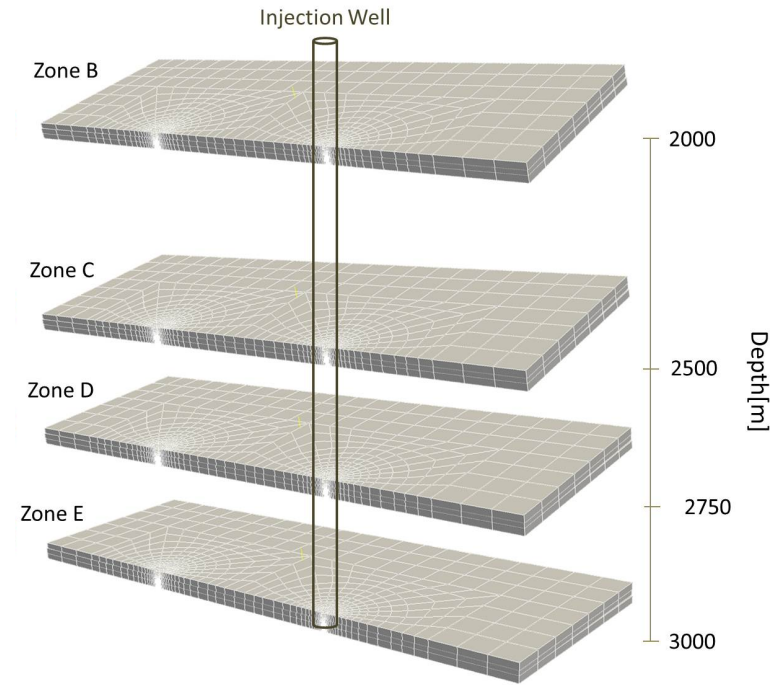
Permeability improvement in all zones is radially symmetric.



Parametric Analysis

$$\log M_0 = 1.5M_s + 9.1$$

Shear stress drop
Fracture size, spacing



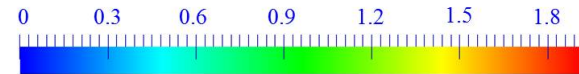
Two different models applied:

Moment magnitude evolution

- 1) Fracture density is the same at shallow to deep zones (0.9 m^{-1})
- 2) Fracture density is not the same at shallow to deep zones (0.5 m^{-1} , 0.9 m^{-1} , 0.26 m^{-1})

Moment Magnitudes - Same Fracture Density

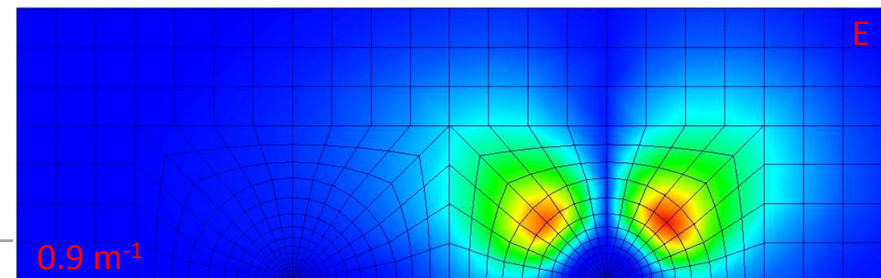
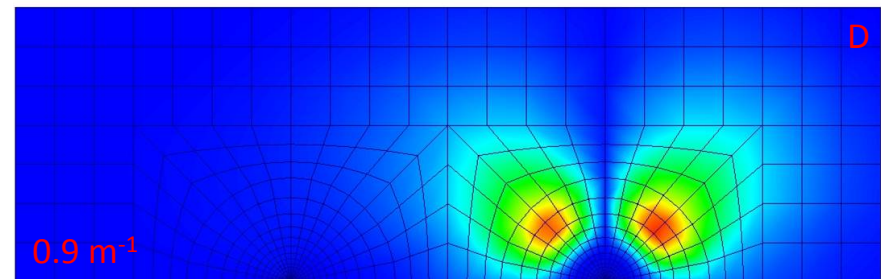
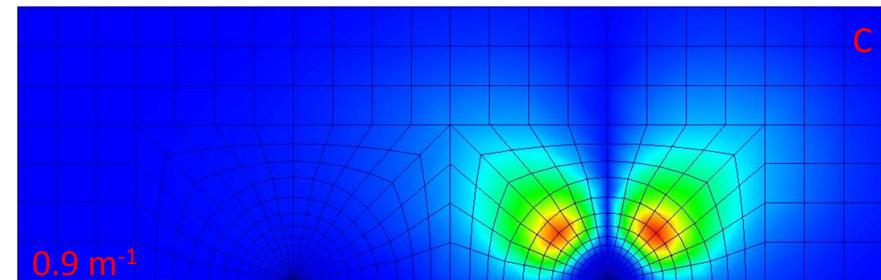
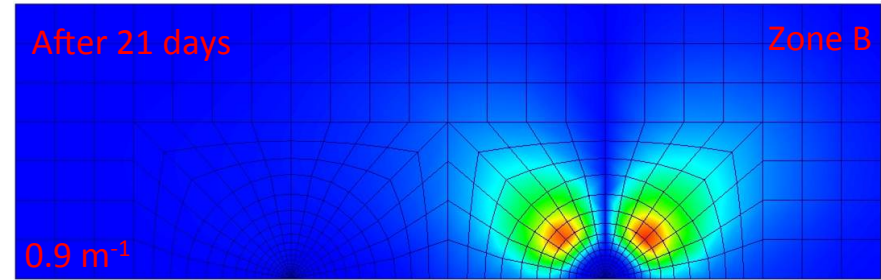
Moment Magnitude



For the same fracture density:

With increasing stresses (reaching the deeper reservoir):

Migration rate of seismic event with time and location changes little - these events may form at the same rate for shallow to deep zones when the same fracture network is present.

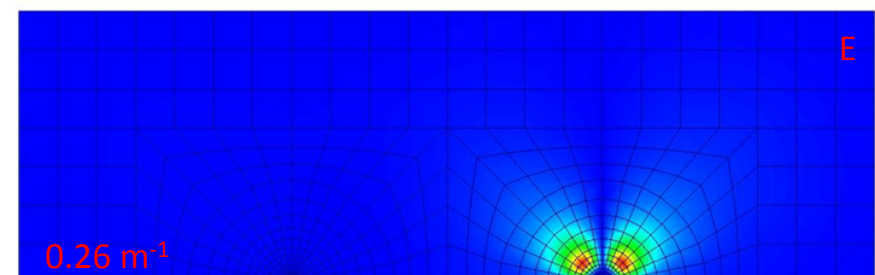
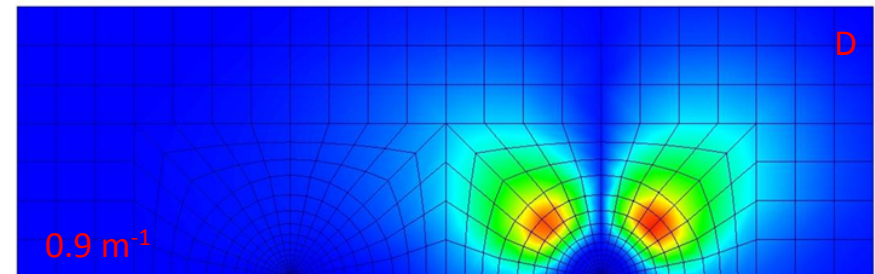
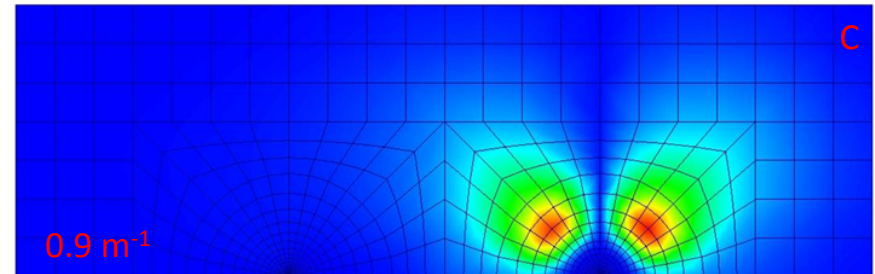
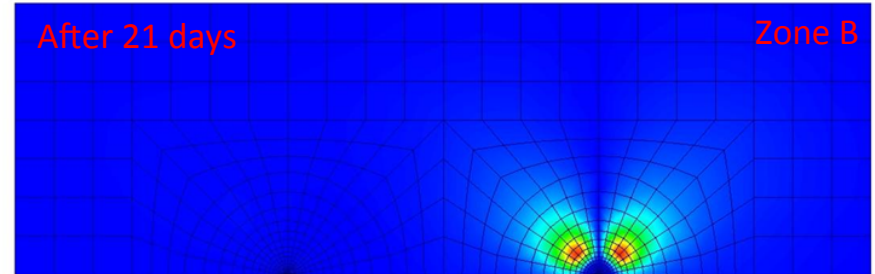
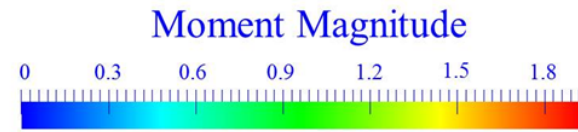


Moment Magnitudes - Variable Fracture Density

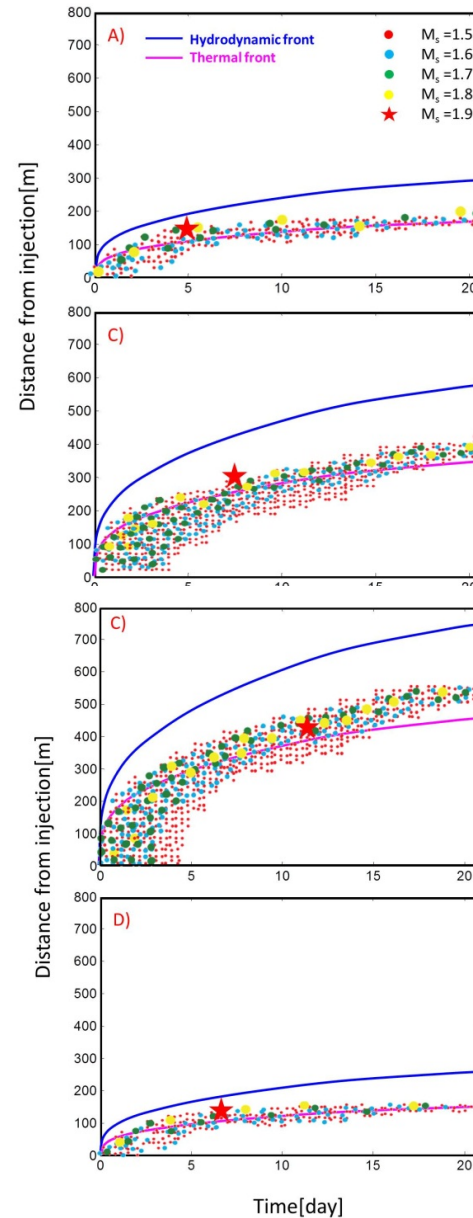
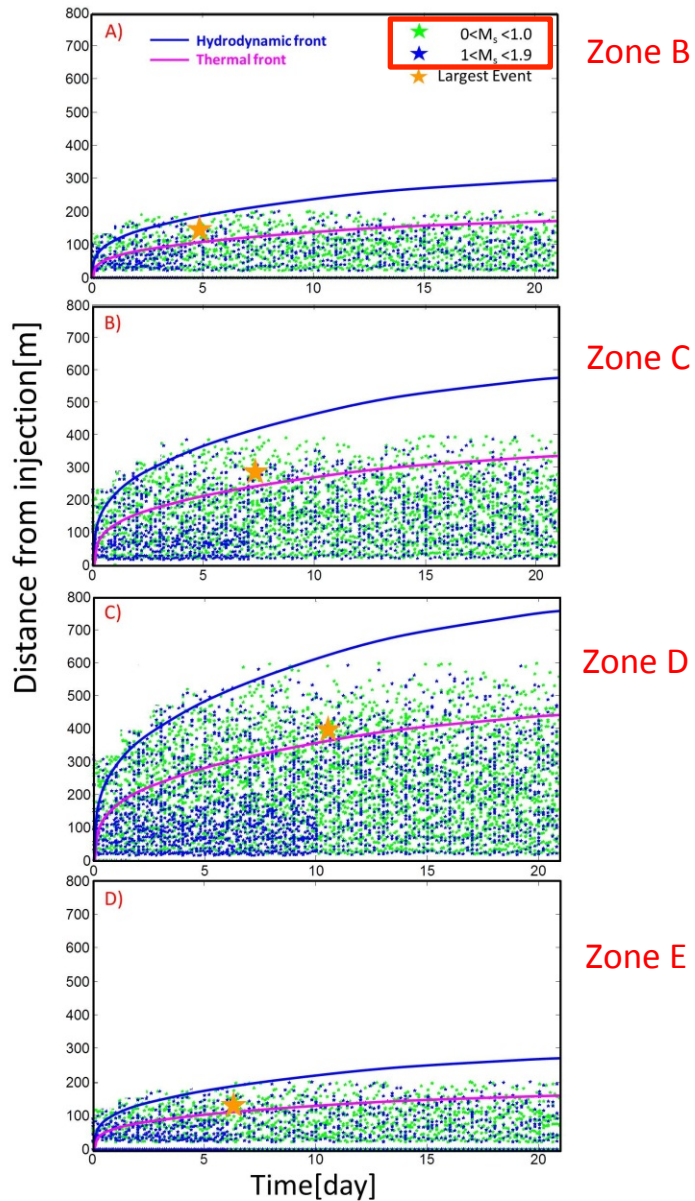
When we apply a differing fracture density:

The rate of seismic event migration within the reservoir is controlled principally by the density and spacing of the fractures.

Highest fracture density generates both the most and the largest seismic events.



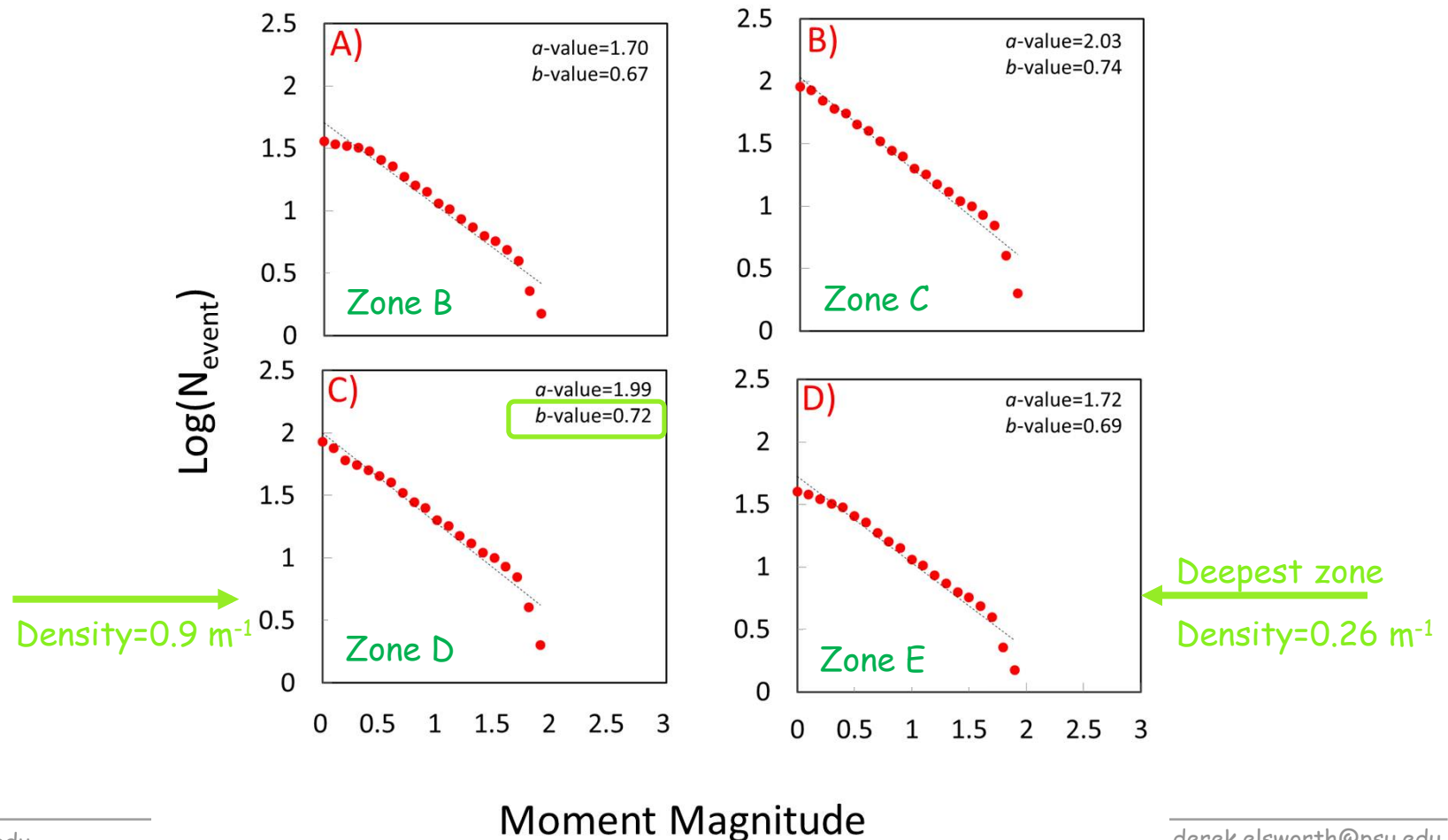
Event Distribution over 21 Days



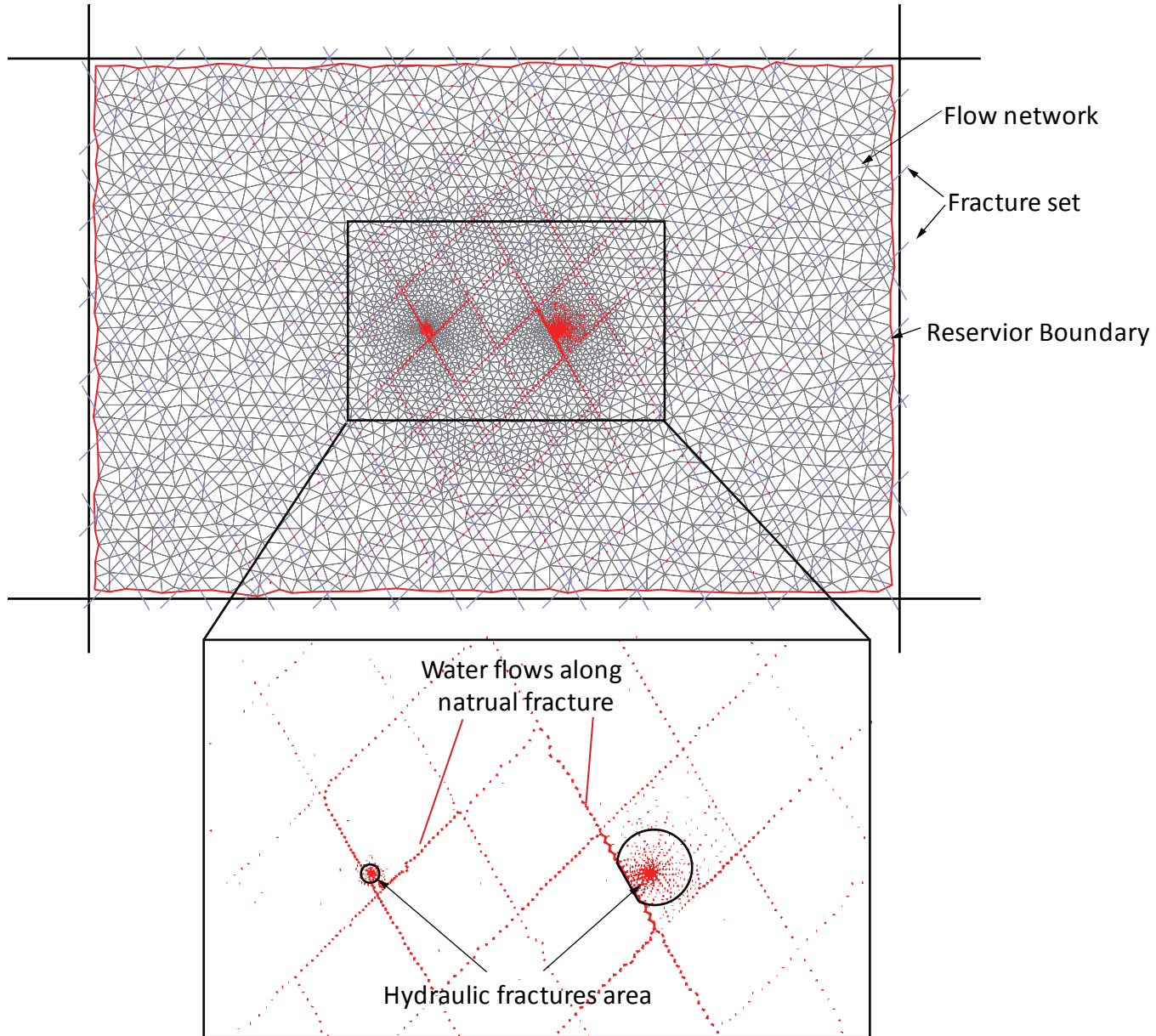
b-value evolution over 21 Days

b-value magnitude [21 days Stimulation]

We characterize the induced seismicity by the *b*-value for three different fracture geometries (high to low density):



Discontinuum Approaches



Conclusions

Complex THM and THC Interactions Influence Reservoir Evolution

Permeability evolution is strongly influenced by these processes

In some instances the full THMC quadruplet is important

Effects are exacerbated by heterogeneity and anisotropy

Spatial and Temporal Evolution

Physical controls (perm, thermal diffusion, kinetics) control progress

Effects occur in order of fluid pressure (M), thermal dilation (TM), chemical alteration (C)

Spatial halos also propagate in this same order of pressure, temperature, chemistry

Induced Seismicity

Mechanisms that control stress effects also influence seismicity

Event magnitudes controlled by stress-drop and fracture size

Distribution controlled by fracture location and sizes (if no new fractures created)

Timing controlled by:

Relative magnitude of stress change effects (pressure, temp, chem)

Rates of propagation and self-propagation of those stress-change fronts

Isolating principal mechanisms is one key to mitigating effect